Pyrolysis of Wood/Biomass for Bio-oil: A Critical Review

- Dinesh Mohan
,
- Charles U. Pittman Jr.
, and
- Philip H. Steele

View Author Information

Cite this: *Energy Fuels* 2006, 20, 3, 848–889
Publication Date:March 10, 2006
https://doi.org/10.1021/ef0502397

SUBJECTS:
- Biofuels,
- Biomass,

- Lipids,
- Pyrolysis,
- Wood

Energy & Fuels

1. Abstract

Fast pyrolysis utilizes biomass to produce a product that is used both as an energy source and a feedstock for chemical production. Considerable efforts have been made to convert wood biomass to liquid fuels and chemicals since the oil crisis in mid-1970s. This review focuses on the recent developments in the wood pyrolysis and reports the characteristics of the resulting bio-oils, which are the main products of fast wood pyrolysis. Virtually any form of biomass can be considered for fast pyrolysis. Most work has been performed on wood, because of its consistency and comparability between tests. However, nearly 100 types of biomass have been tested, ranging from agricultural wastes such as straw, olive pits, and nut shells to energy crops such as miscanthus and sorghum. Forestry wastes such as bark and thinnings and other solid wastes, including sewage sludge and leather wastes, have also been studied. In this review, the main (although not exclusive) emphasis has been given to wood. The literature on wood/biomass pyrolysis, both fast and slow, is surveyed and both the physical and chemical aspects of the resulting bio-oils are reviewed. The effect of the wood composition and structure, heating rate, and residence time during pyrolysis on the overall reaction rate and the yield of the volatiles are also discussed. Although very fast and very slow pyrolyses of biomass produce markedly different products, the variety of heating rates, temperatures, residence times, and feedstock varieties found in the literature make generalizations difficult to define, in regard to trying to critically analyze the literature.

*

To whom correspondence should be addressed. Tel.: (662) 325-7616. Fax: (662) 325-7611. E-mail: dm_1967@hotmail.com.

†

Department of Chemistry, Mississippi State University.

‡

Environmental Chemistry Division, Industrial Toxicology Research Centre.

§

Forest Products Department, Mississippi State University.

2. 1. Introduction

Pyrolysis dates back to at least ancient Egyptian times, when tar for caulking boats and certain embalming agents were made by pyrolysis.[1] Pyrolysis processes have been improved and are now widely used with coke and charcoal production. In the 1980s, researchers found that the pyrolysis liquid yield could be increased using fast pyrolysis where a biomass feedstock is heated at a rapid rate and the vapors produced are also condensed rapidly.[1]

About 97% of all transportation energy in the United States is derived currently from nonrenewable petroleum.[2] Energy for transportation consumes 63% of all oil used in the United States. Foreign oil accounts for more than half of all oil used in the United States. The fact that oil is nonrenewable and the fact that the United States is heavily reliant on foreign sources for energy are excellent incentives for developing renewable energy sources. The accelerated rate of growth of energy consumption in Asia, particularly China and India, raises this incentive for all countries. In addition, the burning of fossil fuels, which produces carbon dioxide, has serious environmental consequences.

In contrast to fossil fuels, the use of biomass for energy provides significant environmental advantages. Plant growth needed to generate biomass feedstocks removes atmospheric carbon dioxide, which offsets the increase in atmospheric carbon dioxide that results from biomass fuel combustion. There is currently no commercially viable way to offset the carbon dioxide added to the atmosphere (and the resultant greenhouse effect) that results from fossil fuel combustion. The climate change effects of carbon dioxide from fossil fuels are now generally recognized as a potential serious environmental problem. To meet the goals of the Kyoto agreement, the United States must reduce greenhouse gas (GHG) emissions to a level 7% below the 1990 emissions in 2008. Carbon dioxide is the predominant contributor to the increased concentration of GHGs. The combustion of fossil fuels accounts for two-thirds of global anthropogenic CO_2 emissions, with the balance attributed to land use changes.

Although it makes up only about 5% of global population, the United States was responsible for 22% of global anthropogenic CO_2 emissions in 1995.[3] Nearly one-third of the U.S. emissions are attributed to transportation, including motor vehicles, trains, ships, and aircraft.[4] The global share of CO_2 emissions by other countries, particularly China and India, is rapidly rising, even as the CO_2 emissions from the United States increase.

In 1998, GHG emissions in the United States were nearly 10% higher than 1990 levels and could rise 47% above 1990 levels by 2020, according to two new reports from the U.S. Department of Energy's Energy Information Adminstration (EIA) (http://www.eia.doe.gov/). The Emissions of Greenhouse Gases, which is the eleventh annual report,[5] presents the Energy Information Administration's latest estimates of emissions for carbon dioxide and other GHGs. According to this report, U.S. emissions of GHGs in 2003 totaled 6935.7 million metric tons of carbon dioxide equivalent, 0.7% more than in 2002 (6890.9 million metric tons of carbon dioxide equivalent). Although the emissions of carbon dioxide and methane grew by 0.8% and 0.5%, respectively, those increases were partially balanced by reductions in emissions of nitrous oxide (−0.9%) and hydrofluorocarbons, perfluorocarbons, and sulfur hexafluoride (−0.3%). U.S. GHGs emissions have averaged 1.0% annual growth since 1990.

Renewable biomass sources can be converted to fuels and are a logical choice to replace oil. By deriving more energy from renewable feedstocks, the United States and other countries might be able to significantly decrease their reliance on foreign petroleum. For this reason, efforts have been made to develop new processes for converting renewable biomass to energy. The land base of the United States, for example, encompasses nearly 2263 million acres, including the 369 million acres of land in Alaska and Hawaii.[6] About 33% of the land

area is classified as forest land, 26% as grassland pasture and range, 20% as cropland, 8% as special uses (e.g., public facilities), and 13% as miscellaneous other uses, such as urban areas, swamps, and deserts.[7,8] About half of the land in the continental United States has agricultural potential for growing biomass. Currently, slightly more than 70% of biomass consumption in the United States (about 142 million dry tons) comes from forestlands. The remainder, which includes bio-based products, biofuels, and some residue biomass, comes from cropland. In 2003, biomass contributed nearly 2.9 quadrillion BTUs (quads) to the nation's energy supply, nearly 3% of total U.S. energy consumption of about 98 quads.[6] Biomass, which comprises 47% of the total renewable energy consumption, is the single-largest renewable energy resource currently being used. Recently, it surpassed hydropower[6] as an energy source.

Most processes that convert biomass to liquid fuels begin with pyrolysis, followed by catalytic upgrading of the resulting biocrude liquids. Kinetics and thermal decomposition mechanisms for the pyrolysis of plant biomass and its constituents have been extensively studied. In contrast, few studies have focused on the use of catalysts for biomass cracking (in situ upgrading) to generate chemicals. Furthermore, the wood preservative industry is interested in finding a low-cost and environmentally friendly means to dispose of treated wood products. This represents another opportunity to convert waste to fuels or chemicals with environmental benefits.

The biological potential of the forestlands of the United States is 29.1−34.6 billion cubic feet per year.[9] Keeping this in mind, the maximum utilization of our forest productivities is becoming increasingly essential. Logging generates considerable residues, which, to date, have been discarded as waste or simply not used. For example, the commercial forest lands of east Texas alone provide an annual harvest of 475 million cubic feet and produce as much as 5 million tons of logging residues annually.[10] This material, which has been ignored in the past, is now being considered as a valuable resource. Increased residue utilization in the future may come as a result of several conversion processes currently under development.[11] One of the most promising is the thermal degradation of lignocellulosic material. This is being studied with great interest as a possible route to alternate energy sources and chemical raw materials. Table 1 summarizes the material and energy balances available from one example process, the Tech Air Process,[12] to illustrate these possibilities. The bio-oil data given in Table 1 are produced from a 50-ton/day demonstration plant operated by the Tech-Air Corporation of Cordele, GA. The process operates continuously in a porous, vertical bed and uses temperatures in the range of 316−982 °C. The feed materials are pine saw dust and bark waste generated from saw mills. Because of the use of some process air, the Tec-Air process is not a true pure pyrolysis.

Table 1. Material and Energy Balance of the Tech Air Process[a]

component	material balance		energy balance
Input			
pine bark/sawdust	100	100	8755 BTU/lb
air and moisture	49		
Output			

char	23	35	11000−13500 BTU/lb
oil	25	35	10000−13000 BTU/lb
gas	68	22	200−500 BTU/scf
water	33		
losses		8	

[a] Data taken from ref 12.

The pyrolytic breakdown of wood produces a large number of chemical substances. Some of these chemicals can be used as substitutes for conventional fuels.

Thermal degradation processes include liquefaction, gasification, and pyrolysis. Liquefaction in a reducing medium also generates solids and gases. Gasification produces hydrogen, carbon monoxide, carbon dioxide, and water by partial combustion. Gasification also produces hydrocarbons, particularly in the lower temperature ranges in fluidized-bed reactors. Pyrolysis converts organics to solid, liquid, and gas by heating in the absence of oxygen. The amounts of solid, liquid, and gaseous fractions formed is dependent markedly on the process variables, as are the distribution of products within each solid, liquid, and gas phase produced. Processing carbonaceous feedstocks to produce heat, chemicals, or fuels offers an alternative to landfills and provides a supplement to fossil fuel use.

Fast pyrolysis has been developed relatively recently. It is the least understood of the thermal degradation processes. The products produced from fast pyrolysis are complex. Presently, there are many laboratories around the world (National Renewable Energy Laboratory, University of Nancy, Colorado School of Mines, University of Twente, University of Laval, Mississippi State University, BBC Engineering, Ltd., Interchem Industries, Inc., Aston University, Irish Bio-energy Association, Naples University, BFH−Institute of Wood Chemistry, VTT Processes, etc.) trying to commercialize "fast wood pyrolysis" to a liquid. [13]

Bio-oil has several environmental advantages over fossil fuels as a clean fuel. [14] Bio-oils are CO_2/GHG neutral. Therefore, they can generate carbon dioxide credits. No SO_x emissions are generated, because plant biomass contains insignificant amounts of sulfur. Therefore, bio-oil would not be subjected to SO_x taxes. Bio-oil fuels generate more than 50% lower NO_x emissions than diesel oil in a gas turbine. Reneawable and locally produced bio-oil can be produced in countries with large volumes of organic wastes. Thus, bio-fuels are cleaner and cause less pollution. [15,16] The thermochemical conversion of biomass (pyrolysis, gasification, combustion) is a promising, non-nuclear form of future energy. [17]

The research and technology concerning bio-oil have advanced significantly. A large number of publications are appearing every year. [18-28] We have selected and reviewed many significant papers from the literature published during last two decades on this subject. The term "significant" is, of course, our own interpretation, with which others may differ.

Commercial pyrolysis processes have been reviewed.[18-22,29-31] Bridgwater and Peacocke[18] summarized the key features of the fast pyrolysis and described the major processes developed over the past 20 years. Bridgwater[20,21,30] reviewed fast pyrolysis design considerations and upgrading. The technical and economic performances of thermal

processes to generate electricity from a wood chip feedstock by combustion, gasification, and fast pyrolysis have been assessed.[20,21] These reviews cover fast pyrolysis process design, pyrolysis reactors, the current status of pyrolysis processes in various countries, and commercialization. However, to the best knowledge of the authors, no review is available where the pyrolysis chemistry of many different types of biomass are discussed for producing bio-oil. Previous reviews covered pyrolysis, with an emphasis on making bio-oil fuels. While generally providing a broad introduction to bio-oil, this review provides a more chemical point of view on fast pyrolysis of lignocellulosic feeds. Many papers published during past decade are discussed that are not found in other reviews. Solvent fractionation methods, which are used to extract lignin-rich bio-oil fractions, are mentioned. If fast pyrolysis liquids are to become as a source of chemical products (as opposed to fuels), separation technology will be important.

3. 2. Introduction to Biomass Pyrolysis Considerations

Pyrolysis is the thermal decomposition of materials in the absence of oxygen or when significantly less oxygen is present than required for complete combustion. It is important to differentiate pyrolysis from gasification. Gasification decomposes biomass to syngas by carefully controlling the amount of oxygen present. Pyrolysis is difficult to precisely define, especially when applied to biomass. The older literature generally equates pyrolysis to carbonization, in which the principal product is a solid char. Today, the term pyrolysis often describes processes in which oils are preferred products. The time frame for pyrolysis is much faster for the latter process.

The general changes that occur during pyrolysis are enumerated below.[250]

(1) Heat transfer from a heat source, to increase the temperature inside the fuel;

(2) The initiation of primary pyrolysis reactions at this higher temperature releases volatiles and forms char;

(3) The flow of hot volatiles toward cooler solids results in heat transfer between hot volatiles and cooler unpyrolyzed fuel;

(4) Condensation of some of the volatiles in the cooler parts of the fuel, followed by secondary reactions, can produce tar;

(5) Autocatalytic secondary pyrolysis reactions proceed while primary pyrolytic reactions (item 2, above) simultaneously occur in competition; and

(6) Further thermal decomposition, reforming, water gas shift reactions, radicals recombination, and dehydrations can also occur, which are a function of the process's residence time/temperature/pressure profile.

Over the last two decades, fundamental research on fast or flash pyrolysis has shown that high yields of primary, nonequilibrium liquids and gases, including valuable chemicals, chemical intermediates, petrochemicals, and fuels, could be obtained from carbonaceous feedstocks. Thus, the lower value solid char from traditional slow pyrolysis can be replaced by higher-value fuel gas, fuel oil, or chemicals from fast pyrolysis.[32]

Characteristics of wood pyrolysis products are dependent on whether a hardwood or softwood species is pyrolyzed. The term “hardwood” is a rather imprecise term identifying

the broad class of angiospermae trees. The term “softwood” identifies the class of gymnospermae trees. The terms hardwood and softwood can be misleading, because they have little relation to the wood hardness.

4. 3. Major Components of Wood/Biomass

The chemical composition of biomass is very different from that of coal oil, oil shales, etc. The presence of large amounts of oxygen in plant carbohydrate polymers means the pyrolytic chemistry differs sharply from these other fossil feeds. Wood and other plant biomass is essentially a composite material constructed from oxygen-containing organic polymers. The major structural chemical components (Figure 1) with high molar masses are carbohydrate polymers and oligomers (65%−75%) and lignin (18%−35%). Minor low-molar-mass extraneous materials mostly organic extractives and inorganic minerals are also present in wood (usually 4%−10%). [33] The major constituents consist of cellulose (a polymer glucosan), hemicelluloses (which are also called polyose), lignin, organic extractives, and inorganic minerals. The weight percent of cellulose, hemicellulose, and lignin varies in different biomass species of wood. The typical lignocellulose contents of some plant materials are given in Table 2.

Figure 1 General components in plant biomass.

Table 2. Typical Lignocellulose Content of Some Plant Materials

	Lignocellulose Content (%)		
plant material	hemicellulose	cellulose	lignin
orchard grass (medium maturity)[a]	40.0	32.0	4.7
rice straw[b]	27.2	34.0	14.2
birchwood[b]	25.7	40.0	15.7

[a] Data taken from van Soest.[240] [b] Data taken from Solo.[241]

Biomass pyrolysis products are a complex combination of the products from the individual pyrolysis of cellulose, hemicellulose, and extractives, each of which has its own kinetic characteristics. In addition, secondary reaction products result from cross-reactions of primary pyrolysis products and between pyrolysis products and the original feedstock molecules. Various chemicals derived from biomass have been discussed by Elliott. [34,35] Pyrolysis of each constituent is itself a complex process that is dependent on many factors. To emphasize this chemistry, the major chemical components of plant biomass are introduced. The general features of the thermal decomposition of these components then are discussed, because these processes must be considered simultaneously during biomass pyrolysis.

3.1. Cellulose. Cellulose fibers provide wood's strength and comprise ∼40−50 wt % of dry wood.[33] Cellulose is a high-molecular-weight (10^6 or more) linear polymer of β-(1→4)-D-glucopyranose units in the $^4C_1$ conformation (Figure 2). The fully equatorial conformation of β-linked glucopyranose residues stabilizes the chair structure, minimizing flexibility. Glucose anhydride, which is formed via the removal of water from each glucose, is polymerized into long cellulose chains that contain 5000−10000 glucose units. The basic repeating unit of the cellulose polymer consists of two glucose anhydride units, called a cellobiose unit.

Figure 2 Chemical structure of cellulose.

Cellulose is insoluble, consisting of between 2000 and 14000 residues, and is crystalline (cellulose I_α). Intramolecular (O3−H → O5‘ and O6 → H−O2‘) and intrastrand (O6−H → O3‘) hydrogen bonds hold the network flat, allowing the hydrophobic ribbon faces to stack.[36] Each residue is oriented 180° to the next within the chain. Individual strands of cellulose are intrinsically no less hydrophilic, or no more hydrophobic, than are some other soluble polysaccharides (such as amylose). However, cellulose's tendency to form crystals utilizing extensive intramolecular and intermolecular hydrogen bonding makes it completely insoluble in normal aqueous solutions (although it is soluble in more exotic solvents, such as aqueous *N*-methylmorpholine-*N*-oxide (NMNO), CdO/ethylenediamine (cadoxen), or LiCl/*N,N‘*-dimethylacetamide, or near supercritical water and in some ionic liquids).[37,38] Cellulose forms long chains that are bonded to each other by a long network of hydrogen bonds (Figure 3). Groups of cellulose chains twist in space to make up ribbonlike microfibril sheets, which are the basic construction units for a variety of complex fibers. These microfibrils form composite tubular structures that run along a longitudinal tree axis. The crystalline structure resists thermal decomposition better than hemicelluloses. Amorphous regions in cellulose exist that contain waters of hydration, and free water is present within the wood. This water, when rapidly heated, disrupts the structure by a steam explosion-like process prior to chemical dehydration of the cellulose molecules.

Figure 3 Intrachain and interchain hydrogen-bonded bridging.

Cellulose degradation occurs at 240−350 °C to produce anhydrocellulose and levoglucosan. When cellulose is pyrolyzed at a heating rate of 12 °C/min under helium in DTA experiments, an endotherm is observed at 335 °C (temperature of maximum weight loss). The reaction is complete at 360 °C.[39] Levoglucosan is produced when the glucosan radical is generated without the bridging oxygen from the preceding monomer unit (see Scheme 1). The C-6 hydroxyl moiety transfers a proton to the C-1 cation during formation of a I-6 oxygen bridge.[40] Pakhomov[41] also proposed that intermediate radicals form and degradation occurs through one of two biradicals. Specifically, a hydroxy group in radical I is transformed from C-6 to C-4, which occurs during the C-1 to C-6 oxygen bridge formation.

Scheme 1

3.2. Hemicellulose. A second major wood chemical constituent is hemicellulose, which is also known as polyose. A variety of hemicelluloses usually account for 25%−35% of the mass of dry wood, 28% in softwoods, and 35% in hardwoods.[33] Hemicellulose is a mixture of

various polymerized monosaccharides such as glucose, mannose, galactose, xylose, arabinose, 4-*O*-methyl glucuronic acid and galacturonic acid residues (see Figure 4). Hemicelluloses exhibit lower molecular weights than cellulose. The number of repeating saccharide monomers is only ∼150, compared to the number in cellulose (5000−10000). Cellulose has only glucose in its structure, whereas hemicellouse has a heteropolysaccharide makeup and some contains short side-chain "branches" pendent along the main polymeric chain.

Figure 4 Main components of hemicellulose.

Hemicellulose decomposes at temperatures of 200−260 °C, giving rise to more volatiles, less tars, and less chars than cellulose.[11] Most hemicelluloses do not yield significant amounts of levoglucosan. Much of the acetic acid liberated from wood during pyrolysis is attributed to deacetylation of the hemicellulose. Hardwood hemicelluloses are rich in xylan and contain small amounts of glucomannan. Softwood hemicelluloses contain a small amount of xylan, and they are rich in galactoglucomannan. The onset of hemicellulose thermal decomposition occurs at lower temperatures than crystalline cellulose. The loss of hemicellulose occurs in slow pyrolysis of wood in the temperature range of 130−194 °C, with most of this loss occurring above 180 °C.[42] However, the relevance of this more-rapid decomposition of hemicellulose versus cellulose is not known during fast pyrolysis, which is completed in few seconds at a rapid heating rate.

3.3. Lignin. The third major component of wood is lignin, which accounts for 23%−33% of the mass of softwoods and 16%−25% of the mass of hardwoods.[30] It is an amorphous cross-linked resin with no exact structure. It is the main binder for the agglomeration of fibrous cellulosic components while also providing a shield against the rapid microbial or fungal destruction of the cellulosic fibers. Lignin is a three-dimensional, highly branched, polyphenolic substance that consists of an irregular array of variously bonded "hydroxy-" and "methoxy-"substituted phenylpropane units.[43] These three general monomeric phenylpropane units exhibit the *p*-coumaryl, coniferyl, and sinapyl structures (Figure 5). In lignin biosynthesis, these units undergo radical dimerization and further oligomerization, and they eventually polymerize and cross-link. The resonance hybrids of the radical formed on oxidation of coniferyl alcohol illustrates the positions where radicals dimerizations occur during lignin formation.

Figure 5 *p*-Coumaryl, coniferyl, and sinapyl structures and resonance hybrid structures of phenoxy radicals produced by the oxidation of coniferyl.

Hardwood and softwood lignin have different structures. "Guaiacyl" lignin, which is found predominantly in softwoods, results from the polymerization of a higher fraction of coniferyl phenylpropane units. "Guaiacyl-syringyl" lignin, which is typically found in many hardwoods, is a copolymer of both the coniferyl and sinapyl phenylpropane units where the fraction of sinapyl units is higher than that in softwood lignins. Lignin has an amorphous structure, which leads to a large number of possible interlinkages between individual units, because the radical reactions are nonselective random condensations. Ether bonds predominate between lignin units, unlike the acetal functions found in cellulose and hemicellulose, but carbon-to-carbon linkages also exist. Covalent linking also exists between lignin and polysaccharides,[44] which strongly enhances the adhesive bond strength between

cellulose fibers and its lignin “potting matrix”. A small section of a lignin polymer is presented in Figure 6, illustrating some typical lignin chemical linkages.

Figure 6 Partial structure of a hardwood lignin molecule from European beech (*Fagus sylvatica).* The phenylpropanoid units that comprised lignin are not linked in a simple, repeating way. The lignin of beech contains units derived from coniferyl alcohol, sinapyl alcohol, and *p*-coumaryl alcohol in the approximate ratio of 100:70:7 and is typical of hardwood lignin. Softwood lignin contains relatively fewer sinapyl alcohol units. (After Nimz 1974.[45]).

The physical and chemical properties of lignins differ, depending on the extraction or isolation technology used to isolate them. Because lignin is inevitably modified and partially degraded during isolation, thermal decomposition studies on separated lignin will not necessarily match the pyrolysis behavior of this component when it is present in the original biomass. Lignin decomposes when heated at 280−500 °C.[11] Lignin pyrolysis yields phenols via the cleavage of ether and carbon−carbon linkages. Lignin is more difficult to dehydrate than cellulose or hemicelluloses. Lignin pyrolysis produces more residual char than does the pyrolysis of cellulose. In differential thermal analysis (DTA) studies at slow heating rates, a broad exotherm plateau extending from 290 °C to 389 °C is observed, followed by a second exotherm, peaking at 420 °C and tailing out to beyond 500 °C.[46] Lignin decomposition in wood was proposed to begin at 280 °C and continues to 450−500 °C, with a maximum rate being observed at 350−450 °C.[47]

The liquid product, which is known as pyroligneous acid, typically consists of ∼20% aqueous components and ∼15% tar residue, calculated on a dry lignin basis. The aqueous portion is composed of methanol, acetic acid, acetone, and water, whereas the tar residue consists mainly of homologous phenolic compounds. The gaseous products represent 10 wt % of the original lignin and contain methane, ethane, and carbon monooxide.

3.4. Inorganic Minerals. Biomass also contains a small mineral content that ends up in the pyrolysis ash. Table 3 shows some typical values of the mineral components in wood chips, expressed as a percentage of the dry matter (DM) in the wood (http://www.woodenergy.ie/biomass_fuel/biomass3.asp).

Table 3. Typical Mineral Components of Plant Biomass

element	percentage of dry matter
potassium, K	0.1
sodium, Na	0.015
phosphorus, P	0.02
calcium, Ca	0.2
magnesium, Mg	0.04

3.5. Organic Extractives. A fifth wood component is comprised of organic extractives. These can be extracted from wood with polar solvents (such as water, methylene chloride, or alcohol) or nonpolar solvents (such as toluene or hexane). Example extractives include fats, waxes, alkaloids, proteins, phenolics, simple sugars, pectins, mucilages, gums, resins, terpenes, starches, glycosides, saponins, and essential oils. Extractives function as intermediates in metabolism, as energy reserves, and as defenses against microbial and insect attack.

5. 4. Types of Pyrolysis

Pyrolysis processes may be conventional or fast pyrolysis, depending on the operating conditions that are used. [48] Conventional pyrolysis may also be termed slow pyrolysis. The terms “slow pyrolysis” and “fast pyrolysis” are somewhat arbitrary and have no precise definition of the times or heating rates involved in each. Many pyrolyses have been performed at rates that are not considered fast or slow but are conducted in a broad range between these extremes. Thermogravimetric (TG) and differential TG studies of beechwood flour illustrated that wood decomposition began at ∼200 °C, reached a maximum rate of mass loss at 350 °C, and continued to ∼500 °C, illustrating the complex contributions of all the chemical constituents. [49]

4.1. Conventional Pyrolysis. Conventional slow pyrolysis has been applied for thousands of years and has been mainly used for the production of charcoal. In slow wood pyrolysis, biomass is heated to ∼500 °C. The vapor residence time varies from 5 min to 30 min.[32,50,51] Vapors do not escape as rapidly as they do in fast pyrolysis. Thus, components in the vapor phase continue to react with each other, as the solid char and any liquid are being formed. The heating rate in conventional pyrolysis is typically much slower than that used in fast pyrolysis. A feedstock can be held at constant temperature or slowly heated. Vapors can be continuously removed as they are formed. Vacuum pyrolysis at slow or fast heating rates is another variant. The definition of a “slow” heating rate versus a “fast” heating rate is arbitrary in many respects.

4.2. Fast Pyrolysis. Fast pyrolysis is a high-temperature process in which biomass is rapidly heated in the absence of oxygen.[28,50,52,53] Biomass decomposes to generate vapors, aerosols, and some charcoal-like char. After cooling and condensation of the vapors and aerosols, a dark brown mobile liquid is formed that has a heating value that is about half that of conventional fuel oil (http://www.pyne.co.uk). Fast pyrolysis processes produce 60−75 wt % of liquid bio-oil, 15−25 wt % of solid char, and 10−20 wt % of noncondensable gases, depending on the feedstock used. No waste is generated, because the bio-oil and solid char can each be used as a fuel and the gas can be recycled back into the process.

Fast pyrolysis uses much faster heating rates than traditional pyrolysis. Advanced processes are carefully controlled to give high liquid yields. There are four essential features of a fast pyrolysis process. [54] First, very high heating and heat transfer rates are used, which usually requires a finely ground biomass feed. Second, a carefully controlled pyrolysis reaction temperature is used, often in the 425−500 °C range. Third, short vapor residence times are used (typically <2 s). Fourth, pyrolysis vapors and aerosols are rapidly cooled to give bio-oil.

Heating rates of 1000 °C/s, or even 10000 °C/s, at temperatures below ∼650 °C have been claimed.[54] Rapid heating and rapid quenching produced the intermediate pyrolysis liquid

products, which condense before further reactions break down higher-molecular-weight species into gaseous products. High reaction rates minimize char formation. Under some conditions, no char is formed.[55] At higher fast pyrolysis temperatures, the major product is gas. Many researchers have attempted to exploit the complex degradation mechanisms by conducting pyrolysis in unusual environments. The main pyrolysis variants[55] are listed in Table 4.

Table 4. Pyrolysis Methods and Their Variants[a]

pyrolysis technology	residence time	heating rate	temperature (°C)	products
carbonization	days	very low	400	charcoal
conventional	5−30 min	low	600	oil, gas, char
fast	0.5−5 s	very high	650	bio-oil
flash-liquid[b]	<1 s	high	<650	bio-oil
flash-gas[c]	<1 s	high	<650	chemicals, gas
ultra[d]	<0.5	very high	1000	chemicals, gas
vacuum	2−30 s	medium	400	bio-oil
hydro-pyrolysis[e]	<10 s	high	<500	bio-oil
methano-pyrolysis[f]	<10 s	high	>700	chemicals

[a] Data taken from refs 55 (with permission from Elsevier) and 242. [b] Flash-liquid = liquid obtained from flash pyrolysis accomplished in a time of <1 s. [c] Flash-gas = gaseous material obtained from flash pyrolysis within a time of <1 s. [e] Hydropyrolysis = pyrolysis with water. [f] Methanopyrolysis = pyrolysis with methanol. [d] Ultra(pyrolysis) = pyrolyses with very high degradation rate.

Emmons and Atreys[56] estimated that more than 200 intermediate products formed during the pyrolysis of biomass. Cellulose is the major constituent of wood, and its pyrolysis occurs over almost the entire range of pyrolysis temperatures.[57] Pure cellulose pyrolysis has been investigated to help understand its decomposition mechanism during wood pyrolysis.[22] An excellent review by DiBlasi[58] has described the classes of mechanisms that had been previously proposed for wood pyrolysis and that of other cellulosic materials. Bridgwater[21] reviewed the principles and practice of biomass fast pyrolysis processes and the variables influencing process design considerations. Design variables required for fast pyrolysis include the following: feed drying, particle size, pretreatment, reactor configuration, heat supply, heat transfer, heating rates, reaction temperature, vapor residence

time, secondary cracking, char separation, ash separation, and liquid collection. Each of these aspects was reviewed and discussed.

6. 5. What Is Bio-oil?

Bio-oils are dark brown, free-flowing organic liquids that are comprised of highly oxygenated compounds. [59-62] The synonyms for bio-oil include pyrolysis oils, pyrolysis liquids, bio-crude oil (BCO), wood liquids, wood oil, liquid smoke, wood distillates, pyroligneous acid, and liquid wood. Throughout this review, the terms pyrolysis oil, tar, pyrolytic tar, and bio-oil will be used.

Pyrolysis liquids are formed by rapidly and simultaneously depolymerizing and fragmenting cellulose, hemicellulose, and lignin with a rapid increase in temperature. Rapid quenching then "freezes in" the intermediate products of the fast degradation of hemicellulose, cellulose, and lignin. Rapid quenching traps many products that would further react (degrade, cleave, or condensate with other molecules) if the residence time at high temperature was extended. Bio-oils contain many reactive species, which contribute to unusual attributes. Chemically, bio-oil is a complex mixture of water, guaiacols, catecols, syringols, vanillins, furancarboxaldehydes, isoeugenol, pyrones, acetic acid, formic acid, and other carboxylic acids. It also contains other major groups of compounds, including hydroxyaldehydes, hydroxyketones, sugars, carboxylic acids, and phenolics. [63] Oligomeric species in bio-oil are derived mainly from lignin, but also cellulose. Oligomer molecular weights from several hundred to as much as 5000 or more can be obtained. They form as part of the aerosols. Free water in the biomass explosively vaporizes upon fast pyrolysis. It shreds the feed particles and aids heat transfer. Cellulose and hemicellulose also lose water, which contributes to the process. Oligomeric species may never be vaporized but simply "blown apart" into aerosols as decomposition rapidly occurs. The molecular mass distribution is dependent on the heating rate, residence time, particle size, temperature, and biomass species used. Most oligomeric structures are unable to be seen using gas chromatography (GC) or gas chromatography−mass spectroscopy (GC-MS). High-pressure liquid chromatography, followed by electrospray mass spectroscopy (HPLC/ES-MS), can provide some separation and molecular mass determinations. Bio-oil can be considered a microemulsion in which the continuous phase is an aqueous solution of holocellulose decomposition products and small molecules from lignin decomposition. The continuous liquid phase stabilizes a discontinuous phase that is largely composed of pyrolytic lignin macromolecules.[63] Microemulsion stabilization is achieved by hydrogen bonding and nanomicelle and micromicelle formation. The exact chemical nature of each bio-oil is dependent on the feedstock and the pyrolysis variables, as defined above.

Recently, Fratini et al.[64] performed a small-angle neutron scattering (SANS) analysis of microstructure evolution during the aging of pyrolysis oils from biomass. The BCOs are nanostructured fluids constituted by a complex continuous phase and nanoparticles mainly formed by the association of units of pyrolysis lignins. The aggregation of these units with time produced branched structures with a fractal dimension of $D_f = 1.4-1.5$, which is responsible for BCO aging.[64]

An excellent study of the bio-oils's multiphase structure was reported by Roy et al. [65] They described the physical state as follows: "The multiphase complex structure of biomass pyrolysis oils can be attributed to the presence of char particles, waxy materials, aqueous

droplets, droplets of different nature, and micelles formed of heavy compounds in a matrix of hollocellulose-derived compounds and water."

Bio-oil ages after it is first recovered; this is observed as a viscosity increase. Some phase separation may also occur. This instability is believed to result from a breakdown in the stabilized microemulsion and to chemical reactions, which continue to proceed in the oil. In some ways, this is analogous to the behavior of asphaltenes found in petroleum.[59] Biomass pyrolysis oils contain aldehydes, ketones, and other compounds that can react via aldol condensations during storage or handling to form larger molecules. These reactions cause undesirable changes in physical properties. Viscosity and water content can increase, whereas the volatility will decrease. The most important variable driving this "aging" is temperature.[66-68] Bio-oil is produced with ~25 wt % water, which cannot readily be separated. In contrast to petroleum fuels, bio-oil contains a large oxygen content, usually 45%−50%. Thus, its elemental composition resembles the biomass from which it was derived far more than it resembles petroleum oils. For example, wood can be approximately represented by $CH_{1.4}O_{0.6}$, or 42 wt % oxygen. This oxygen is present in most of the more than 300 compounds that have been identified in the oils.[59] The presence of oxygen is the primary reason for the difference in the properties and behavior between hydrocarbon fuels and biomass pyrolysis oils.[68] Although the pyrolysis liquid is called "bio-oil", it actually is immiscible with liquid hydrocarbons, because of its high polarity and hydrophilic nature.

Typical properties and characteristics of wood-derived BCO are presented in Table 5. Bio-oil has many special features and characteristics. These require consideration before any application, storage, transport, upgrading or utilization is attempted. These features are summarized in Table 6.[21]

Table 5. Typical Properties and Characteristics of Wood Derived Crude Bio-oil[20]

property	characteristics
appearance	from almost black or dark red-brown to dark green, depending on the initial feedstock and the mode of fast pyrolysis.
miscibility	varying quantities of water exist, ranging from ~15 wt % to an upper limit of ~30−50 wt % water, depending on production and collection.
	pyrolysis liquids can tolerate the addition of some water before phase separation occurs.
	bio-oil cannot be dissolved in water.
	miscible with polar solvents such as methanol, acetone, etc., but totally immiscible with petroleum-derived fuels.
density	bio-oil density is ~1.2 kg/L, compared to ~0.85 kg/L for light fuel oil

viscosity	viscosity (of as-produced bio-oil) varies from as low as 25 cSt to as high as 1000 cSt (measured at 40 °C) depending on the feedstock, the water content of the oil, the amount of light ends that have collected, the pyrolysis process used, and the extent to which the oil has been aged
distillation	it cannot be completely vaporized after initial condensation from the vapor phase
	at 100 °C or more, it rapidly reacts and eventually produces a solid residue from ∼50 wt % of the original liquid
	it is chemically unstable, and the instability increases with heating
	it is always preferable to store the liquid at or below room temperature; changes do occur at room temperature, but much more slowly and they can be accommodated in a commercial application
ageing of pyrolysis liquid	causes unusual time-dependent behavior
	properties such as viscosity increases, volatility decreases, phase separation, and deposition of gums change with time

[a] Data taken from ref 20 with permission from Elsevier.

Table 6. Characteristics of Bio-oil and Methods for Modification[a]

characteristic	effect	solution
contains suspended char	Leads to erosion, equipment blockage, combustion problems due to slower rates of combustion; ‘sparklers' can occur in combustion leading to potential deposits and high CO emissions	Hot vapor filtration; liquid filtration; modification of the char for example by size reduction so that its effect is reduced; modification of the application
contains alkali metals	Causes deposition of solids in combustion applications including boilers, engine and turbines; in turbines the damage	Hot vapor filtration; processing or upgrading of oil; modification of application; pretreat feedstock to remove ash

	potential is considerable, particularly in high performance	
low pH	Corrosion of vessels and pipe work	Careful materials selection; stainless steel and some olefin polymers are acceptable
incompatibility with some polymers	Swelling of destruction of sealing rings and gaskets	Careful materials selection
high-temperature sensitivity	Liquid decomposition and polymerization on hot surfaces leading to decomposition and blockage; adhesion of droplets on surfaces below 400 °C	Recognition of problem and appropriate cooling facilities; avoidance of contact with hot surfaces >500 °C
high viscosity	High-pressure drops in pipelines leading to higher cost equipment and/or possibilities of leakage or even pipe rupture. Higher pumping costs.	Careful low temperature heating, and/or addition of water, and/or addition of cosolvents, such as methanol or ethanol
water content	Complex effect on viscosity, lowers heating value, density, stability, pH, homogeneity, etc. Can lead to phase separation.	Recognition of problem; optimization with respect to application
inhomogeneity	Layering or partial separation of phases; filtration problems	Blending with methanol or ethanol

[a] Data taken from ref 21 with permission from Elsevier.

7. 6. Feedstock for Bio-oil Generation

Bio-oil can be made from a variety of forest and agricultural biomass wastes. Waste biomass feedstocks with good potential include bagasse (from sugar cane), rice hulls, rice straw, peanut hulls, oat hulls, switchgrass, wheat straw, and wood. In North America and Europe, bio-oil is produced from forest residues (sawdust, bark, and shavings). In Central and South America, the Caribbean and South Pacific, Australia, Asia, and Africa, it is produced from sugar cane bagasse and other agricultural wastes. Other abundant potential feedstocks include

wheat and other straws, rice hulls, coconut fiber, etc. As-received biomass has a moisture content in the range of 50%−60% (wet basis).[69] Passive drying during summer storage can reduce this to ∼30%. Active silo drying can reduce the moisture content to 12%. Drying can be simply accomplished by near-ambient solar drying or drying using waste heat flows. Alternatively, specifically designed dryers can be used.

8. 7. Bio-oil Yield

Yields of bio-oil from wood, paper, and other biomass were in the range of ∼60−95 wt %, depending on the feedstock composition.[70] The bio-oil yields from wood are in the range of 72−80 wt %, depending on the relative amount of cellulose and lignin in the material.[70] High lignin contents, such as that found in bark, have a tendency to give lower liquid yields (60%−65%). However, these are offset somewhat by a higher energy density than in the liquid materials that are high in cellulose-derived content. These give bio-oil yields in the yield range of 75%−93%. Yields in excess of 75 wt % are typical of a mixed paper stream.[70]

9. 8. Properties of Bio-oil

Bio-oils are composed of differently sized molecules derived primarily from the depolymerization and fragmentation reactions of three key biomass building blocks: cellulose, hemicellulose, and lignin, as previously discussed. Perfect reproduction of all the bio-oil processing conditions can produce varying bio-oils, because the feed composition (biomass or wood) influences the nature of the final product. The physical properties of bio-oils are well-described in the literature.[59,70] The lower heating value (LHV) of bio-oils is only 40−45 wt % of that exhibited by hydrocarbon fuels.[59] The LHV of bio-oils on a volume basis is ∼60% of the heating value of hydrocarbon oils,[59] because of the high oxygen content, the presence of water, and the higher bio-oil density. A typical heating value of bio-oil is ∼17 MJ/kg. Bio-oil is miscible with ethanol and methanol but immiscible with hydrocarbons. Bio-oil can be stored, pumped, and transported in a manner similar to that of petroleum-based products and can be combusted directly in boilers, gas turbines, and slow- and medium-speed diesel engines for heat and power applications.[59] Basic data for bio-oils and conventional petroleum fuels are compared in Table 7,[59] whereas typical properties of bio-oil, light oil, and heavy oils are compared in Table 8.

Table 7. Typical Properties of Wood Pyrolysis Bio-oil and Heavy Fuel Oil[a]

	Value	
physical property	bio-oil	heavy fuel oil
moisture content (wt %)	15−30	0.1
pH	2.5	

specific gravity	1.2	0.94
elemental composition (wt %)		
C	54−58	85
H	5.5−7.0	11
O	35−40	1.0
N	0−0.2	0.3
ash	0−0.2	0.1
HHV (MJ/kg)	16−19	40
viscosity, at 500 °C (cP)	40−100	180
solids (wt %)	0.2−1.0	1
distillation residue (wt %)	up to 50	1

[a] Data taken from ref 59 with permission from the American Chemical Society.

Table 8. Typical Properties of Bio-oil, Compared to Those of Light and Heavy Fuel Oil[a]

property	BioTherm bio-oil	light fuel oil	heavy fuel oil
heat of combustion			
BTU/lb	7100	18200	17600
MJ/L	19.5	36.9	39.4
viscosity (centistokes)			
at 50°C	7	4	50
at 80°C	4	2	41
ash content (wt %)	<0.02	<0.01	0.03
sulfur content (wt %)	trace	0.15−0.5	0.5−3
nitrogen content (wt %)	trace	0	0.3

pour point (°C)	−33	−15	−18
turbine emissions (g/MJ)			
NO_x	<0.7	1.4	N/A
SO_x	0	0.28	N/A

[a] Data taken from ref 106.

8.1. Chemical Nature of Bio-oil. Wood pyrolysis causes bond cleavage and produces fragments of the original polymers (cellulose, hemicellulose, and lignin). Most of the original oxygen is retained in the fragments that collectively comprise bio-oil. A small amount of CO_2 and CO is formed, along with a substantial amount of water. Bio-oil contains 45−50 wt % oxygen,[68] but the oxygen content is dependent on the bio-oil's water content. Proximate analysis of the bio-oil gives a chemical formula of $CH_{1.9}O_{0.7}$, which corresponds to ∼46 wt % oxygen (versus ∼42 wt % oxygen in wood). The difference in oxygen content present in the feed versus that in the bio-oil is related to the oxygen content in the gases and the amount present as water in the oil. Oxygen is present in most of the more than 300 compounds that have been identified in bio-oil.[11] The compounds found in bio-oil have been classified into the following five broad categories:[63](1) hydroxyaldehydes, (2) hydroxyketones, (3) sugars and dehydrosugars, (4) carboxylic acids, and (5) phenolic compounds.

The phenolic compounds are present as monomeric units and oligomers derived from the coniferyl and syringyl building blocks of lignin. Oligomer molecular weights range from several hundred to as much as 5000 or more, depending on the details of the pyrolysis process used. These phenolic compounds are derived from lignin. A more-detailed classification organizes compounds under following categories: acids, alcohols, aldehydes, esters, ketones, phenols, guaiacols, syringols, sugars, furans, alkenes, aromatics, nitrogen compounds, and miscellaneous oxygenates.[63,71] The highest concentration of any single chemical compound (besides water) is hydroxyacetaldehyde (at levels up to 10 wt %), followed by acetic and formic acids (at ∼5 wt % and ∼3 wt %, respectively).[63] This accounts for the acidic pH of 2.0−3.0 that is exhibited by bio-oil.

The chemistry of bio-oils can be manipulated by changing the thermal conditions of the process or by conducting pyrolysis in the presence of catalysts. Increasing the cracking severity (time−temperature relationship) lowers the molecular weight distribution in the resulting oils and produces more gas. At very high temperatures, dehydrogenation/aromatization reactions can eventually lead to larger polynuclear aromatic hydrocarbons and, eventually, increases in carbonization. Elliot[72] described the relationship between the types of compounds in the products and the temperature to which the vapors were exposed before quenching. That relationship is described as

As the temperature is increased, alkyl groups cleave from aromatic compounds. Eventually, the aromatic compounds condense into polycyclic aromatic hydrocarbons (PAHs) at the higher temperatures.

8.1.1. Chemical Characterization Methods. Complete chemical characterization of bio-oil is difficult (or impossible). The bio-oil contains higher-molecular-weight species, including degradation products of pentoses, hexoses, and lignin. Only a portion of the bio-oil can be detected via GC, even using robust columns and high-temperature programs. In addition, the bio-oil contains polar, nonvolatile components that are only accessible by HPLC or GPC analysis[24] (Figure 7). Whole pyrolysis liquids can be analyzed by GC-MS (volatile compounds), HPLC and HPLC/electrospray MS (nonvolatile compounds), Fourier transform infrared (FTIR) spectroscopy (functional groups), gel permeation spectroscopy (GPC) (molecular weight distributions), and nuclear magnetic resonance (NMR) (types of hydrogens or carbons in specific structural groups, bonds, area integrations).

Figure 7 Typical portions of the important fractions in bio-oil.

Analysis is especially difficult because complex phenolic species from lignin decomposition can have molecular weights as high as ∼5000 amu. A variety of these fragmented oligomeric products exist with varying numbers of acidic phenolic and carboxylic acid hydroxyl groups as well as aldehyde, alcohol, and ether functions. They exist in a variety of hydrogen-bonded aggregates, micelles, droplets, gels, etc. Thus, GPC analysis can overestimate the molecular weights, because of aggregation. During HPLC analysis, the combination of polarity differences and molecular-weight differences interact to produce broadened envelopes of peaks that are difficult to analyze by subsequent MS analysis.

8.2. Physical Properties. Bio-oil's physical properties are well documented in the literature[60-62,72-80] Thus, only limited comments are added here.

Pyrolysis liquids contain compounds that self-react during handling at ambient temperatures to form larger molecules. Oasmma and Peacocke[81] discussed various physical and chemical properties and their methods of estimation. The various methods[81] necessary for the characterization of bio-oil fuels and the sample sizes required for each analysis are provided in Table 9.

Table 9. Analytical Methods for Wood-Based Pyrolysis Liquids[a]

analysis	method	sample size
water content (wt %)	ASTM 203	1 g
solids content (wt %)	ethanol insolubles	30 g
	methanol−dichloromethane insolubles	30 g
particle size distribution	microscopy + particle counter	1 g
Conradson carbon residue content (wt %)	ASTM D189	2−4 g

ash content (wt %)	EN 7	40 mL
CHN content (wt %)	ASTM D5291	1 mL
sulfur and chlorine content (wt %)	capillary electrophoresis	2−10 mL
alkali metals content (wt %)	AAS	50 mL
metals content (wt %)	ICP, AAS	50 mL
density, at 15 °C (kg/dm^3)	ASTM D4052	4 mL
viscosity, at 20 and 40 °C (cSt)	ASTM D445	80 mL
viscosity (mPa s)	rotational viscometry	40 mL
pour point (°C)	ASTM D97	80 mL
heating value (MJ/kg)		
calorimetric value, HMV	DIN 51900	1 mL
effective value, LHV	DIN 51900	1 mL
flash point (°C)	ASTM D93	150 mL
pH	pH meter	50 mL
water insolubles content (wt %)	water addition	5 mL
stability	80 °C for 24 h	200 mL
	40 °C for 1 week	200 mL

[a] Data taken from ref 81.

Oasmma and Meier [26,82] presented the results from 12 laboratories that participated in a round-robin test aimed at comparing the accuracy of chemical and physical characterization methods. Four laboratories performed chemical characterization. Four different types of pyrolysis liquids were provided from different producers. The analytical methods used in the round-robin test are presented in Table 10.

Table 10. Analytical Methods for Round-Robin Test[a]

property	method	units

water content	Karl−Fischer titration	wt % water based on wet oil
viscosity	capillary or rotary viscosimeter, two temperatures (at 20 and 40 °C)	cSt at 20 and 40 °C
solids	insolubles in ethanol, filter pore size of ≤3 μm	wt % based on wet oil
pH	use pH meter	pH units
stability[78]	store samples for (i) 6 h at 80 °C, (ii) 24 h at 80 °C, and (iii) 7 days at 50 °C	cSt, wt % water based on wet oil
	viscosity at 20 and 40 °C and water by Karl−Fischer titration	
elemental analysis	elemental analyzer (complete oxidation)	wt % C, wt % H, wt % N, wt % O, based on wet oil
pyrolytic lignin	add 60 mL oil to 1 L of ice-cooled water under stirring, filter and dry precipitate at <60 °C	wt %, based on wet oil
gas chromatography, GC	column type DB 1701, with dimensions of 60 m × 0.25 mm; film thickness: 0.25 μm; injector: 250 °C, split 1:30; FID detector: 280 °C; oven program: 45 °C, 4 min constant, 3 °C/min to 280 °C, hold 20 min; sample concentrated: 6 wt %, solvent acetone	

[a] Data taken from ref 26 with permission from Elsevier.

The round-robin tests led to the following recommendations.[26,82]

(1) The homogeneity of the sample should be verified by water distribution and/or by microscopic determination.

(2) Karl−Fischer titration is recommended for analyzing water in pyrolysis liquids. Water standards and water addition method are suggested for calibration.

(3) pH determination is recommended and the pH level should be reported to one decimal place. Accurate determinations of acidity changes are needed and require frequent calibration.

(4) The kinematic viscosity at 40 °C is accurate for homogeneous pyrolysis liquids. The Newtonian behavior should be checked for extractive-rich liquids, using a closed-cup rotaviscotester.

(5) Stability tests should be performed each time, in exactly the same manner. If the weight loss is >0.1 wt % during the test, the results should be excluded. Stability testing is recommended for comparison of pyrolysis liquids from one specific process. The best comparisons can be obtained when the differences in the water contents of the samples are small. The viscosity is measured at 40 °C, where the measuring error is smaller.

(6) The sample size for elemental analysis should be as large as possible, and analyses should be performed at least in triplicate.

(7) Ethanol (or methanol) can be used for the solids determination of white-wood pyrolysis liquids. For new feedstocks, such as bark and forest residue, the solubility of the liquid should be checked using solvents of different polarity.

(8) Definitions and reliable determination methods for “water insolubles” and “pyrolytic lignin” are necessary.

(9) It might be necessary to calibrate the gas and liquid chromatographic systems, using standard solutions of known amounts of compounds during chemical characterization.

The following measures were recommended for future round-robin studies.[26,82]

(1) Pyrolysis liquids produced from industrially important biomass feedstocks should be included.

(2) Water, solids, homogeneity, viscosity, stability, water insolubles, average molecular weight, and GC/MS should be included as analyses.

(3) Detailed and clear instructions on the handling, pretreatment, and analysis of needed reference samples should be provided.

10. 9. Methods of Bio-oil Preparation

Fast pyrolysis is the leading method for producing liquid biofuels.[83-86] The advantages include low production costs, high thermal efficiency, low fossil fuel input, and CO_2 neutrality. Pyrolysis to a liquid offers the possibility of decoupling (time, place, and scale), easy handling of the liquids, and more-consistent quality, compared to any solid biomass. A liquid intermediate is produced for a variety of applications by fast pyrolysis. The typical yields obtained by different modes of pyrolysis of wood are presented in Table 11.

Table 11. Typical Product Yields (Dry Wood Basis) Obtained by Different Modes of Pyrolysis of Wood[a]

	Product Yield (%)		
process	liquid	char	gas
fast pyrolysis (moderate temperature and short residence time)	75	12	13

carbonization (low temperature and long residence time)	30	35	35
gasification (high temperature and long residence time)	5	10	85

[a] Data taken from ref 25 with permission from Elsevier.

Several fast pyrolysis processes have been developed. Examples include the Tech-Air process,[12] Waterloo fast pyrolysis,[87] Ensyn rapid thermal pyrolysis,[88] Georgia Tech entrained flow pyrolysis,[89] NREL vortex ablative pyrolysis,[90] Pyrovac vacuum pyrolysis,[27,28,91-105] and Dynamotive's fluidized bed.[106] A fast pyrolysis process includes drying the feed to a water content of typically <10% (although up to 15% can be acceptable), to reduce the water content in the product oil (http://www.pyne.co.uk). The feed must be ground (to ∼2 mm, in the case of fluidized-bed reactors) to give sufficiently small particles to ensure rapid heat transfer and reaction (http://www.pyne.co.uk). After pyrolysis, the solids (char) must be separated and the vapors and aerosol are quenched. The liquid bio-oil then is collected. Free moisture in the biomass feed should not be removed entirely, because it assists in high heat transfer upon rapid conversion to steam. This assists in rupturing the biomass particle structure, thereby enhancing pyrolysis.

9.1. Heat-Transfer Requirements. High heat-transfer rates are required to heat the feed particles quickly. The heat required for pyrolysis is the total amount to provide all the sensible, radiation, and reaction heat for the process to proceed to completion. The heat of reaction for the fast pyrolysis process is marginally endothermic. It has been well-documented[19] that heat fluxes of 50 W/cm^2 are required to achieve true fast pyrolysis. The two important modes of heat transfer in fast pyrolysis are conduction and convection. Depending on the reactor configuration, each one can be optimized or a contribution from both can be achieved. In a circulating fluidized bed, the majority of the heat transfer is achieved from the hot circulating sand, typically at a sand-to-feed ratio of 20−25. This requires an effective sand reheating system. On the other hand, in a conventional fluidized bed, sand requires an external heat source, which can be obtained from char in an integrated system. Slow pyrolysis produces ∼30% liquid, ∼35% char, and ∼35% gas, whereas in fast pyrolysis, the liquid, char, and gas contents can be 75%, 12%, and 13% respectively.[91] The total heat required to obtain a bio-oil yield of 62% (including radiation and exhaust gas losses) is ∼2.5 MJ/kg of bio-oil produced[107] for a prepared feedstock. The net heat required from an external fuel source, such as natural gas, is only 1.0 MJ/kg of bio-oil produced. This applies when produced non-condensable gases are directly injected into the reactor burner. This represents approximately 5% of the total calorific value of the bio-oil being produced.[107]

11. 10. Bio-oil Production from Various Feedstocks

It is difficult to divide bio-oil feedstocks into different categories, because such classifications are dependent on the species, age, portion of the plant selected, and many other variables. We have selected some very general feedstock categories. Readers may compare the difference in bio-oil properties obtained from these different feedstock groups. These categories are bark, wood, agricultural wastes/residues, nuts and seeds, algae, grasses, forestry residues, cellulose and lignin, and miscellaneous.

10.1. Bio-oil from Bark. Bark is removed from wood in lumber manufacture and in many papermaking processes. Thus, bark is often available where wood is not prepared for the generation of secondary products, such as bio-oil. Furthermore, bark has different heat-transfer characteristics, different moisture contents, and, in most cases, a higher lignin content than the underlying wood. These differences must be considered when the fast pyrolysis of bark to bio-oil is undertaken. It is possible that the pyrolytic lignin fraction from various bark feeds may exhibit different properties than the pyrolytic lignin fraction from wood or other forms of plant biomass. It should be noted that wood and its bark are often copyrolyzed.

The development of the vacuum pyrolysis process was an important contribution that was made by Roy and co-workers[27,28,92-105] at Universite Laval, Canada. Vacuum pyrolysis is typically performed at a temperature of 450 °C, under a pressure of <20 kPa. This enables the production of very large quantities of pyrolysis oils and a charcoal product with specific properties. Solid wastes must be shredded and dried (via air drying, steam drying, or flue-gas drying) prior to pyrolysis, depending on the nature of the waste to be pyrolyzed. The solid wastes are first introduced into the reactor using a vacuum-feeding device. Wastes are then transported into the reactor in horizontal plates heated with molten salts. The heat is supplied by the noncondensable process gas, which is burned in place. The reactor temperature is maintained at 530 °C. Heating decomposes the feedstock into vapors that are rapidly removed by means of a vacuum pump. The vapors are condensed in towers, where the pyrolytic oils and the aqueous phase are recovered. The aqueous phase is then treated before being discarded. The solid residue (charcoal) is cooled and recovered. This group's recent contributions are further discussed in the subsequent paragraphs.

Roy and co-workers vacuum-pyrolyzed softwood bark and reported the properties of the bio-oil in different articles.[96-99] Various vacuum pyrolysis conditions were described.[94,95] TGA, differential scanning calorimetry (DSC), and rheological evaluations of the colloidal properties of softwood bark bio-oils were performed. The bio-oil was separated into top and bottom layers, and their storage stabilities were studied.[96] The upper layer represents ∼16 wt % of the total. The properties of the upper layer, bottom layer, and whole bio-oil are given in Table 12. Microstructures (e.g., waxy materials) were present in the bio-oil matrix and were, in part, responsible for the high viscosity and non-Newtonian behavior that is observed at <50 °C. Newtonian behavior was observed at temperatures above the melting point of these three-dimensional structures. Ba et al.[97] also characterized the water-soluble and water-insoluble fractions of the same oil. The generic composition was obtained by extracting water-insoluble materials (i.e., mostly the lignin-derived compounds). The yield of these lignin derivatives was 29 wt % The chemical composition of the water-soluble materials, as well as the molecular weight distribution of the water-insoluble components, was determined (see Tables 13 and 14).

Table 12. Physicochemical Properties of the Upper Layer, Bottom Layer, and the Whole Bio-oil from Softwood Bark Vacuum Pyrolysis[a]

	Value		
property	upper layer	bottom layer	whole bio-oil
water content (wt %)	3.5	14.6	13.0

density at 28 °C (kg/m^3)	1089	1222	1188
kinematic viscosity (cSt)			
at 50 °C	88	66	62
at 80 °C	14	11	11
at 90 °C	21	15	15
gross calorific value, anhydrous basis (M J/kg)	34.3	26.4	27.9
methanol insoluble materials, MTM (wt %)	1.30	0.6	0.7
solid content, CH_2Cl_2 insoluble (wt %)	0.28	0.58	0.55
Conradson carbon residue, CCR (wt %)	14.3	22.2	20.5
pH	3.03	2.98	3.00
acidity (NaOH g/100 g oil)	3.51	5.00	4.77
elemental analysis, anhydrous basis (wt %)			
C	74.1	61.3	62.3
H	8.5	6.5	7.00
N	0.3	0.6	1.1
S	0.05	0.07	0.07
ash	0.1	0.3	0.3
oxygen content (by difference)	17.0	31.3	29.0

[a] Data taken from ref 96 with permission from the American Chemical Society.

Table 13. Elemental Compositions of Bio-oil from the Vacuum Pyrolysis of Bark: Whole Bio-oil, the Water-Soluble Fraction, and Water-Insoluble Fraction[a]

sample	C	H	N	S + ash + O	C/H molar ratio

water-insoluble fraction, WIF	72.7	7.1	0.7	19.5	0.85
water-soluble fraction, WSF	51.7	6.3	1.2	40.8	0.68
whole bio-oil	62.6	7.0	1.1	29.3	0.74

[a] Data taken from ref 97 with permission from the American Chemical Society.

Table 14. Molecular Weight Distribution (MWD) of the Water-Insoluble Fraction (WIF) of Bio-oils from Vacuum Pyrolysis[a]

	Molecular Weight		
lignin	weight average, M_w	number average, M_n	polydispersity, M_w/M_n
WIF (softwood bark residues)	1163	577	2.0
Biomass Technology Group (BTG) (mixed softwood)	1317	592	2.2
MWL (spruce)	5720	3270	1.8

[a] Data taken from ref 97 with permission from the American Chemical Society.

The corrosion of aluminum, copper, and austenitic steel by bio-oil obtained via the vacuum pyrolysis of softwood bark residues was studied by using X-ray photoelectron spectroscopy (XPS) and Auger electron spectroscopy (AES).[98] The bio-oil was very acidic (the bottom layer was more acidic than the upper layer) and contained significant amounts of water. This caused extensive aluminum corrosion and a smaller degree of copper corrosion. The austenitic steel was not attacked. Chaala et al.[99] showed that vacuum-pyrolyzed bio-oil from softwood bark residues can be stored at 50 °C for 1 week without any significant increase in viscosity and solids content. However, the viscosity, solids content, and average molecular weight of the bio-oil increased considerably at 80 °C. The bio-oil's thermal stability was linked to the thermal stability of the bottom layer's compounds. The upper layer components were less thermally stable and exhibited a dramatic increase in viscosity during the first 65 days.

Roy and co-workers[27,28] also obtained bio-oil via the vacuum pyrolysis of softwood bark residues.[27] The vacuum pyrolysis condtions were the same as those previously discussed.[96-99] The alkali metal content, viscosity, solid content, heating value, surface tension, moisture content, and density of the bio-oil were investigated. The effect of methanol addition and/or a pyrolytic aqueous phase on the physicochemical properties of the bio-oils was also investigated. The pyrolytic aqueous phase is the sum of the water contained in the form of moisture in the feedstock plus the water formed during pyrolysis. This bio-oil appeared to be

valuable as a gas turbine fuel, because it has a relatively low Na/K/Ca content (21 ppm), a low viscosity (5.3 cSt at 90 °C), a high net heating value (32 MJ/kg, on an as-received basis), and a low solids content (0.34 wt %). The addition of methanol to the oil was beneficial. Adding the pyrolytic aqueous phase had no significant effect on the viscosity, but its "flowability" effect was beneficial for other properties. The addition of 10%−15% aqueous phase to the bio-oil seemed to be optimal.

The stability and aging of bark and vacuum-pyrolyzed bio-oil and mixtures thereof were further evaluated.[28] The samples were stored at 40, 50, and 80 °C for up to 168 h and at room temperature for up to one year, after which the phase-separation time, viscosity, solids and water contents, and average molecular weight were measured. The properties of the bio-oil were significantly altered when the bio-oil was heated at 80 °C for 168 h, but the changes after heating at 40 and 50 °C for 168 h were not critical. The molecular weight increase after heating the bio-oil for one week at 80 °C was equivalent to keeping the sample for one year at room temperature. The addition of an aqueous phase pyrolysate to the bio-oil lowered its thermal stability significantly. Rapid phase separation occurred at 80 °C. Therefore, researchers concluded that the total aqueous phase concentration in this oil should be limited to 15%. Aging of the raw bio-oil at room temperature resulted in a dramatic viscosity increase during the first 65 days, after which point a plateau was reached. The addition of methanol to the bio-oil improved its properties and increased its stability and that of its mixtures. Methanol dissolved some structural components of the bio-oil, reducing the rate at which the viscosity increased. Moreover, methanol delayed the phase separation of bio-oil/pyrolytic aqueous phase mixtures. The rate of heating and the pyrolysis temperature exert complex and interdependent effects on the products obtained.

Demirbas [108] determined the high-heating values (HHVs) of biochar (33.2 MJ/kg) and oils (34.6 MJ/kg) from the pyrolysis of beech trunk barks. The effects of both the heating rate and pyrolysis temperature on bio-oil and char yields and their characteristics were investigated. It is important that the heating rates indicated are "external" heating rates and not necessarily the heating rates within the particles. Temperatures of 277, 327, 377, 427, 477, and 527 °C were applied at heating rates of 2, 5, 10, 20, 40, and 100 °C/s. The oil yield increased from 24% to 27%, using a heating rate of 2 °C/s, and from 27% to 34% for a heating rate of 100 °C/s when the temperature is increased from 277 °C to 427 °C.

A maximum pyrolysis oil yield of 36% was obtained at 427 °C and a heating rate of 100 °C/s. However, by increasing the pyrolysis temperature from 427 °C to 527 °C, the bio-oil yield decreased to 32.6 wt % at a heating rate of 100 °C/s. The char yield decreased from 59% (at 277 °C) to 42% (at 527 °C) for a heating rate of 2 °C/s. Similarly, the char yield decreased from 43% to 29% going from 277 °C to 527 °C at a heating rate of for 100 °C/s. Clearly, the char yield decreased as the heating rates increased over the entire temperature range of 277 to 527 °C. Table 15 summarizes the pyrolysis oil yields from beech bark at different heating rates and temperatures, whereas Table 16 shows the char yields at these same heating rates and temperatures.

Table 15. Bio-oil Yield from Pyrolysis of Beech Trunkbarks, as a Function of Temperature and Heating Rates[a]

	Bio-oil Yield (wt %, daf basis)[b]					
temperature range (°C)	2 °C/s	5 °C/s	10 °C/s	20 °C/s	40 °C/s	100 °C/s

25−277	24.2	27.4	27.8	28.5	29.1	31.0
25−327	26.1	28.8	29.9	30.8	31.4	33.7
25−377	27.4	29.9	31.5	32.0	33.2	35.1
25−427	27.8	30.7	32.2	32.9	33.7	35.8
25−477	27.5	30.1	31.7	31.0	32.1	34.0
25−527	26.7	29.6	29.8	30.4	31.0	32.6

[a] Data taken from ref 108 with permission from Elsevier.[b] The term daf represents dry ash free basis.

Table 16. Char Yields from Beech Trunkbark Pyrolysis as a Function of Temperature and Heating Rate[a]

	Char Yield (wt %, daf basis)[b]					
temperature range (°C)	2 °C/s	5 °C/s	10 °C/s	20 °C/s	40 °C/s	100 °C/s
25−277	58.6	53.7	51.0	48.7	46.5	43.2
25−327	53.2	49.0	45.8	44.6	43.1	39.6
25−377	48.8	43.2	42.0	41.1	38.9	35.8
25−427	47.1	41.4	40.2	39.2	37.0	34.2
25−477	43.2	37.8	34.6	33.7	32.0	30.2
25−527	41.9	36.4	33.5	32.6	31.3	28.9

[a] Data taken from ref 108 with permission from Elsevier.[b] The term daf represents dry ash free.

10.2. Bio-oil from Wood. Beaumont[109] described the qualitative and quantitative compositions of the volatile portion of pyrolytic oil from the fast pyrolysis of beech wood. The pyrolytic oil contained more than 50 compounds. The products that formed were compared to the pyrolytic products from cellulose. This study indicated the origin of each product formed from the wood pyrolysis.

Fixed beds of 10-mm beech wood particles were slowly pyrolyzed[110] to a maximum temperature of 525 °C at rates of 3−10 °C/min by a flow of hot nitrogen. The mean gas velocity and residence times are provided in Table 17. The loss of mass versus time during decomposition was recorded. Also, the temperature field inside the beds was measured

continuously. The yields of char, tar, and gas were quantified. Higher temperatures led to an increased carbon content in the char fraction. This resulted in an increase in the calorific value of the char. The pyrolysis onset was observed at temperatures of ∼190 °C. From the temperature measurements inside the bed pores, exothermic reactions were observed to occur above 300 °C. From 300 ° to 400 °C, most of the mass loss occurred. At 500 °C, neither the product yields nor elemental compositions and calorific values differed greatly from the experiments at 400 °C. The time-resolved loss of mass in addition to the temperature distribution provides a useful tool for validating solid bed pyrolysis models.

Table 17. Mean Nitrogen Velocity in the Empty Tube, Resultant Gas Residence Time, and Mean Heating Rate of the Bed in the Test Facility at Various Temperatures[a]

temperature, T (°C)	mean gas velocity in the empty tube (m/s)	nitrogen residence time in the tube (s)	mean heating rate in the bed (K/min)
200	0.064	1.7	3
300	0.077	1.4	4.5
400	0.091	1.2	8.5
500	0.104	1.0	9.5

[a] Data taken from ref 110 with permission from Elsevier.

Branca and co-workers [111,112] studied the thermal behavior of bio-oils obtained from conventional pyrolysis (40-mm cylinders exposed to different radiative heat fluxes of 33−80 kW/m^2, corresponding to steady pyrolysis temperatures of 427−677 °C). These were compared to bio-oil formed by the updraft gasification of beech wood. Thermogravimetric curves in air showed two main reaction stages. The first (at ≤327 °C) involved the evaporation, formation, and release of gases and formation of secondary char (coke). At higher temperatures, heterogeneous combustion of secondary char occurred. A reliable procedure was developed to perform the first stage at a specified temperature. The temperature did not affect the weight loss dynamics and amount of secondary char significantly (∼20% of the liquid on a dry basis). The thermogravimetric curves were predicted well by a global mechanism that consisted of three parallel first-order reactions (with activation energies of 66, 32, and 36 kJ/mol).

Branca et al. [113] characterized the liquids generated from the low-temperature pyrolysis of wood by GC/MS. Conventional beech wood pyrolysis was conducted at a temperature of 327−627 °C, reproducing the conditions of interest in counter-current fixed-bed gasification. A wood layer was exposed to thermal radiation by means of a stainless steel mesh screen, whose sides were wrapped on two titanium rods (the uniform heated zone is ∼2.6 cm in the axial direction of the reactor). Aluminum supports connected the sample holder to a precision (0.1 mg) balance. A continuous nitrogen flow at ambient temperature (1×10^{-3} m^3/min, nominal velocity of 3.0 cm/s; residence time of 14 s) established an inert environment, reduced the residence time of vapors inside the reactor, and cooled both the gas-phase environment during pyrolysis and the solid residue after complete devolatilization. Liquid yields (water and tars) increase from ∼40% to ∼55% of dry wood mass with increasing

temperature. Approximately 90 product species were identified. GC/MS identification of 40 compounds from the pyrolysis liquid, corresponding to 40%−43% of the organic fraction (tars), demonstrated that this analysis reflects the combined thermal responses of holocellulose and lignin. The holocellulose leads to the formation of furans and carbohydrates, whereas the lignin generates phenolics. The high number of liquid compounds quantified represents a significant advance in the current state of the art. This analytical approach can be used to improve reactor development/optimization and to formulate detailed reaction mechanisms. Syringols and guaiacols, originating from primary degradation of lignin, reach their maximum levels in the bio-oils during pyrolyses at ∼477−527 °C. In contrast, secondary degradations continuously increase production of phenols with increasing temperature. Conventional pyrolysis and fast pyrolysis exhibit enhanced levoglucosan and hydroxyacetaldehyde formation at faster heating rates with lower yields of carboxylic acids.

Both stepwise and one-step vacuum pyrolyses of birch-derived biomass (birch bark and birch sapwood) were conducted by Murwanashyaka et al.,[92] to monitor the evolution of phenols. The feedstock was shredded to fibrous particles with the longest dimension ranging between 5 mm and 20 mm. Before pyrolysis, the sample was split into two parts. One portion was pyrolyzed in one step and the second was pyrolyzed in stepwise modes under a 0.7 kPa vacuum. Dry ice in limonene condensers were used to trap the pyrolysis vapors at −72 °C. A stepwise pyrolysis of the birch feed was performed by increaing the temperature from 25 °C to 550 °C. After heating to a selected temperature and holding for 1 h, the reactor was cooled to room temperature and kept under nitrogen until the next step. Before each subsequent temperature step, the liquids formed in the previous step were collected. The residual solids were weighed and placed back into the reactor for further pyrolysis. Table 18 lists the different pyrolysis steps and product yields obtained.

Table 18. Product Yields from the Stepwise Pyrolysis of Birch (Birch Bark and Birch Sapwood), as a Function of Increasing Temperature[a]

	Yield (wt %, Anhydrous Feed Basis)				
stepwise pyrolysis (°C)	solid residue	pyrolysis oil	gas	water	phenols
1. 25−200	93.96	6.02	0.02	5.91	0.00
2. 200−275	70.46	18.14	5.36	6.19	0.40
3. 275−350	37.85	27.28	5.33	6.95	2.18
4. 350−450	25.67	9.47	2.71	0.70	1.83
5. 450−550	23.25	1.48	0.94	0.41	0.01
cumulative (steps 1−5)	25.25	62.39	14.36	20.16	4.42
one-step, 25−500	24.79	63.43	11.78	19.79	2.51

[a] Data taken from refs 92 and 93 with permission from Elsevier.

The stepwise thermal decompositions of birch bark and birch sapwood under vacuum at low temperatures were less destructive.[92] The evolution of pyrolysis oil and phenols during the stepwise vacuum pyrolysis of a mixture of birch sapwood and birch bark followed a similar trend. The most active zone was observed to be within the range of 275−350 °C. Guaiacol derivatives result at low temperatures, followed by syringol derivatives. Their transformation to pyrocatechols occurs at high temperatures. The evolution of phenols was determined to occur in the following order: methylguaiacol, ethylguaiacol, guaiacol, propenylsyringol, phenol, and catechol. The maximum rate of evolution was observed at 275−350 °C. Phenols were converted sequentially into catechols by demethylation of the methoxy groups at 350−450 °C. The pyrolysis is almost complete at 450 °C. The total phenolic yields obtained by stepwise and one-step pyrolysis were 4.43 and 2.51 wt %, respectively, on an anhydrous feed basis.

Murwanashyaka et al.[93] also conducted a vacuum pyrolysis on 116 kg of a mixture of birch bark (*Betula papyrifere*) (ca. 46%) and birch sapwood (ca. 54%). Syringol was separated from the pyrolytic oil. The total pressure inside the reactor was <3 kPa, the final temperature was 500 °C, and the heating rate was 100 °C/min. The pyrolysis was held at a temperature of 500 °C for at least 30 min. The pyrolytic oil obtained was stored at 4 °C to prevent aging. The products yields included 53.9% condensates (i.e., 45.9% anhydrous pyrolysis oil and 8% of miscible reaction water), 24.0% gas, and 22.1% wood charcoal (on a weight-percent feedstock moisture-free basis). The mass balance accounted for 96.8% of the feed. Steam distillation of the oil recovered the phenols at various steam/pyrolysis oil ratios. A volatile fraction (14.9 wt %, based on the total feed oil) was recovered at a steam:oil ratio of 27. The distillate analyzed by GC/MS after acetylation contained 21.3 wt % of phenolic compounds. The distillate was then vacuum-distilled at 0.7 kPa. Sixteen sub-fractions were recovered. The steam-distilled fractions were observed to be chemically and thermally stable, when subjected to further purification. The 2,6-dimethoxyphenol (syringol)-rich fraction was separated and purified. Syringol was obtained in a purity of 92.3 wt %.

Amen-Chen et al.[105] isolated phenol, cresols, guaiacol, 4-methylguaiacol, catechol, and syringol from Eucalyptus wood pyrolysis tar. The approach included a primary conversion of the raw wood tar into lighter oil. Phenolic compounds were further separated from the oil by liquid−liquid extraction, using aqueous alkali and organic solvents. GC/MS analysis of acetyl-derivatized phenolic compounds was used to evaluate the separation method. The primary conversion allowed the isolation of lighter oil without causing major chemical changes in the original wood tar. Liquid−liquid extraction by alkali and organic solvents produced a phenolic fraction. Removal of phenols was efficient under highly alkaline conditions.

Few papers have discussed pyrolysis under irregular heating rates. Demirbas[55] pyrolyzed beech wood in the absence of oxygen in a stainless steel horizontal cylindrical reactor inserted vertically into an electrically heated furnace. Irregular heating rates were used from 25 °C to 502 °C. The average heating rate was higher than 6 °C/s from 60 s to 90 s for three samples with particle sizes of <0.063 mm, 0.060 mm, and >0.150 mm. The average temperature increase was low, from 170 s to 350 s. The temperature increase was highly regular, in periods of 450−600 s. The time to complete pyrolysis decreased when the particle size increased from <0.063 mm to >0.150 mm and then increased as the particle size increased. The completion time was lower (445 s) at 397 °C for >0.150 mm particle size. Important variables affecting the yield are the biomass species, chemical and structural

composition of the biomass, particle size, temperature, heating rate, atmosphere, pressure, and reactor configuration.

Şensöz and Can[114,115] pyrolyzed bark-free Turkish red pine (*Pinus brutiaTen*.) chips in a laboratory-scale fixed-bed reactor. Pyrolyses were performed at temperatures of 300−550 °C with slow heating rates of 7 and 40 °C/min. The sweep gas (N_2) flow rates were 50, 100, 200, and 300 cm^3/min. The char, gas, and liquid yields obtained were in the ranges of 23−36 wt %, 11−23 wt %, and 21−30 wt %, respectively. The highest liquid yield was obtained at 500 °C and a heating rate of 40 °C/min. Chemical fractionation showed that the oxygenated and polar fractions dominated. The empirical formula of bio-oils obtained in a static pyrolysis atmosphere and in a nitrogen atmosphere are $CH_{1.32}O_{0.54}N_{0.0014}$ and $CH_{1.38}O_{0.37}N_{0.002}$, respectively. Oil heating values from pyrolyses at 300 and 500 °C varied from 23.1 MJ/kg to 25.4 MJ/kg. The H/C and O/C molar ratios were 1.38 and 0.37, respectively.

Guerrero et al.[116] reported eucalyptus pyrolysis at 600−900 °C in a fixed-bed reactor at a low heating rate (LHR) (∼10 °C/min). A fluidized-bed reactor was also used at 800 and 900 °C to prepare chars at a high heating rate (HHR). The elemental composition, pore volume, and surface area of the chars were also determined. The surface area was determined via CO_2 adsorption at 0 °C, using the Dubinin−Radushkevich method. Scanning electron microscopy (SEM) analysis of the chars probed the differences in the macroscopic morphology obtained using LHR versus HHR. Various properties are given in Table 19.

Table 19. Char Yields, Elemental Compositions, Surface Areas, Micropore Volumes, and N, C, and H Yields (Relative to the Amount of Eucalyptus Sample) of Chars Obtained at Low (LHR) and High (HHR) Heating Rates[a]

	LHR Char				HHR Char	
property	600 °C	700 °C	800 °C	900 °C	800 °C	900 °C
char yield (wt %, db[b])	24.0	22.9	21.8	21.4	18.5	18.3
C	87.4	87.99	88.23	89.54	81.85	81.22
H	1.22	0.87	0.71	0.52	1.55	1.25
N	0.52	0.62	0.74	0.95	0.55	0.64
O	11.0	10.52	10.32	8.99	16.05	16.89
surface area[c] (m^2/g)	570	588	589	362	528	539
micropore volume (mm^3/g)	218	224	225	138	202	206
nitrogen yield (%)	44.6	50.7	57.6	72.6	36.4	41.8
carbon yield (%)	43.1	41.4	39.5	39.4	31.1	30.6

hydrogen yield (%)	4.8	3.2	2.5	1.8	4.7	3.7

[a] Data taken from ref 116 with permission from Elsevier. [b] Dry basis. [c] Surface areas were measured from the CO_2 adsorption isotherm at 0 °C, using the Dubinin−Radushkevich method.

Commercial wood pellets are increasingly used for residential heating in Sweden. Therefore, the oxidative pyrolysis of integral softwood pellets was studied by Olsson et al. [117] The major primary semivolatile compounds released during flame burning were six lignin-derived 2-methoxyphenols with antioxidant properties and 1,6-anhydroglucose from cellulose.

The combustion behavior of bio-oils derived from wood fast pyrolysis technologies (BTG, Dynamotive, Ensyn, Pyrovac) has been investigated by measuring weight-loss curves in air under controlled thermal conditions.[112] Two separate sets of experiments were performed: (1) devolatilization (evaporation and cracking reactions) at 327 °C with the formation of secondary char, and (2) heterogeneous combustion of secondary char at 600 °C. A heating rate of 5 °C/min was applied. Heating only to 327 °C caused evaporation/cracking of the oil and secondary char formation. The process involved swelling and solidification. After the char was collected and milled, a second set of heterogeneous combustion experiments was performed on the secondary char, to temperatures of 600 °C. Although the details of the rate curves are dependent on which commercial process (BTG, Dynamotive, Ensyn, Pyrovac) was applied to produce the oil, the same general features are always observed. Secondary char formation and sample modification begin at 187−217 °C. The secondary char exhibits weight-loss curves from a thermal gas evolution (devolatilization) stage and a combustion stage occurs similar to that of primary char produced during wood fast pyrolysis. Secondary char has a lower reactivity, because it completely lacks micropore networks.

Luo et al. [118] conducted the fast pyrolysis of wood feedstocks such as *Pterocarpus indicus*, *Cunninghamia lanceolata*, and *Fraxinus mandshurica* and rice straw in a fluidized-bed reactor (at a maximum feed rate of 3 kg/h) with an inert atmosphere. The 80-mm-diameter reactor had a height that varied over a range of 700−1200 mm. The reaction temperature varied over a range of 500−700 °C. The nitrogen flow for fluidizing the sand bed was in the range of 3−6 Nm^3/h. Bio-oil production was greatest at 500 °C. Using the yield, heating value, and low water content as evaluation criteria, *Pterocarpus indicus* produced the best bio-oil, followed by *Cunninghamia lanceolata* and *Fraximus mandshurica*. Rice straw was the worst (see Table 20). This was mainly due to the higher water and ash content in the rice straw.

Table 20. Bio-oil Yields Obtained[a] at 550 °C from Pyrolysis of *Pterocarpus indicus*, *Cunninghamia lanceolata*, and *Fraxinus mandshurica* and Rice Straw with a Maximum Feed Rate of 3 kg/h

biomass species	particle size (μm)	bio-oil yield (%)	heating value (kJ/kg)	water in bio-oil[b] (%)
F. mandshurica	74−154	40.2	22 000	39.6

C. lanceolata	74−154	53.9	19 000	31.4
P. indicus	250−355	55.7	19 000	24.6
rice straw	154−250	33.7	19 000	53.5

[a] Data taken from ref 118 with permission from Elsevier.[b] Water in bio-oil determined using the Karl−Fischer method.

Pakdel and Roy[100,101] reported the large-scale vacuum thermochemical conversion of several common wood species. Various conditions for vacuum pyrolysis have been described by Garcia-Perez et al.[94,95] The separation and quantitative analysis of steroids were studied and steroid distributions in softwood and hardwood species were compared. Fifty steroids were identified with significant abundances. Most of the compounds detected had not been identified earlier in biomass-derived vacuum pyrolysis oils and rarely reported in plants. Steroid concentrations were observed to be higher in softwoods than hardwoods. Steroids were present in trace amounts in tropical woods.

Paris et al.[119] investigated the pyrolysis of spruce and pine softwood in the temperature range of 25−1400 °C. The wood sections were sandwiched between two alumina plates, to prevent warping, and placed in a Heraeus furnace that was equipped with a quartz tube that was continuously flushed with nitrogen to ensure a non-oxidizing atmosphere. A 2°C/min heating rate and the use of thin wood sections allow full preservation of the original cellular wood structure without the formation of cracks. Thermal degradation of the wood biopolymers and the evolution of the carbonaceous material's molecular and mesoscopic structure was studied by wide-angle X-ray scattering, small-angle X-ray scattering, and Raman spectroscopy. Formation of an isotropic and almost structureless material occurs in a clear transition region between 307 °C and 347 °C. Here, the cellulose microfibril crystal structure is completely degraded. The scattering contrast, based on the density difference between cellulose microfibrils and polyoses/lignin, has fully disappeared. After this decomposition of the wood's nanocomposite structure, charring commences. Aromatic structures form and a strongly increasing scattering signal, at small angles, confirms the formation and growth of nanopores. Developing graphene sheets show a slightly preferred orientation, with respect to the oriented cellular structure of the wood. The unique cellulose microfibril orientation in the native wood cell wall might affect the carbonaceous material.

Stamatov et al.[120] derived bio-oil via slow pyrolysis process of two indigenous Australian tree species: red gum (*Eucalyptus camaldulensis*) from the Murray basin in Victoria, and blue gum (*Eucalyptus* globulus) from the region of Mount Gambier, South Australia. The bio-oil was blended with ethanol and burned in a circular jet spray at atmospheric pressure. Bio-oil flames were shorter, wider, and brighter than diesel fuel flames under the same conditions. Adding flammable polar additives (e.g., ethanol) to bio-oil improved some of the undesired properties of the fuel such as poor atomization, low calorific value, and high NO_x emission from the flame.

Diebold and Czernik[121] studied the fast pyrolysis of hybrid poplar in the vortex reactor (high heat transfer rate, moderate temperature (450−550 °C), and a short (<1 s) vapor residence time in the reactor) at the National Renewable Energy Laboratory (NREL). Vapor generation was followed immediately by hot gas filtration. The properties are listed in Table 21.

Additives to reduce and stabilize the viscosity during storage were also studied.[121] Additives were selected on the basis of their cost and their potential to shed light on the relative importance of the several types of chemical reactions thought to contribute to aging. These reactions include esterification, transesterification, phenol/aldehyde condensation, aldol condensation, and etherification. Methanol and water were added in varying amounts to the pyrolysis bio-oils as part of an extensive evaluation of these two additives. Ethanol, acetone, methyl isobutyl ketone, and the methyl ester of soybean oil were also chosen as additives. These represent three chemical families that all demonstrated the ability to drastically reduce the aging rate of biocrude. The additives reduced the initial viscosity at 40 °C by half and also reduced the aging rate (viscosity increase) of hybrid poplar hot-gas-filtered pyrolysis oil by factors of 1:18, compared to original pure oil. Methanol was the best additive at 10 wt % of the pyrolysis oil. This methanol-modified biocrude was still a single-phase liquid and it met the ASTM No. 4 diesel fuel specification for viscosity, even after 96 h of exposure at 90 °C.

Table 21. Properties of the Bio-oil Produced by Fast Pyrolysis from Hybrid Poplar in the NREL (Run 175) Vortex Reactor[a]

	Value	
property	pyrolysis oil, dry basis	pyrolysis oil, wet basis
empirical formula	$CH_{1.3}O_{0.47}$	$CH_{1.3}O_{0.47} + 0.27H_2O$
analysis		
C	57.3 wt %	46.5 wt %
H	6.3 wt %	7.2 wt %
O	36.2 wt %	46.1 wt %
S	0.02 wt %	0.02 wt %
N	0.18 wt %	0.15 wt %
ash	<0.01 wt %	<0.01 wt %
moisture	0 wt %	18.9 wt %
high heating value, HHV	22.3 MJ/kg	18.7 MJ/kg
low heating value, LHV	21.2 MJ/kg	17.4 MJ/kg
specific gravity	∼1.25	∼1.15−1.2
flash point		64 °C

potassium content	2.7 ppm
sodium content	7.2 ppm
calcium content	2.2 ppm
chlorine content	7.9 ppm
aluminum content	2.6 ppm
titanium content	<0.2 ppm
vanadium content	0.002 ppm
manganese content	0.063 ppm

[a] Data taken from ref 121 with permission from the American Chemical Society.

Elliott[122] studied pyrolysis oils obtained from three sources: a hardwood (oak), a softwood (southern pine), and a high-growth-rate herbaceous biomass (switch grass). All the bio-oils were produced at ∼520 °C in a residence time of <1 s in the Vortex flash pyrolysis reactor at the NREL in Golden, CO, using a feed particle size of 105−250 μm. The bio-oils were analyzed and compared with others reported in the literature. The inorganic components include the alkali metals, which are distributed throughout the oil, in both the homogeneous oil phase and the char.

Nilson et al.[123] pyrolyzed small (15−150 mg) samples from eight different birch (Betula) species at 550 °C and analyzed the products using GC, direct injection with GC/FTIR/FID (where FID denotes flame ionization detection), and preconcentration with GC/MS. Aldehydes, acids, ketones, substituted furans, and methoxylated phenols were formed. The chromatograms were similar for all eight wood species, both with direct injection and preconcentration. Larger amounts of products were formed in the molecular-weight range of 60−130 from birch wood than in similar studies on pine and spruces. Conifer pyrolysis oils had more peaks, with a molecular weight above 200 amu. A thermogravimatric study of the pyrolysis of three different types of wood (viz., forest wood, old furniture, and used pallets) using dynamic and isothermal techniques was reported.[124] Both dynamic and isothermal pyrolyses were performed. Isothermal runs were conducted at two different temperatures. The low-temperature range (225−325 °C) was chosen, where the main degradation processes of pyrolysis occur. The remaining residue pyrolyzed in the range of 700−900 °C. Five different heating rates were used in the dynamic experiments (2, 20, 35, 50, and 100 °C/min), to observe their influence on the thermal decomposition. The kinetic parameters obtained from both dynamic and isothermal techniques agreed closely.

10.3. Bio-oil from Agricultural Wastes/Residues. Pyrolysis of agricultural residues, such as olive husks, corncobs, and tea waste, at high temperature (677−977 °C) in a cylindrical batch reactor was studied by Demirbas.[17] When the pyrolysis temperature was increased, the bio-char yield decreased. The bio-char yield increased as the sample particle size increased. The use of higher temperatures and smaller particles increases the heating rate, resulting in

decreased bio-char yields. The higher lignin content in olive husks results in a higher bio-char yield, compared to that from corncobs.

The effect of temperature and particle size on bio-char yield from the pyrolysis of agricultural residues (wheat straw, corncobs, corn stover, tobacco stalks, tobacco leaves, olive wastes, walnut shells, and almond shells) was studied at 800−1000 °C and a heating rate of 10 °C/s in a free-fall reactor.[17] When the temperature was increased, the char yield decreased. The char yield increased as the particle size increased. A high temperature and smaller particles increased the heating rate, resulting in lower char yields. The higher lignin content in olive husk resulted in a higher char yield than corncobs. Char from olive husks was more reactive in gasification than bio-char from corncob because of the higher ash content.

Putun et al. [125] studied the pyrolysis of cotton stalks in a Heinze-type reactor in both a static atmosphere and with nitrogen as the carrier gas. The 400-cm^3 (70-mm inner diameter (id)) stainless steel Heinze retort was heated externally by an electric furnace. Various temperatures (400−700 °C), particle sizes (0.25−1.8 mm), and nitrogen gas flow rates (50−400 cm^3/min) were studied. Particle size and nitrogen flow rate did not exert significant influence on the pyrolysis, whereas temperature was significant. At the slow heating rate (7 °C/min) employed in all reactions, each particle has time to heat to about the same temperature in the pyrolytic temperature range. The liquid products and their pentane-soluble subfractions were characterized by elemental analysis, FT-IR spectroscopy and ^{1}H NMR spectroscopy. The pentane subfraction was also analyzed by GC. Char was characterized by elemental composition, surface area, and FT-IR spectroscopy. The H/C and O/C ratios of the chars decreased as the pyrolysis temperature increased. FT-IR-confirmed hydroxyl and carbonyl functionalities were lost at high temperatures. Putun[16] further reported the fast pyrolysis of cotton straw and stalk in a fixed tubular reactor. Pyrolysis temperature, heating rate, and sweep gas atmosphere were examined. The highest yield 39.5% was obtained at 550 °C, with a heating rate of 550 °C/min. The pyrolysis oil and the pentane-soluble subfractions were characterized by elemental analysis, GC, infrared (IR), and ^{1}H NMR spectroscopy. The product analysis can be compared to that obtained at a much slower (7 °C/min) heating rate.[125]

Rice straw pyrolyses were also reported [126] in a stainless steel fixed-bed Heinze reactor (350 mL). Ten-gram samples of rice straw were heated at a slow rate (5 °C/min). The temperature, particle size, sweep gas flow rate, and steam velocity were studied. The highest bio-oil yield of 27.3%, achieved at 400−900 °C, was obtained at 550 °C. Liquid products obtained from pyrolysis, inert atmosphere pyrolysis, and steam pyrolysis were then fractionated into asphaltanes and maltanes. The aliphatic subfractions obtained by column chromatography were then analyzed by GC/MS. Further structural analyses of the pyrolysis oils and aliphatic subfractions were conducted, using ^{1}H NMR and FT-IR spectroscopy. ^{1}H NMR and FT-IR spectra were obtained from the bio-oil samples produced under normal, nitrogen, and steam atmospheres. Larger proportions of aliphatic structural units exist in the bio-oil from steam pyrolysis. The O−H stretching vibrations between 3150 and 3400 cm^{-1} indicated the presence of phenols and alcohols. No peaks exist between these wavenumbers for the aliphatic subfractions. This indicated that aliphatic subfractions did not contain oxygenated compounds like the whole bio-oils did.

The effects of temperature, particle size, heating rate, and nitrogen flow rate on the product yields and compositions of sesame stalk pyrolysis were studied in a fixed-bed reactor[127] (8 mm id × 90 cm height). Temperatures of 400−700 °C, particle sizes (diameters) of 0.224−1.8 mm, heating rates of 100−700 °C/min, and nitrogen flow rates of 50−800 cm^3/min were used.

The maximum oil yield was 37.2 wt %, which was obtained at 550 °C, a heating rate of 500 °C/min, and a nitrogen flow rate of 200 cm^3/min. Bio-oil yields were unchanged for the four particle-size ranges that were studied: 0.224 mm < d_P < 0.425 mm, 0.425 mm < d_P <0.85 mm, 0.85 mm < d_P <1.25 mm, or 1.25 mm < d_P <1.8 mm. Liquid column chromatography was used to fractionate the pyrolysis oils to chemical class compositions. Oil was separated on a 0.2 m × 0.025 m activated silica gel (70−230 mesh) column pretreated at 170 °C for 6 h, by successive elution with *n*-pentane, toluene, and methanol. Aliphatic, aromatic, and polar fractions were produced. After solvent removal and weighing, the residues were subjected to elemental, IR, and GC analyses. Subfractions of oil were analyzed by elemental analysis and IR spectroscopy (Table 22), and the *n*-pentane subfraction was analyzed by GC to determine hydrocarbon distribution. The sesame stalk bio-oil could be used as a potential renewable fuel source, based on its chemical composition(62% carbon, 8% hydrogen, 0.98% nitrogen, and 29% oxygen; H/C molar ratio = 1.55 and O/C molar ratio = 0.36; calorific value = 27 MJ/kg). The aromatic protons account for 7% of all protons in this bio-oil. Specifically, the methylene protons and protons α to an aromatic ring dominate, constituting 31% of the total protons present. Naphthenic protons and β-CH_3, CH_2, and CHγ or further from an aromatic ring protons of the oil were observed only at levels of 10.2% and 12.0%, respectively. CH_3 protons located at the γ-position or further from an aromatic ring were observed. Finally, the H/C ratio of the *n*-pentane fraction (2.12) is almost the same as that of gasoline.

Table 22. ^{1}H NMR Determination of the Hydrogen Distribution in Sesame Stalk Pyrolysis Oil[a]

type of hydrogen	chemical shift (ppm)	oil content (% of total hydrogen)
aromatic	6.5−9.0	7.7
phenolic(OH) or olefinic protons	5.0−6.5	2.8
ring-joined methylene (Ar−CH_2−Ar)	3.3−4.5	31.0
CH_3, CH_2, and CH α to one aromatic ring (benzylic)	2.0−3.3	31.0
CH_2, and CH β to an aromatic ring (naphtenic)	1.6−2.0	10.2
β-CH_3, CH_2, and CH γ or further from an aromatic ring	1.0−1.6	12.0
CH_3γ or further from an aromatic ring	0.5−1.0	5.3

[a] Data taken from ref 127 with permission from Elsevier.

Şensoz et al.[128] studied the pyrolysis of olive bagasse (*Olea europeaL.*) in a fixed-bed reactor at 350−550 °C with heating rates of 10 and 50 °C/min, particle sizes of 0.224−1.8 mm, and sweep gas flow rates of 50−200 cm^3/min. The bio-oil yield was greatest at 500 °C, where a heating value of 31.8 MJ/kg was observed. An empirical formula of $CH_{1.65}O_{0.25}N_{0.03}$ was

established. Şensoz et al.[129] studied the pyrolysis of *Brassica napus L*. in a Heinze reactor under a static atmosphere at 500 °C and a heating rate of 40 °C/min. The oil and char yields were largely independent of particle size, with maximum yields of ca. 46 wt % in the particle size range of 0.85−1.8 mm.

Pütün et al.[130] pyrolyzed hazelnut shells in a fixed-bed tubular reactor. The effects of pyrolysis temperature and a N_2 atmosphere on pyrolysis yields and bio-oil chemical composition were investigated. A maximum bio-oil yield (23.1 wt %) was obtained under nitrogen at 500 °C and a heating rate of 7 K/min. The pyrolysis products were characterized by elemental analysis, high-performance size exclusion chromatography (HPSEC), GC, GC/MS, FT-IR, and ^{1}H NMR. Bio-oil was also fractionated to pentane-soluble and pentane-insoluble compounds (asphaltenes). The pentane-soluble fraction was then fractionated to pentane, toluene, ether, and methanol subfractions, using column chromatography. The aliphatic and low-molecular-weight aromatic subfractions of the bio-oil were analyzed by capillary column GC and GC/MS analyses. Further structural analysis of hazelnut shell bio-oil and its aromatic and polar subfractions by FT-IR and ^{1}H NMR spectra were obtained.[130] The ^{1}H NMR spectra of the bio-oil and its toluene, ether, and methanol subfractions are summarized in Table 23. The aromaticity of the unfractionated bio-oil was lower than that of its toluene subfraction (6.2% versus 12.3%). High-molecular-weight polycyclic compounds and phenolic OH groups can be observed in the ^{1}H NMR spectra of the polar methanol subfraction from the hazelnut shell bio-oil was quite similar to the crude oil and shale oil.

Table 23. ^{1}H NMR Spectra of Hazelnut Shell Bio-oil and Its Subfractions (Toluene, Ether, Methanol) from Fixed-Bed Pyrolysis Expressed as the Percentage of Total Hydrogen Determined by Area Integration[130]

		Percentage of Total Hydrogen (%)			
type of hydrogen	chemical shift (ppm)	bio-oil (total)	toluene subfraction	ether subfraction	methanol subfraction
aromatic	6.5−9.0	6.45	12.25	19.58	17.78
phenolic(OH) or olefinic proton	5.0−6.5	1.59		1.19	45.19
ring-join methylene (Ar−CH_2−Ar)	3.3−4.5	33.90		34.90	
CH_3, CH_2 and CH α to an aromatic ring	2.0−3.3	23.0		12.31	
CH_2, and CH to an α ring(naphtenic)	1.6−2.0	25.57			

β-CH_3, CH_2 and CH γ or further from an aromatic ring	1.0−1.6	7.22	73.47	27.19	29.63
CH_3 γ or further from an aromatic ring	0.5−1.0	1.81	14.29	4.84	7.41

[a] Data taken from ref 130 with permission from Elsevier.

Mass transfer limitations on product yields were determined by Kockar et al.[131] during the fixed-bed pyrolysis of hazelnut shells. Two different pyrolysis reactors (viz., a fixed-bed Heinze reactor and a well-swept fixed-bed tubular retort) were used and the oils were characterized. The effects of heating rate, pyrolysis temperature, particle size, and sweep gas velocity on both the pyrolysis yields and chemical compositions were investigated. The maximum oil yield via a slower pyrolysis (at a heating rate of 7 °C/min) in the Heinze reactor was 22.5% under flowing nitrogen using a feed particle size of 0.85 mm < d_P < 1.8 mm at 550 °C. The maximum fast pyrolysis oil yield (34%) was obtained at a heating rate of 300 °C/min in fixed-bed tubular reactor.

Garcia-Perez et al.[94] pyrolyzed sugarcane bagasse at bench and pilot scales. Sugarcane bagasse samples (80 g; 6 wt % moisture) were pyrolyzed in a cylindrical stainless steel retort that was placed in a Lindberg three-zone vertical electric furnace. The temperature was increased at a rate of 12 °C/min to 500 °C. The total pressure was maintained below 8 kPa throughout the test. Vapors were rapidly pumped from the reactor through the biomass bed (250 mm in height). The organic vapors and steam were condensed in three traps, which were connected in series and maintained at −30, −78, and −78 °C, respectively. A large-scale pyrolysis test was performed in a pilot-plant reactor, where air-dried bagasse (20 kg; 8 wt % moisture) was placed in four pans and introduced into a cylindrical horizontal reactor 3 m long and 0.6 m in diameter. The bagasse bed height was 140 mm. The sample was heated at a slow rate (over a period of 200 min) until the feed attained a temperature of 530 °C. The pilot reactor was operated in batch mode at 530 °C for 1 h. The solid residue was cooled to room temperature under a flow of nitrogen. The average total pressure during the pyrolysis was ∼12 kPa. Four traps that were maintained at 25, 0, −30, and −80 °C were used as a condensation train.

Laboratory-scale vacuum pyrolysis of sugarcane bagasse yielded more oil (34.4% versus 30.1%)[94] and less charcoal (19.4 wt % versus 25.7 wt %) than pilot-scale runs. The bio-oil seemed to be valuable as a liquid fuel, because it had a low ash content (0.05 wt %), a relatively low viscosity (4.1 cSt at 90 °C), a high calorific value (22.4 MJ/kg), and a low methanol-insoluble content (0.4 wt %). Accelerated aging of this bio-oil at 80 °C indicated that its thermal instability was similar to that of oils obtained from other biomass sources. Table 24 lists the product yields for laboratory-scale tests versus pilot-scale tests. This group further compared the physicochemical properties of the bagasse bio-oil with those of other bio-oils, as given in Table 25. The bagasse bio-oil has low moisture content, viscosity, and acidity, as well as high calorific values, when compared to a variety of other bio-oils.

Table 24. Evaluation of Product Yields Obtained from Laboratory-Scale versus Pilot-Scale Pyrolysis of Sugar Cane Bagasse[a]

	Product Yield (wt %)[b]	
property	laboratory scale	pilot-plant scale
liquid organic compounds	43.2 ± 2.9	31.0
pyrolytic water	18.8 ± 2.5	20.3
gas	17.6 ± 2.2	22.0
charcoal	19.4 ± 1.2	25.6
losses	1.0 ± 0.5	1.1
total	100	100

[a] Data taken from ref 94 with permission from Elsevier. [b] Value given on a weight-percent bagasse (anhydrous) basis.

Table 25. Evaluation of Physicochemical Properties of Bagasse Bio-oil versus Bio-oils from Other Feedstocks[a]

property	bagasse bio-oil	other bio-oils
moisture (wt %)	13.8	10.2−35
density (kg/m^3)		
at 20 °C	1211	1208−1238
at 40 °C	1195	1190−1211
at 60 °C	1180	1171−1197
at 80 °C	1160	
kinematic viscosity (cSt)		
at 20 °C	116.5	50−672
at 40 °C	26.7	35−53
at 50 °C	16.4	9−137
at 60 °C	11.2	

at 70 °C	8.2	
at 80 °C	5.4	11
at 90 °C	4.1	
flash point (°C)	>90	64 to >106
gross calorific value (MJ/kg, as-received basis)	22.4	15−24.3
elemental composition (wt %, anhydrous basis)		
C	54.60	48.0−63.5
H	6.45	5.2−7.2
N	0.73	0.07−0.39
S	<0.10	0.00−0.05
O	38.07	32−46
ash	0.05	0.03−0.3
solids content, as methanol-insoluble material (wt %)	0.38	0.17−1.14
Conradson carbon residue (wt %)	18.6	18−23
acidity (g NaOH/100 g oil)	8.2	
pH	2.7	2.0−3.8

[a] Data taken from ref 94 with permission from Elsevier.

Garcia-Perez et al.[95] reported the simultaneous vacuum pyrolysis of sugarcane bagasse combined with petroleum residue (PR). Bagasse, PR, and their mixtures were pyrolyzed in a cylindrical stainless steel retort that was placed in a Lindberg three-zone vertical electric furnace. The average heating rate was slow (12 °C/min, from 25 °C to 500 °C). The sample (80 g) was held at 500 °C for 1 h at a pressure of 8 kPa. Vapors were rapidly pumped out of the reactor and condensed in three traps that were connected in series at −30, −78, and −78 °C, respectively. Noncondensable gases were evacuated and stored in a stainless steel vessel at room temperature. Important synergetic effects leading to increased charcoal yields were observed. Maximum charcoal and minimum oil yields were obtained when 15 wt % PR was mixed with bagasse. At this concentration, sugarcane bagasse charcoal is almost completely covered with PR-derived pyrolytic carbon. At concentrations greater than 15 wt % PR, hydrocarbon vapors interacted less with the bagasse charcoal. Consequently, an appreciable

increase in oil yield was observed. These oils were complex emulsions that consisted of oxygenated compounds (originating from bagasse) and hydrocarbons (originating from PR and water). Oils obtained from feedstocks with up to 15 wt % PR were stable emulsions that consisted of PR-derived products in bagasse-derived oil. The oil obtained from a 30-wt % PR−bagasse blend was an unstable emulsion. However, the emulsion obtained at 50 wt % PR was stable and the PR-derived oil constituted the continuous phase. This emulsion exhibited a Conradson carbon residue (CCR) value (9 wt %) similar to that of PR-derived oil.

Drummond and Drummond[132] performed the fast pyrolysis of sugarcane bagasse in a wire-mesh reactor. In this reactor, pyrolysis tars were rapidly swept from the hot zone of this reactor and quenched. Thus, secondary reactions were greatly diminished. The effects of the peak temperature and heating rate on the ultimate tar yield were investigated. Particular emphasis was given to the measurement of the pyrolysis yields for sugarcane bagasse, which is an abundant agricultural waste. The role of peak temperature and heating rate in defining the ultimate tar yield was investigated. The highest value obtained for bagasse was 54.6% at 500 °C with a very fast heating rate (1000 °C/s). The yields of bio-oil obtained by the pyrolysis of silver birch were also reported and compared to those of bagasse.[132]

The Waterloo fast pyrolysis fluidized sand was used at atmospheric pressure for the pyrolysis of Italian sweet sorghum and sweet sorghum bagasse.[133] Temperatures were varied over a range of 400−560 °C and residence times for volatiles were varied over a range of 222−703 ms. The maximum liquid yield (dry basis) for sorghum bagasse was 69.4% at 510 °C (500 ms). At a shorter residence time (225 ms) and 525 °C, a slightly higher yield was obtained.

Lee et al.[134] studied the production of bio-oil from rice straw by fast pyrolysis using a fluidized bed that was equipped with a char removal system. Experiments were conducted over a range of 400−600 °C at a feed rate of ∼1 kg/h. The mass balances were established, and the gases and oils were analyzed using GC and GC-MS. The effect of prewashing rice straw on the alkali-metal content was investigated, as well as its effect on the yield of bio-oil. The char removal system and prewashing effectively reduced the alkali-metal content in the resulting bio-oil (see Table 26). The optimum reaction temperature range for the bio-oil production is 410−510 °C.

Table 26. Alkali Metals in the Rice Straw Bio-oils Produced in Fluidized-Bed Pyrolysis[a]

	Concentration (ppm)	
alkali metal	after washing	before washing
Na	2.8	12.0
Mg	7.7	3.3
Ca	55.2	12.5
K	22.6	8.9

[a] Data taken from ref 134 with permission from the American Chemical Society.

Gonzalez et al.[135] studied the slow pyrolysis of almond shell residues under nitrogen in a laboratory fixed-bed reactor. The influence of the temperature (300−800 °C) and the heating rate (5−20 °C/min) on the composition and properties of the different fractions were analyzed. As the pyrolysis temperature increased, a decrease in the char yield and an increase in the gas yield was observed. A maximum in the yield of the oil fraction was observed at temperatures in the range of 400−500 °C.

Increasing the heating rate led to a slight decrease of the char and oil yields and an increase of the gas yield. These yields were in the range of 21.5%−47.3% for char, 31%−51.5% for oil, and 11.4%−47.5% for gas. These three product fractions exhibited maximum heating values of 29.0 MJ/kg, 14.1 MJ/kg, and 15.5 MJ/Nm^3, respectively. The char had a high fixed-carbon content (>76%), as well as a high heating value. Therefore, it could be used as a solid precursor in the manufacture of activated carbon (which has a specific surface area (BET) of 121 m^2/g), or it could be used to obtain category-A briquettes. Aliphatic and aromatic hydrocarbons and hydroxyl and carbonyl compounds were a majority of the components in the oil fraction.

The effects of initial moisture content and temperature on the oil yields from slow pyrolysis (slow heating rates, low-to-intermediate temperatures, and long residence times) of spruce wood, hazelnut shell, and wheat straw were studied.[69] Bio-oil yields increased when the pyrolysis temperature was increased from 302 °C to 427 °C, and then the bio-oil yields decreased at temperatures of >427 °C. The total oil yield increased as the initial moisture content increased. The total oil yield (aqueous phase + tarry materials phase) from spruce wood (with a moisture content of 6.5%), hazelnut shell (with a moisture content of 6.0%), and wheat straw (with a moisture content of 7.0%) increased as the temperature increased from 302 °C to 427 °C. Thus, yields of 8.4%, 6.7%, and 6.2% at 302 °C increased to 33.7%, 30.8%, and 27.4%, respectively, at 427 °C. The bio-oil yields from spruce wood (with a moisture content of 60.5%) increased from 17.2% to 39.7% when the pyrolysis temperature was increased from 327 °C to 416 °C.[69] These values can be compared to the bio-oil yields from spruce wood (where all free moisture content was removed). Yields increased from 12.6% to 26.7% when the temperature was increased from 327 °C to 416 °C in nitrogen.

The total oil yields from hazelnut shells (with a moisture content of 30.7%) increased from 14.6% to 35.9% when the pyrolysis temperature was increased from 327 °C to 416 °C, whereas the total bio-oil yields increased from 10.8% (327 °C) to 23.8% (416 °C) using hazelnut shells with a moisture content of 0% in nitrogen. Clearly, the effect of free water in the biomass is temperature-dependent and the presence of water benefits the conversion to oil.

The oil yields from wheat straw (which has a moisture content of 34.7%) increased from 12.1% at 327 °C to 33.6% at 416 °C, whereas the total oil yields from wheat straw (with a moisture content of 0%) increased only from 10.3% at 327 °C to 23.0% at 430 °C in nitrogen. Again, we see that the presence of moisture significantly influenced the degree of biomass thermal degradation during pyrolysis. Dry feed led to the production of very viscous oils, particularly at higher reaction temperatures. The highest liquid yield from spruce wood pyrolysis (39.7% on a dry feed basis) was observed when the initial moisture content was 60.5% at 416 °C. These conditions also gave the lowest viscosity.

Cashew nut shell (CNS) biomass represents a renewable and abundant source of energy in India.[136,137] CNS was vacuum-pyrolyzed in a fixed-bed reactor at 175 °C to give a dark brown oil (CO1), which was extracted. After the CO1 oil was removed, the CNS was again pyrolyzed under vacuum. A stainless steel reactor (600 mm in length) was used. Initial

reactor vacuum pressures of 5 kPa were used at various maximum temperatures of 400−600 °C, at increments of 50 °C for each experiment. The product distribution at each of these temperatures was analyzed. The volatiles removed by pyrolysis were fractionally condensed in a preweighed condensing train, using temperatures of 20−25 °C to conduct condensation in an ice bath (5−7 °C). The first three fractions were directly combustible without any further treatment and were designated as bio-oil CO2. The other fractions, which are noncombustible, contained water and light organics.

The detailed chemical composition analysis of both the CO1 and CO2 oils, as well as the aqueous fractions, were explored using HPLC, ^{1}H NMR, ^{13}C NMR, FT-IR, and GC-MS. The combination of both oils totals ∼40 wt % of the shells. Cardanol and cardol are the major constituents of CNS oil from pyrolysis at 175 °C, whereas CNS pyrolysis oil is a mixture of cardanol, di-*n*-octyl phthalate, *bis*-(2-ethyl hexyl) phthalate, cardol, and di-*n*-decylphthalate. The absence of anacardic acid in cashew nut shell oil is attributed to its decarboxylation during pyrolysis. The presence of long (C-6 to C-15) linear chain compounds in CO1 and CO2 CNS produced excellent solubility of CNS oil in diesel oils. Phenolic groups induced antioxidant characteristics, which was confirmed by the very small viscosity change that occurs when this oil is stored at high temperatures. These oils had little corrosivity toward copper and stainless steel. The physical properties of both the oils are given in Table 27.

Table 27. Physical Properties of Cashew Nut Shell Vacuum Pyrolysis Oils (CO1 and CO2[a])[b]

		Value	
property	test method	oil CO1	oil CO2
ash	ASTM D482	0.01	0.01
moisture	ASTM 1744	3.5	3
density at 28 °C (kg/m^3)	ASTM D4052-86 and IP 365/84	0.993	0.987
absolute viscosity (cSt)	ASTM D93 and IP 34/88		
at 30 °C		159	166
at 60 °C		33	39
at 80 °C		17	16
pour point (°C)	ASTM D97-87 and IP 15/67	−5.0	−0.5
elemental composition (wt %, db)[c]			

C		76.4	79.9
H		10.5	11.8
N		<0.2	<0.2
O, by difference		12.9	8.1
calorific value (MJ/kg)	ASTM D240	33	44
solids content, as methanol-insoluble material (%)		nil	nil
miscibility (%)			
hexane		100	73
methanol		100	100
acetone		100	100
diesel, HSD		100	100

[a] CO2 was condensed at 5−7 °C, after CO1 was already condensed.[b] Data taken from refs 136 and 137 with permission from Elsevier.[c] db = Dry basis.

10.4. Bio-oil from Nuts and Seeds. Nuts are composed of the outer shell and the nut within. In the preceding section on agricultural wastes, the shells of walnuts, almonds, and hazelnuts have already been mentioned. Other examples of nutshells are also included in this section.

Extractions and characterizations were performed on the important lignin-derived compounds present in walnut (*Juglans regia*) shell oil.[138] The oil was extracted using a novel method in which the shells were roasted at 250−300 °C. The lignin breakdown compounds in the oil were isolated by solvent extraction using petroleum ether (with a boiling-point range of 60−80 °C) and separated by preparative thin-layer chromatography (TLC). After separation, these compounds were fully identified using GC-MS, ^{1}H NMR, ultraviolet (UV), FT-IR, and high-performance liquid chromatography (HPLC) data. The major compounds that resulted from lignin breakdown during this pyrolysis were guaiacol, 4-methylguaiacol, 4-ethylguaiacol, 4-propylguaiacol, syringol, 4-methylsyringol, 4-ethylsyringol, and 4-propylsyringol.

Zensor et al.[139] pyrolyzed rapeseed (*Brassica napus L.*) at different particle sizes and sweep gas velocities. The maximum oil yield (53%) was obtained at 500 °C, at a slow heating rate of 7 °C/min, under nitrogen, using a particle size range of 0.85−1.8 mm. Ozcimen and Karaosmanoglu[140] studied the production and characterization of bio-oil and bio-char from rapeseed cake under static and nitrogen atmospheric conditions in a Heinze retort 316 stainless steel fixed-bed reactor that had a length 104 mm and an inner diameter of 70 mm. The sweep gas velocity did not have a significant effect on the product yields for the pyrolysis temperature and heating rate that was examined. A carbon-rich char was obtained

with a high heating value. This char was considered a relatively pollution-free, potential solid fuel, whereas the bio-oil product was an environmentally friendly bio-fuel candidate.

The fast pyrolysis of rapeseed performed in a well-swept fixed-bed reactor[141] produced a maximum oil yield of 68% at 550 °C, using a particle size range of 0.6−0.85 mm and a heating rate of 300 °C/min with a nitrogen flow. The bio-oil was first separated into *n*-pentane-soluble and *n*-pentane-insoluble compounds (asphaltenes). The *n*-pentane-soluble compounds were further separated by adsorption chromatography over a silica gel (70−230 mesh), which had been preheated at 105 °C for 2 h prior to use. Successive elution with *n*-pentane, toluene, and methanol produced aliphatic, aromatic, and polar fractions, respectively. Each fraction was dried, weighed, and then subjected to elemental, GC, and IR analysis. The elemental compositions of various oil fractions (as determined via chromatography) are given in Table 28. The average composition can be expressed as $CH_{1.758}N_{0.0538}O_{0.300}$. The ^{1}H NMR confirmed a high aliphatic content (chemical-shift range of 0.4−1.8 ppm) and low aromatic content in this oil (Table 29).

Table 28. Elemental Compositions of Column Chromatographic Fractions from Rapeseed Fast Pyrolysis Oil[a]

	Elemental Composition (wt %)		
component	*n*-pentane	toluene	methanol
C	81.4	77.4	68.8
H	13.8	12.7	9.4
N		0.3	2.8
O	4.8	10.2	19.0
H/C	2.03	1.96	1.64

[a] Pyrolysis conditions were as follows: pyrolysis temperature, 550 °C; particle size range, 0.6−1.8 mm; heating rate, 300 °C/min; and nitrogen flow rate, 100 cm^3/min. Elemental compositional data were taken from ref 141 with permission from Elsevier.

Table 29. ^{1}H NMR of Rapeseed Fast Pyrolysis Oil[a]

hydrogen environment	molar content in pyrolysis oil (% of total hydrogen)
aromatic/alkene, including the peak at 5.5 ppm	2
aliphatic adjacent to oxygen, 3.3−4.5 ppm	9

aliphatic adjacent to aromatic/alkene group, 1.8−3.3 ppm	14
other aliphatic, bonded to aliphatic only, 0.4 −1.8 ppm	75

[a] Pyrolysis conditions were as follows: pyrolysis temperature, 550 °C; particle size range, 0.6−1.8 mm; heating rate, 300 °C/min; and nitrogen flow rate, 100 cm^3/min. Elemental compositional data were taken from ref 141 with permission from Elsevier.

Haykiri-Acma et al.[142] studied the effect of heating rate on rapeseed pyrolysis yields at 1000 °C. Heating rates of 5, 10, 20, 30, 40, and 50 °C/min were used in a dynamic nitrogen flow of 40 cm^3/min. Mass losses (solid to vapors) were examined using derivative TGA profiles. At the lower heating rates, the maximum mass rate loss was low. These loss rates increased as the heating rate increased, showing the importance of rapid heat transfer to achieve high temperatures quickly.

Rapid pyrolysis of the *Linum usitatissimum L.* (linseed) plant produced a maximum oil yield (57.7%) at 550 °C using a particle size range of 0.6 mm < d_P < 1.8 mm, a heating rate of 300 °C/min, and a nitrogen flow rate of 100 cm^3/min (the reactor had dimensions of 0.8 cm id and 90 cm in length).[143] Linseed fast pyrolysis oil had an empirical formula of $CH_{1.64}N_{0.03}O_{0.11}$. The small amount of aliphatic carbon bound to oxygen (with an NMR peak of δ = 3.5−4.5 ppm) was smaller than that from rapeseed. Yorgun et al.[144] conducted a similar pyrolysis of sunflower oil cake in a tubular transport reactor at atmospheric pressure under nitrogen. A maximum oil yield of 45% was obtained at a pyrolysis temperature of 550 °C, with a gas flow rate of 300 cm^3/min and a particle size of 0.425−0.850 mm. Chromatography and spectroscopic studies demonstrated that this bio-oil contained a mixture of aliphatic and aromatic compounds (the net empirical formula was $CH_{1.512}N_{0.070}O_{0.175}$).

10.5. Bio-oil from Algae. Rapidly growing algae represent a promising pathway to liquid fuels. Algae are more readily and rapidly bioengineered than trees and might be easily cultured. Algae are comprised of several different groups of photosynthetic organisms. The most conspicuous are the seaweeds, multicellular green, red, and brown algae that often closely resemble terrestrial plants. These and other algal groups also include various single-celled creatures that are simple collections of cells, without differentiated tissues.

Miao and co-workers[145,146] performed the fast microalgae pyrolysis at 500 °C at a heating rate of 600 °C/s in nitrogen sweep gas, using a vapor residence time of 2−3 s. Microalgae usually have greater photosynthetic efficiency and faster growth than lignocellulosic plants.[147-150] More high-quality bio-oil was produced via fast pyrolysis than via slow pyrolysis. Oil yields of 18% and 24% were obtained from fast pyrolysis of *Chllorella protothecoides* and *Microcystis areuginosa.* Typical properties of fossil oil and bio-oil from the fast pyrolysis of wood versus microalgae are compared in Table 30.[19,57,145,151,152] The saturated and polar fractions account for 1.14% and 31.17% of the bio-oils from microalgae, whereas the saturated fraction accounts for <1% of the bio-oil from wood and the polar fraction is 12%. The microalgae bio-oil exhibited a higher carbon and hydrogen content, lower oxygen content, and, importantly, a 26%−27% greater heating value than wood bio-oil.

Table 30. Comparative Evaluation of Fossil Oil and Bio-oil from Fast Pyrolysis of Wood and Microalgae[a]

Typical Yield Values					
Bio-oils					
C. protothecoides					
property	wood[b]	microalgae[b]	autotrophic (AC)[b]	heterotrophic (HC)[b]	fossil oil
C (%)	56.4	61.52	62.07	76.22	83.0−87.0
bio-oil yields, at 600 °C			17.5	23.7	
H (%)	6.2	8.50	8.76	11.61	10.0−14.0
O (%)	37.3	20.19	19.43	11.24	0.05−1.5
N (%)	0.1	9.79	9.74	0.93	0.01−0.7
S (%)	na[c]	na[c]	na[c]	na[c]	0.05−5.0
density (kg/L)	1.2	1.16	1.06	0.92	0.75−1.0
viscosity, at 40 °C (Pa s)	0.04−0.20	0.10	0.10	0.02	2−1000[d]
heating value (MJ/kg)	21	29	30	41	42
stability	not as stable as fossil fuels	not as stable as fossil fuels, but more stable than the bio-oil from wood			

[a] Data taken from refs 145 and 146 with permission from Elsevier. [b] Maximum yield. [c] Not available. [d] Depending on temperature.

The fast pyrolysis of autotrophic and heterotrophic *C. protothecoides* was studied.[145,146] Samples with masses of 200 g (0.5 mm in size) were subjected to pyrolysis in the fluidized-bed reactor. The biomass-feeding rate was 4 g/min. Two groups of experiments were performed. In the first group, cells of autotrophic and heterotrophic *C.*

protothecoides were pyrolyzed at a temperature of 500 °C with a heating rate of 600 °C/s, a gas (N_2) flow rate of 0.4 m^3/h, and a vapor residence time of 2−3 s. The second group was performed to determine the effect of temperature (in the range of 400−600 °C) on the pyrolysis yields of heterotrophic *C. protothecoides*. The heating rate, sweep gas flow rate, and vapor residence time were maintained the same as that for the first group.[145,146]

Bio-oil yields from the algae fast pyrolysis can be increased by manipulating the microalgae metabolic pathways through heterotrophic growth.[145,146] The bio-oil yield (57.9%) from heterotrophic *C. protothecoides* cells was 3.4 times greater than that from the fast pyrolysis of autotrophic cells. This combination of bioengineering and fast pyrolysis is a feasible and effective method for the production of high-quality oils in high yields from microalgae. Maximum bio-oil yields of 57.9%−57.2% were obtained from heterotrophic *C. protothecoides* (HC) microalgae at temperatures of 450−500 °C. In contrast, higher plants such as pinewood, cotton straw and stalk, tobacco stalk, and sunflower bagasse generated maximum oil yields of 40%−49% at 500−550 °C.[16,153,154] This may be due to chemical composition differences between these species. The bio-oil from heterotrophic microalgae was characterized by a lower water content, a higher heating value (41 MJ/kg), a lower density (0.92 kg L^{-1}), and a lower viscosity (0.02 Pa s) than that of bio-oil from autotrophic microalgae cells or wood.

10.6. Bio-oil from Grasses. Various fast-growing grasses could possibly give higher annual energy yields than trees, when compared over a multiyear periods. Also, various topographies favor grasses over trees. The pyrolysis of switchgrass (*Panicum virgatum*) of the lowland ecotype "Cave-in-Rock" cultivar harvested at three stages of maturity was studied in an on-line pyrolysis−gas chromatography/mass spectrometry (PY−GC/MS) system in the temperature range of 600−1050 °C.[155] These decompositions were complete within 20 s, yielding char and both condensable and noncondensable pyrolysis gases. The condensable gas consisted of acetaldehyde (CH_3CHO), acetic acid (CH_3COOH), and higher-molecular-weight compounds. Noncondensables mainly included CO, CO_2, and C_1−C_3 hydrocarbons. At 900 °C, a dramatic change occurred in their evolution rates. Below 900 °C, CO_2 decreased but CO and the C_1−C_3 hydrocarbons increased almost linearly with temperature. Above 900 °C, the hydrocarbons leveled off, but a rapid increase in CO and CO_2 evolution at a constant CO/CO_2 ratio was observed. Secondary or tertiary pyrolysis reactions apparently occur, involving the release of CO and CO_2 from the tightly bonded oxygen functionalities. At <750 °C, there were modest increases in the condensable gas yield and a decrease in noncondensable gas. Slow vapor evolution at this temperature (<750 °C) is probably due to the strong bonds in the lignin and the extra lignin gained at plant maturity, which increase cell wall structural rigidity. At 900 and 1050 °C, gas yields are relatively constant at all three grass maturity levels. Evidence of this lies in the declining CO_2 yield, and the absence of (and the declining evolution trends for) some of the hydrocarbon gases, particularly CH_4 and C_3H_8. At higher temperatures, however, the effect of plant maturity on the release rates is diminished or is only marginal. At these temperatures, no extent of structural bond strengthening as the plant reaches maturity could withstand the thermal degradation. The energy content of the noncondensable gas was ∼68% of the gross biomass energy content for the early harvest crop and 80% for the mature crop.

10.7. Bio-oil from Forestry Residues. Oasmaa and co-workers[83-85,156] have studied the fast pyrolysis of forestry post- harvest residues at 520 °C and residence times of 1−2 s. Pyrolysis was performed using a 20-kg/h capacity Process Development Unit (PDU) at VTT. Ensyn Technology initially designed and delivered the transport bed reactor to VTT in 1995. This reactor has subsequently been modified by VTT. The ground, sieved, and dried (moisture

content of 3−6 wt %) forestry residue feedstock was fed to the reactor. Vapors were condensed using pyrolysis liquid condensers, and the liquid was transferred to phase-separation towers. The towers were equipped with warm-water circulation to adjust the temperature. After a certain amount of storage time, the liquid was recovered from the bottom of the tower as "bottom" and "top" phases. The bio-oil was composed of an extractive-rich upper phase, which varies over a range of 10%−20% of the total product. The bottom phase closely resembled the normal bark-free bio-oil product from wood feedstock.

Phase separation occurred in this forestry residue bio-oil because of the higher hydrophobic extractive content of the residues. Extractives separate because of their lower oxygen content and solubility, polarity, and density differences between the extractives and the polar pyrolysis liquid compounds.[83] The extractives are composed of fatty acids, fatty alcohols, terpenes, resin acids, and terpenoids. They form an upper phase that has a higher viscosity and higher heating value than the bottom phase. Phase separation was enhanced by an increase in temperature and/or storage time. Brown, partially dried forestry residue contained less extractives and produced less of this top phase than green feedstock.

Oasmaa et al.[84] also studied the uses, properties, and behavior of forestry residue pyrolysis liquids. The chemical composition of forestry residue liquid (bottom phase) is similar to that of pine pyrolysis liquids. It is composed of volatile acids (8−10 wt %); aldehydes and ketones (10−15 wt %); water (25−30 wt %); sugar-derived constituents (30−35%); water-insoluble, mainly lignin-based constituents (15−20 wt %); and extractives (2−6 wt %). Brown forestry residue produced more (35−37 wt %) water-insoluble lignin-derived components than pine (32−35 wt %) or green forestry residue (17−22 wt %).

The typical forestry residue pyrolysis[84] liquids contained ∼28 wt % water and exhibited pH 3.0, a viscosity of ∼15 cSt at 40 °C, a lower heating value (LHV) of 14 MJ/kg (21 MJ/kg, dry basis), and <0.05 wt % solids. Pyrolysis oils from these residues contain reactive organics that can polymerize during storage. Thus, they behave like other bio-oils, undergoing viscosity increases during "aging".[25,66-68] The stability of this pyrolysis oil was monitored by analyzing changes in the physical properties and chemical composition during storage at ambient conditions.[85] The main physicochemical changes occurred during the first six months, similar to the behavior observed with other bio-oils. The high-molecular-mass, water-insoluble fraction (lignin-derived fraction) underwent oligomerization and polymerization. Condensation reactions of carbohydrate-derived constituents, aldehydes, and ketones occurred, which increased the average molecular mass and the viscosity. Finally, Oasmaa et al.[156] studied the improvement of the product quality by the addition of solvents. Alcohols improved the homogeneity, decreased the viscosity and density, lowered the flash point, and increased the heating value of the pyrolysis liquids. Alcohols addition also reduced the viscosity and decreased the molecular mass increase during aging. Alcohols convert aldehydes, ketones, and anhydrosugars to acetals, slowing the condensation reaction.

Gerdes et al.[24] used a continuous pilot-scale fluidized-bed plant for lignocellulosic biomass fast pyrolysis, which gave bio-oil yields of 65 wt %. The average reactor gas residence time was only 1.2 s. The gas and charcoal yields were 15−20 wt %, respectively. The main monomeric products of carbohydrate thermal degradation were acetic acid, hydroxyacetaldehyde, hydroxypropanone, and levoglucosan.[24]

10.8. Bio-oil from Cellulose and Lignin. Fullana et al.[157] utilized multidimensional gas chromatography (MDGC) to analyze products generated from primary and secondary pyrolyses of cellulose, lignin, and sewage sludge samples. These three feeds produced compounds with very different polarities, thus making them ideal for MDGC applications.

More than 70% of the total MDGC chromatogram peaks could be identified, versus only 47% in the best case of conventional GC; this was due to improved separations. This increased understanding of the pyrolytic product distribution can be used to enhance our understanding of the formation mechanisms of important pyrolytic products such as PAHs. Furthermore, the MDGC technique can be easily implemented in most pyrolysis laboratories. Microsoft Excel and Visual Basic commercial software can be used to handle vast amounts of MDGC data effectively. The data treatment methods discussed by Fullana et al.[157] successfully divided MDGC data into manageable groups, which were then used to obtain insights into the pyrolytic processes.

Studies have been performed on the characterization of pyrolytic lignin obtained from pyrolysis oils after it has been precipitated as a fine powder.[138,158,159] Analyses were obtained for various pyrolytic lignins from different fast pyrolysis processes. Chromatography, spectroscopy, and wet chemical techniques were used. In one study, the research group of Scholze and Meier[158,159] characterized the water-insoluble fraction pyrolysis oil (pyrolytic lignin) by PY−GC/MS, FT-IR, GPC, and ^{13}C NMR. The average molecular weight of pyrolytic lignin, using GPC, was determined to be in the range of 650−1300 g/mol. This demonstrated that pyrolytic lignin was comprised mainly of trimers and tetramers. The weight-average molecular weight (M_w) of softwood pyrolytic lignin is larger than that of hardwood samples. Softwood pyrolytic lignins have a larger tendency to polymerize, because unsubstituted positions ortho to the phenol hydroxyl exist in softwood lignins.

10.9. Bio-oil from Miscellaneous Feeds. One of the largest genera of flowering plants is euphorbia, which is a large genus of *Euphorbiaceae*, a family of laticiferous herbs, shrubs, and small trees that is distributed in the tropical and warm temperature regions of the world. Many of the species are succulent and inhabit dry places. They resemble cacti in appearance but can be distinguished from them by the presence of milky latex. About 2000 species have been reported throughout the world, chiefly in tropical regions. Some species of this family have been investigated and identified as promising candidates for renewable fuels and chemical feedstocks.[154,160]

The hydropyrolysis (pyrolysis under a hydrogen atmosphere) of extracted *Euphorbia rigida* was conducted at a moderate heating rate (100 °C/min) in a well-swept fixed-bed tubular reactor.[154] The effects of the hydropyrolysis temperature and heating rate on the yields and product chemical compositions were investigated. A maximum bio-oil yield of 39.8 wt % was obtained at 550 °C at a hydrogen pressure of 150 bar, and a hydrogen flow rate of 5 dm^3/min.

Slower pyrolysis of *Euphorbia macroclada*[148] produced maximum oil yields at 550 °C and a heating rate of 7 °C/min. Distinct conversion increments occurred in the temperature range of 500−550 °C, because of the rapid gas evolution from cellulose and hemicelluloses.

12. 11. Effect of Various Parameters on Pyrolysis/Bio-oil Production

11.1. Influence of Metal Ions and Salts on Wood Pyrolysis Products. The addition of metal ions can be used to alter or tailor the products produced by biomass pyrolysis. Catalyzed biomass pyrolysis is not yet well-studied. However, it does offer tremendous

potential for future development as a route for chemical production or to modify fuel properties.

The presence of alkaline cations in biomass is known to affect the mechanism of thermal decomposition during the fast pyrolysis. These cations cause fragmentation of the monomers that comprise the natural polymer chains, rather than the predominant depolymerization that occurs in their absence.[161-166] Potassium and calcium are the major cations present, along with minor amounts of sodium, magnesium, and other elements. Richards and Zeng[161] purposely incorporated several different metal ions, individually, into cottonwood via ion exchange and then investigated the products of vacuum pyrolysis. The cations K^+, Li^+, and Ca^{2+} induced high char and low tar yields. The tar was very low in levoglucosan. In contrast, all of the other ions investigated, especially the transition metals, gave increased yields of levoglucosan (as much as 15.8% from wood exchanged with ferrous ions). This corresponds to a 32% conversion of cellulose to levoglucosan. When salts were sorbed into the wood (instead of ion-exchanged), smaller, but significant, levoglucosan increases were again obtained, especially when indigenous salts in the wood were first removed by acid washing.

The effect of the anion on pyrolysis was investigated with sorbed salts. Wood impregnated with acetate salts behaved similarly to ion-exchanged wood. Chlorides (especially copper chlorides and iron chlorides) increased the levoglucosan yield. Low levels of sorbed $FeSO_4$ catalyzed the formation of both levoglucosan (LG) and levoglucosenone (LGone).

Dobele et al.[165] estimated the effect of added phosphoric acid and Fe^{3+} ions on 1,6-anhydrosaccharides, LG, and LGone in volatile products produced by the fast analytical pyrolysis of wood and microcrystalline cellulose. Approximately 50 μg samples were pyrolyzed in a quartz boat (2.5 cm × 2 mm) at 500 °C and a heating rate of 600 °C/s, using a Pyroprobe 100 (CDS) coil probe directly coupled to a GC/MS system. The LG and LGone contents were influenced by the biomass pretreatment. $Fe_2(SO_4)_3$ was introduced by soaking biomass in an iron(III) sulfate solution alone or in the presence of ammonium (NH_4^+) ions. This formed oxyhydroxides of iron. Previous decationization of wood has an important role in the subsequent pyrolysis products formed after Fe^{3+} ion treatment. The 1,6-anhydrosaccharides content in volatile products and the LG/LGone ratio is governed by the phosphoric acid concentration. The same is true for cellulose soaked by iron sulfate: at higher iron concentrations, the LGone content increases and the LG/LGone ratio decreases. Iron ions act according to a mechanism, which is dependent on the iron species formed during iron sulfate pretreatment. Adsorbed iron sulfate increases the amount of both LG and LGone formed in the volatile products through the acidic catalysis mechanism, because of sulfate anions. Pretreatment by ion-exchange could be an efficient technique for obtaining bio-oil that contains high levoglucosan contents: 44.8% from cellulose and 27.3% from wood.

Metal ions have profound effects on biomass pyrolysis, but this topic is understudied. The volatile products from wood pyrolysis in air have been determined[144,163] by coupled thermogravimetry/Fourier transform infrared spectrometry (TG/FTIR), both isothermally at 250 °C and with progressive heating to 477 °C. Replacement of indigenous metal ions by K^+ ions catalyzed both pyrolysis and oxidation. At higher temperatures, K^+ ions catalyzed char oxidation by air, resulting in ignition and the sudden formation of carbon monoxide, carbon dioxide, and water. In contrast, calcium does not act as a catalyst in pyrolytic reactions. The principal effect of removing alkaline or alkaline-earth cations, followed by fast pyrolysis, is the production of an anhydrous liquid that is rich in LG (anhydrous glucose) and anhydropentoses.[166]

Scott et al.[162] described a preliminary study of the removal of indigenous alkaline cations in a poplar wood. Potassium and calcium were removed via ion exchange, using dilute acid. The exchange process is rapid. Potassium is more easily removed than calcium. Washing with hot water alone was able to remove a major portion of the alkaline cations from wood. The deionized wood was used as the feed for a fast pyrolysis process that converts cellulose and hemicellulose to good yields of anhydrosugars for use in synthesis or as a source of fermentable sugars. Table 31 compares the yields and liquid compositions obtained by fast pyrolysis of natural poplar wood versus deionized popular wood.[162]

Table 31. Fast Pyrolysis of Natural versus Deionized Poplar[a]

	Value	
feedstock	poplar	deionized poplar
temperature (°C)	497	493
moisture (wt %)	3.3	11.4
particle size (mm)	<0.5	<0.5
yield (wt % mf feed)		
gas	10.8	2.6
char	7.7	5.4
organic liquid	65.8	75.9
product water	12.1	14.0
recovery (%)	96.5	97.9
liquid components (wt % mf feed)		
levoglucosaan	3.0	17.1
other anhydrosugars/sugars	5.7	6.7
hydroxyacetaldehyde	10.0	2.0
acetic acid	5.4	1.3
glyoxal	2.2	2.7
pyrolytic lignin[b]	16.2	22.4

[a] Data taken from ref 162 with permission from Elsevier.[b] Precipitate formed upon the dilution of bio-oil to ∼50% water content.

French and Milne [167] studied the emission of alkali vapor species by molecular-beam mass spectrometry (MBMS) during combustion. A free-jet sampling system cooled the products of combustion extremely rapidly with little condensation, making it possible to identify the alkali species that are active in high-temperature vapor transport. The release mechanisms and the implications for the use of biomass in gasification and combustion systems were discussed.

11.2. Influence of Catalysis on Wood Pyrolysis Products. Catalytic pyrolysis can profoundly alter the pyrolytic product distribution. Adam et al. [168] conducted a pyrolysis of spruce wood in the presence of Al−MCM-41-type mesoporous catalysts. The catalysts were used for further conversion of the pyrolysis vapors from spruce wood to attempt to improve bio-oil properties. Four Al−MCM-41- type catalysts were tested. The catalytic properties of Al−MCM-41 were modified by both pore enlargement, which allows the processing of larger molecules, and the introduction of Cu cations into the structure. Spruce wood pyrolysis was performed at 500 °C, and the products were analyzed via PY−GC/MS. In addition, TG/MS was used to monitor product evolution under slow heating conditions (20 °C/min) from 50 °C to 800 °C. Levoglucosan was completely eliminated, whereas acetic acid, furfural, and furans become important cellulose pyrolysis products over an unmodified Al−MCM-41 catalyst. The quantity of higher-molecular-mass phenolic compounds is strongly reduced in the lignin-derived products. The increase in acetic acid and furan and the decrease of large methoxyphenols are both somewhat repressed over catalysts with enlarged pores. The copper-modified catalyst performed similarly to the enlarged pore catalyst in converting the wood pyrolysis vapors, although its pore size was similar to the unmodified Al−MCM-41.

A HZSM-5 zeolite catalyst was used[169] in situ in a conical spouted-bed reactor in the flash pyrolysis of sawdust at 400 °C. HZSM-5 promoted major changes in the yields of gas, liquid, and chars. The gas yields increased as the catalyst amount was increased, while the liquid yields decreased significantly and the char yields decreased slightly. A kinetic scheme was proposed for the catalytic pyrolysis and the values of the kinetic constants were calculated. This scheme includes two new steps that are different from those of thermal pyrolysis. First, the transformation of the liquid into gas and char proposed. Catalyst use caused the bio-oil composition to undergo a drastic change. The heavy organic fraction was proposed to be partially transformed to the aqueous fraction due to cracking, whereas the aqueous liquid fraction was hypothesized to undergo dehydration, decarboxylation, and decarbonylation.

Barks from four common Mediterranean trees were subjected to thermal pyrolysis with acid catalysts at moderate temperature (130 or 150 °C). The products were analyzed by pyrolysis−molecular beam mass spectrometry (PY−MBMS). [170] Both the concentration of acid catalyst and the phenolysis temperature impacted the chemical compositions of the isolated oils and the solid residue. Acid concentration had the greatest influence. The primary phenolysis products included phenolics and furans. Higher acid concentrations favored the generation of fewer carbohydrates and more phenolic fragments. These phenolysis oils should be useful as feedstocks for the production of phenol formaldehyde resins. PY−MBMS was an effective and convenient method to understand bark phenolysis.

Pinewood was pyrolyzed in a heated, 7.5-cm-diameter, 100-cm-high fluidized-bed pyrolysis reactor with nitrogen as the fluidizing gas. [171] A downstream section of the reactor was packed with the ZSM-5 zeolite catalyst. The pyrolysis oils obtained both before and after exposure to the ZSM-5 zeolite catalyst were collected, condensed, and analyzed. HPLC, GC/MS, FT-IR,

and size exclusion chromatography (SEC) were used for the analysis. Oils were highly oxygenated before catalysis. After catalysis, the oils had markedly less oxygenated species present, a higher aromatic content, and an increase in biologically active polynuclear aromatic (PAHs) species. The gases that evolved during the biomass pyrolysis were CO_2, CO, H_2, CH_4, C_2H_4, C_3H_6, and minor amounts of other hydrocarbons. The amounts of CO_2 and CO increased during catalysis. Oxygen in the oxygenated compounds was catalytically converted mainly to H_2O at lower catalyst temperatures and CO_2 and CO at high catalyst temperatures. The amounts of PAHs increased as the catalyst temperature increased. The oxygenated compounds remaining in the oil formed over the ZSM-5 bed were mainly phenols and carboxylic acids. Exposure to ZSM-5 progressively decreased the concentration of phenolics and acids as the bed temperature increased.

Ateş et al.[172] studied the catalytic pyrolysis of the perennial shrub *Euphorbia rigida*, using a commercial Co−Mo catalyst (Criterion-534) in a water vapor atmosphere and a well-swept fixed-bed Heinze reactor. The stainless steel fixed-bed reactors had a volume of 400 cm^3 (70 mm id). A 10-g sample, which had a particle size of 0.55 mm, was mixed with different amounts of catalyst (5, 10, 20, and 25 wt %) and then was placed in the reactor. The experiments were performed to a final pyrolysis temperature of 550 °C, using a slow heating rate (7 °C/min) at water vapor velocities of 0.6, 1.3, or 2.7 cm/s. The oil yield (21.7% without a catalyst) progressively increased to 29.4%−30.9% in the static atmosphere, using 5, 10, 20, and 25 wt % of catalyst. The oil yield increased only slightly when the amount of catalyst is achieved, reaching its maximum using 20 wt % of catalyst. The oil yields were 38.8% with 5 wt % of catalyst, 39.4% with 10 wt % of catalyst, and 39.7% with 20 wt % of catalyst at a steam velocity of 0.6 cm/s. These yields increased to 40.6%, 42.1%, and 42.6%, respectively, when a steam velocity of 1.3 cm/s was used. In both atmospheres, increasing the catalyst charge to 25 wt % did not change the results. The oil yield was 21.7% in a static atmosphere with no catalyst present. The yields increased to a maximum value of 42.6% at a flow rate of 1.3 cm/s.

Biomass pyrolysis that was performed in a fixed-bed reactor with Criterion-534, activated alumina, and natural zeolite (klinoptilolite) catalysts[154] gave oil yields of 27.5% with natural zeolite, 31% with Criterion-534, and 28.1% with activated alumina.[173] The yield was only 21.6% when no catalyst was used.

Garcia et al.[174] studied the influence of catalyst pretreatment on gas yield in catalytic biomass (sawdust) pyrolysis based on the Waterloo Fast Pyrolysis Process (WFPP) technology. This technology achieves a very fast biomass heating rate and a low gas residence time in the reaction bed. The gas spatial time in the fluidized-bed reactor was ∼0.34 s for the two operating temperatures (650 and 700 °C) under a nitrogen flow. A Ni/Al coprecipitated catalyst was used in the reaction bed where biomass thermochemical decomposition occurred. A decrease was observed in the H_2 and CO yields at both 650 and 700 °C when the sawdust feed rate increased; this could result from catalyst deactivation. Higher H_2 and CO yields were observed at both temperatures after the catalyst had been reduced using hydrogen for 1 h.

Borgund and Barth[175] performed the pyrolysis of a pure thermomechanical pulp (TMP) from softwood (Norwegian spruce) that was comprised of 46.6% carbon, 6.2% hydrogen, and 47.2% oxygen. The TMP was dried at 100 °C to a constant weight. Sodium hydroxide (NaOH) was used as a basic catalyst to increase oil yield and decrease coke generation. The addition of a catalyst caused a decrease in coke formation, along with an increase in the extractable organic matter. Polar compounds dominated in the extracted matter. The amount

of water present in the biomass had the largest effect on yields. The temperature and the amount of starting material exerted minor effects.

13. 12. Kinetics of Pyrolysis

Knowledge of the kinetics helps to achieve control of the pyrolysis and gasification and assists in optimizing system design. Kinetic analysis is complicated by wood's complex composite structure. Hemicellulose, cellulose, lignin, and extractives each have their own pyrolysis chemistry. Kinetic modeling can incorporate the following simplifying steps (http://www.zju.edu.cn/jzus/2003/0304/030411.pdf): (1) degradation of the virgin biomass materials into primary products (tar, gas, and semi-char), (2) decomposition of primary tar to secondary products, and (3) continuous interaction between primary gas and char. The last step is disregarded completely by kinetic models in the literature. Furthermore, neither the effects of the wood composite morphology on heat-transfer differences nor the actual chemical degradation kinetics of individual wood components have been modeled. Several kinetic models have appeared in the literature.[176-186]

The pyrolysis and gasification of aspen, beach, and larch wood were compared.[187] Their formal kinetics and main pyrolysis liquids, char, carbon dioxide, carbon monoxide, methane, and hydrogen were described. Luo et al.[188] modeled wood pyrolysis operating parameters in a fluidized-bed reactor (bed temperature, suspension bed temperature, particle size, feed rate). Reaction temperature, not surprisingly, has a major important role in wood pyrolysis, according to the model. Good agreement between the experimental and modeling results was obtained. Through the use of particle sizes of <500 μm, a heating rate that was high enough to permit true fast pyrolysis was achieved.

The effective thermal conductivity (ETC) of softwood bark and softwood char in highly polydispersed particle beds was measured experimentally.[189] The ETC was also calculated theoretically, using liner packing theory and a unit-cell model of heat conduction. Excellent agreement was obtained with experimental results. This approach can predict the ETC of any size distribution for beds of softwood bark or char. Heat transfer is the rate-determining step in fast pyrolysis reactions; therefore, the ETC values are needed to model pyrolysis kinetics.

Tsotsas and Schlunder[190] had previously shown that biomass particle size dispersity affects ETC through variation in bed voidage. Prior to the paper by Gupta, Yang, and Roy,[189] they recommended determining the ETC experimentally. Gupta et al.[191] had proposed a modified ETC prediction strategy that considered the complex particle−particle interaction of the particles' initial porosity and binary packing size ratio.

Knowledge of other thermal properties (including the specific heat) are necessary to model pyrolysis and vacuum pyrolysis reactor kinetics effectively. Very little data are available for softwood, softwood bark, or softwood chars. Recently, DSC studies by Gupta et al.[191] have helped to fill that void. At 40 °C, the specific heats 1172, 1364, and 768 J kg^{-1} $°C^{-1}$ for softwood, softwood bark, and softwood chars, respectively. Specific heat was studied from 40 °C to 444 °C, and the specific-heat-versus-temperature data were fitted to polynomials. Particle thermal conductivities were also measured.

Blasi[192] presented a detailed single-particle model to simulate the fast pyrolysis of wood in fluidized-bed reactors for liquid fuel production. The model included a description of transport phenomena and a global reaction mechanism coupled with a plug-flow assumption

for the extra particle processes of tar cracking. Good agreement was obtained between the predictions and product yield measurements (liquids, char, and gases), as a function of temperature. Particle dynamics were found to be affected by convective transport of volatile products. The average heating rates were in the range 450−455 °C/s. Reaction temperatures varied between 367 °C and 497 °C (for particle sizes of 0.1−6 mm, a reactor temperature of 527 °C was observed). The effects of size, shape, shrinkage of wood particles, and external heat-transfer conditions were also examined.

14. 13. Chemical Analysis

The chemical analysis of solids and pyrolytic vapors from wildland trees has been reported.[193] The pyrolysis chemistry of tree samples commonly found in the forests of the western United States was evaluated and compared with a wet chemical analysis of the original material. Wood, leaves, bark, needles, reaction wood, and sticks are individually examined. Molecular-beam-sampling MS detection of pyrolytic compounds obtained at 500 °C with residence times of ∼100 ms permitted mass spectral analysis of the chemicals in the primary decomposition regime. Multivariate analysis of the pyrolysis mass spectra revealed three principal factors. One factor identified leaf, needle, and bark samples and correlates well with the extractive content of the material. A relationship existed between this factor and the ash content of the material. The other two factors related hardwood and softwood samples; this distinction is based mainly on differences in the structure of lignin degradation products that are evident in the pyrolysis vapors. These measurements suggest that fuel stock biomass extractives content may be a natural chemical indicator, useful for estimating the bulk pyrolysis chemistry in a way that can be practically implemented into wildland fire models.

Brown and co-workers[194,195] reported the design and characterization of a laminar entrained-flow reactor for studying high heating rate biomass pyrolysis chemistry. Peak reactor heating rates[194] were on the order of 10^4 °C/s. The reactor was interfaced with a molecular-beam mass spectrometer for rapid gas-phase chemistry analyses. Computational fluid dynamic simulations predicted an accurate time−temperature profile for the reactants and to better explain the internal reactor processes. Brown et al.[195] further studied cellulose pyrolysis in a laminar entrained flow reactor (LEFR). This reactor was capable of high heating rates (∼10^4 K/s) and was characterized in detail to ensure that pyrolysis of lignocellulosic materials occurred under kinetic control. The extent of cellulose pyrolysis in the LEFR was monitored by gas-phase sampling with a molecular beam MS system and independently by sampling and weighing residues. Quantitative cellulose pyrolysis data were compared to several published reaction rates. Factor analysis of the mass spectral data required two principal components to interpret the gas-phase product composition. This suggests that the primary cellulose pyrolysis products underwent subsequent secondary reactions that directly compete with the primary release of products under these conditions. A rate law was developed that describes the observed thermal destruction of primary pyrolysis products.

15. 14. Solvent Fractionation of Bio-oil

The prevalence of dimeric to tetragmeric phenolic lignin decomposition products in bio-oil, together with water and a plethora of compounds of many classes, makes the fractional distillation of bio-oil impossible. In this respect, bio-oil differs from many grades of petroleum. The huge range of polarities and the large fraction of oxygenated compounds also differ from petroleum. If bio-oils are to be a future source of chemicals production, effective separation methods must be developed to generate fractions of similar polarity and to concentrate the undistillable compounds. Therefore, bio-oil solvent fractionation seems to be a very important topic to consider. Developments in the literature concur with this view.

Bio-oils are easily separated into an aqueous fraction and an organic fraction by adding water to bio-oil. Upon adding water, a viscous oligomeric lignin-containing fraction settles at the bottom, whereas a water-soluble fraction rich in carbohydrate-derived compounds form a top layer. However, much overlap of compound types exists in both fractions. Also, water addition cannot separate compounds of this lignin-rich fraction. The "lignin-rich" fraction usually constitutes 25%−30% of the whole bio-oil.[59] It contains oligomeric fragments originating from native lignin degradation. This lignin-rich fraction has not yet been commercialized, but applications such as the use of the lignin as a phenol replacement in phenol formaldehyde resins has been studied extensively. [196,197] Whole bio-oil and especially the lignin-rich fraction have been proposed for use as a wood preservative to replace CCA and or creosote.[196,197,202]

Wood preservative studies are currently underway at Mississippi State University. The production of chemicals from bio-oil and/or its lignin-rich fraction is possible; however, the complexity makes this a challenge on the commercial scale. Bio-oil fractionation procedures have been developed and several are discussed here. Schematic diagrams have been provided to aid the reader as a rapid visual response. Various fractionation methods are compared in a tabular form.

14.1. Fractionation of Vacuum-Pyrolyzed Softwood Bark Bio-oil.[96,97] Bio-oil obtained via the vacuum pyrolysis of softwood bark residues was solvent-fractionated via a column elution process.[96,97] The pyrolysis was performed in a cylindrical stainless steel retort that was placed in a Lindberg three-zone vertical electric furnace. Unlike fast pyrolysis, the heating rate was only 12 °C/min, from 25 °C to 500 °C. The sample (80 g) was held at 500 °C for 1 h. Bio-oil thus obtained is a multiphase, viscous, unstable system composed of water-soluble and water-insoluble fractions.[96,97] Bio-oil was separated by centrifugation into an upper layer (ca. 16 wt %) and a bottom layer (ca. 84 wt %). Samples of the upper layer, bottom layer, and whole bio-oil (each with a mass of 1 g) were successfully fractionated in a glass column that had an internal diameter (ID) of 16 mm, packed with 15 g of 70−230 mesh silica gel. Five fractions of each sample were collected by successive elution with increasingly polar solvents, as listed in Table 32. Solvents were removed and the recovered bio-oil fractions were weighed and analyzed. The upper layer had a minor methanol-insoluble content, high viscosity, and high calorific value. The properties of the bottom layer are very similar to those of the whole bio-oil, except that the bottom layer contained more ash and water.

Table 32. Solvents Used for the Fractionation of Vacuum-Pyrolyzed Softwood Bark Bio-oil Samples[a]

solvent	polarity index	applications

pentane	0.00	nonpolar to less-polar compounds (e.g., hydrocarbons, olefins)
benzene	3.0	less or moderately polar compounds (e.g., phenols and oxygenated compounds)
dichloromethane	3.4	less to moderately polar compounds (e.g., phenols and oxgenated compounds)
ethyl acetate	4.3	polar compounds (e.g., ketones and aldehydes)
methanol	6.6	strongly polar compounds (e.g., sugars and acids)

[a] Data taken from refs 96 and 97 with permission from American Chemical Society.

14.2. Fractionation of Vacuum-Pyrolyzed Birchwood Bio-oil.[93] Murwanashyaka et al.[93] separated and purified syringol from birchwood-derived vacuum pyrolysis oil. The steps used for the separation of various fractions are described in Scheme 2. A 10-mL fraction was extracted three times with 20 mL of pentane. The pentane-soluble fraction was concentrated under vacuum. The pentane-insoluble fraction was dissolved in 20 mL of toluene and extracted three times with 10 mL of distilled water. The syringol-rich fraction was obtained after the evaporation of toluene. The water fraction was extracted three times with 10 mL of ethyl acetate. The solvent was evaporated under vacuum and water was discarded. The pentane-, toluene-, and ethyl acetate-soluble fractions were subjected to GC/MS analysis.

Scheme 2. Syringol Separation and Purification from Birchwood Vacuum Pyrolysis Oil[93]

14.3. Fractionation of Vacuum-Pyrolyzed Cashew Nut Shell Bio-oil.[136,137] The stepwise procedure shown in Scheme 3 was used for fractionation by column elution and chemical characterization of both cashew nut oil and the pyrolysis aqueous fraction.[136,137] Oil CO1 (described under agricultural wastes/residues), obtained at 100−175 °C (1 g), was adsorbed on 2 g of silica gel and then transferred to a 450-mm-long × 25-mm-ID glass column packed with 60−120 mesh silica gel in hexane. The oil was eluted sequentially with hexane−ethyl acetate mixtures in different proportions, as well as a chloroform−methanol mixture (Scheme 3), to give fractions CO1−I and CO1−II, respectively. Oil fraction CO2 was generated by pyrolysis at 500 °C under vacuum (720 mm Hg). A 1-g sample of oil CO2 was adsorbed on 2 g of silica gel and transferred onto the prewashed and activated silica gel (60−120 mesh) packed in a 450-mm-long × 35-mm-ID glass column. The oil sample was eluted sequentially with the increasingly polar solvent mixtures, as given in Scheme 3.

Scheme 3. Schematic Diagram for Separation and Chemical Characterization of Cashew Nut Shell Oil[136,137]

14.4. NREL Bio-oil Solvent Method. [198] The NREL method[198] to solvent fractionate bio-oil is diagramed in Scheme 4. First, the whole bio-oil (1 kg) was dissolved in ethyl acetate (EA) on

a 1:1 (wt/wt) basis. The oil was then vacuum-filtered through filter paper to remove char. Upon standing, the EA/pyrolysis oil separated into two phases: an organic-rich, EA-soluble (top) phase and an EA-insoluble (bottom) phase. Most of the water formed during pyrolysis was contained in the EA-insoluble phase. The EA-soluble portion of the oil was washed with water (2 × 75 mL) to remove the remaining water-soluble products. The EA-soluble phase was then extracted with aqueous $NaHCO_3$ (5% w/w, 10 × 200 mL) and the basic aqueous layer was saved for isolation of the acidic organic fraction, which contained the phenolic and neutral (P/N) fractions. EA was evaporated from the EA extraction layer. Because EA was not dried prior to evaporation, water was azotroped during distillation (Scheme 2).

Scheme 4. NREL Bio-oil Fractionation Method[198]

14.5. Solvent Fractionation of Biomass-Derived Flash Pyrolysis Oils. [199] Sipila et al.[199] developed a solvent fractionation for the separation and characterization of biomass-based fast pyrolysis oils. Their method (Scheme 5) was based on an initial water fractionation of the oils, followed by further extraction of the water-soluble fraction with diethyl ether. Pyrolysis oil was slowly added dropwise with constant stirring into distilled water in a 1:10 weight ratio. The powderlike water-insoluble fraction was removed by filtration (<0.1 μm). This fraction was further washed with distilled water, vacuum-dried at <40 °C, and weighed. The drying temperature had to be kept low, because the fraction became darker at 60 °C and melted at 80 °C. The complete method is illustrated in Scheme 5.

Scheme 5. Solvent Fractionation for the Separation and Characterization of Biomass-Based Flash Pyrolysis Bio-oil[199]

14.6. Extraction of Phenols from Eucalyptus Wood Pyrolysis Tar.[105] Primary pyrolysis oil (2−6 g) was dissolved in an equal weight of EA, to improve the flowability and to decrease the original oil density. The solution was then mixed with an aqueous NaOH solution in a 1:1 ratio. The phases were clearly visible at this ratio. The mixture was shaken in a separatory funnel, and the phases were separated after standing. The pH then was measured. Alkaline extraction of the solvent phase was repeated five times with fresh alkali solution. An aliquot of the aqueous phases was taken in each stage to determine the phenolic composition in the extract. The combined aqueous phases were collected and the phenols were regenerated by acidifying the solution with 50% sulfuric acid. EA was used as an organic solvent to recover the phenols from aqueous phase. The extraction was repeated four times with an 0.5:1 solvent/aqueous phase ratio. Aliquots were taken from the EA layer to analyze the phenolic content of the extracts and to determine the number of stages required. The extraction procedure was performed using NaOH solutions of 2, 0.3, and 0.05 M, to determine the effect of pH on the recovery of phenols. The complete liquid−liquid extraction procedure is given in Scheme 6.

Scheme 6. Extraction Procedure for the Isolation of Phenols from Eucalyptus Tar[105]

14.7. Bio-oil Extraction Procedure by Shriner et al. [200] This extraction procedure starts with a water wash to isolate the water solubles (see Scheme 7). The water insolubles were extracted with 75 mL of ether. The ether insolubles (residue 1) were filtered. [200,201] The ether solution (solution 1) was extracted next, using 5% HCl. This acid solution, containing the

bases and amphoteric compounds, was discarded, whereas the ether layer was retained. The ether layer was then extracted with 5% NaOH to give ether layer 4 and solution 4. The ether layer was evaporated to yield neutral compounds. The aqueous solution (solution 4) was cooled and saturated with CO_2. The weak acids were then extracted with several portions of ether (ether layer 5), which was then evaporated to concentrate the weak acids that contained the phenols. The aqueous portion (solution 5) was acidified and extracted with ether to yield the stronger acids.

Scheme 7. Bio-oil Extraction Procedure by Shriner et al.[200]

14.8. Bio-oil Extraction Method of Christan et al. [202] Separation of four groups of organic compounds in the bio-oil was performed[202] according to Scheme 8. The first step involved an initial extraction of the total bio-oil with ethyl ether. The ether phase was divided into two parts; one part was retained and identified as the ethyl ether fraction (F1), and the other part was treated with 1 M aqueous NaOH to precipitate the phenols as phenolates. The organic phase remaining after NaOH treatment was evaporated to obtain the neutral fraction (F3). After re-acidification with HCl to pH 4, an extraction was conducted with EA to obtain the "phenolic" fraction (F4). This F4 fraction is considered to be a purified version of the ethyl ether fraction. The remaining aqueous phase was then extracted with EA to obtain another more-polar fraction, which was identified as the EA fraction (F2).

Scheme 8. Aqueous Phase Fractionation of Bio-oil Developed by Christian et al.[202]

14.9. Fractionation Method Developed by Oasmaa and Coworkers.[83-85] The solvent fractionation of bio-oil was performed as shown in Scheme 9 by Oasmaa et al.[83-85] First, the liquid pyrolysis oil samples were washed with water. The water-insoluble fraction precipitated and was removed by filtration. This solid was dried, and the dried residue was weighed. This residue was further extracted with dichloromethane. Dichloromethane solubles and insolubles were evaporated (≤40 °C) and each of these two dried residues were weighed. The water-soluble fraction was further extracted with diethyl ether and dichloromethane. These fractions are called "diethyl ether solubles" and "diethyl ether insolubles". Diethyl ether solubles and diethyl ether insolubles were evaporated (≤40 °C), and residues were dried and weighed.

Scheme 9. Fractionation Scheme Developed by Oasmma and Co-workers[83-85]

The various fractionation methods previously discussed are compared (Table 33).

Table 33. Bio-oil Fractionation Methods

method name	solvents used	mode of separation	targeted chemicals	reference(s)

fractionation of vacuum-pyrolyzed softwood bark derived bio-oil	pentane, benzene, dichloromethane, ethyl acetate, methanol	column separation	−	96, 97
fractionation of vacuum-pyrolyzed birchwood-derived bio-oils	pentane, tolune, water, ethyl acetate	column separation	Syringol	92
fractionation of vacuum-pyrolyzed cashew nut shell bio-oil	hexanes−ethyl acetate mixtures and chloroform methanol mixture	column separation		136, 137
NREL bio-oil solvent method	ethyl acetate, sodium bicarbonate, phosphoric acid, sodium chloride, water	solvent extraction	lignin-rich fraction	198
fractionation of biomass-derived flash pyrolysis oils	diethyl ether	solvent extraction		199
extraction of phenols from eucalyptus wood pyrolysis tar	ethyl acetate, sodium hydroxide	solvent extraction	phenolic fraction	105
bio-oil extraction procedure by Shriner et al.	ether, sodium hydroxide	solvent extraction	acids and neutrals	200
bio-oil extraction method of Christan et al.	ethyl acetate, sodium hydroxide	solvent extraction	acids, neutrals, and phenols	202
fractionation method of Oasmaa et al.	hexane, dichloromethane, diethyl ether	solvent extraction	lignin-rich fraction	83−85

16. 15. Reactors for Fast Pyrolysis

The heart of a fast pyrolysis process is the reactor and considerable research development has focused on reactor types. During the last two decades, several different reactor designs have been explored that meet the rapid heat-transfer requirements. These reactor configurations have been shown to achieve liquid-product yields as high as 70%−80%, based on the starting

dry biomass weight. Bridgewater et al.[19] published an excellent review that classified the reactors within the following categories: (1) fluidized-bed reactors,[87,203] (2) transported and circulating fluidized-bed reactors,[88,204] (3) ablative (vortex and rotating blade) reactors, and (4) rotating cone reactors and vacuum reactors.[13,90,205] Meier and Faix[22] discussed the state-of-the-art of reactors applied to fast pyrolysis of lignocellulosic materials. Various types of pyrolytic reactors were compared and discussed in this review. Scott et al.[29] analyzed several reactors for conducting biomass pyrolysis. This publication noted that only four main technologies are available for the commercialization of "pyrolysis", which generates acceptable yields of liquid products. These are (a) shallow fluidized-bed reactors; (b) vacuum pyrolysis reactors; (c) ablative reactors, both cyclonic and plate type; and (d) circulating fluidized-bed reactors (both dilute and dense types). In addition to these four classifications, we also consider a fifth class: (e) auger reactors**.** The locations of the various operating pyrolysis reactors are given in Table 34. The main highlights of the important reactors are discussed below.

Table 34. Fast Pyrolysis Reactor Type and Locations

reactor type	location(s)
ablative	Aston University, NREL, BBC, Castle capital
auger	ROI and Mississippi State University
circulating fluidized bed	CPERI, CRES, ENEL
entrained flow	GTRI, Egemin
fluidized bed	Aston University, Dynamotive, Hamberg University, Leeds University, NREL, Oldenberg University, VTT
rotating cone	Twente University, BTG/Schelde/Kara
transported bed	Ensyn (at ENEL, Red Arrow, VTT)
vacuum moving bed	Laval University/Pyrovac

15.1. Bubbling Fluidized-Bed Reactors. Bubbling fluidized beds (Figure 8) are usually referred to simply as fluidized beds, as opposed to circulating fluidized beds. Bubbling fluidized beds are a well-understood technology. They are simple to construct and operate, and they provide good temperature control and very efficient heat transfer to biomass particles, because of the high solids density in the bed.[206] Sand is often used as the solid phase of the bed. Bubbling fluidized beds produce good quality bio-oil with a high liquid product yield. Char does not accumulate in the fluidized bed, but it is rapidly eluted. Shallow fluidized beds can be readily scaled up; however, according to Scott et al.,[29] the low bed height-to-diameter ratio causes transverse temperature and concentration gradients to develop in large reactors. Special designs are needed to alleviate the processing problems that result during scaleup. The residence time of solids and vapors is controlled by the fluidizing gas

flow rate. Char has a higher residence time than the vapors. The char acts as an effective vapor cracking catalyst at fast pyrolysis reaction temperatures. Therefore, rapid and effective char separation is important. This is usually achieved by ejection followed by separation in one or more cyclone separators. Thus, careful design of sand and biomass/char hydrodynamics is important. Experience with the process has led to a somewhat different view of the optimal conditions for fast pyrolysis and has resulted in the recent development of a new fluidized-bed process the RTI process.

Figure 8 Bubbling fluidized-bed reactor (Redrawn, with permission, from Bridgwater.[54] (Copyright 2003, Elsevier, Amsterdam.)

15.2. Circulating Fluidized Beds and Transported Bed Reactors. Circulating fluidized bed (CFB) and transported bed reactor systems (Figure 9) have many of the features of bubbling beds (described above), except that the residence time for the char is almost the same as that for the vapors (http://www.pyne.co.uk). Furthermore, the char is more attrited, because of higher gas velocities. This can lead to higher char contents appearing in the condensed bio-oil. Although many studies have been reported, only a few [207] are relevant in regard to investigating CFB reactor performance under suitable pyrolysis conditions. Most circulating beds are dilute phase units. Their heat-transfer rates are not particularly high, because they are dependent primarily on gas−solid convective transfer. Moreover, if the CFB common twin-bed reactor type is used, with the second vessel employed as a char combustor to reheat the circulating solids, ash carryover to the pyrolyzer is possible. This leads to ash buildup in the circulating solids. Biomass ash is known to be a cracking catalyst for the organic molecules in the volatile pyrolysis products. This causes a loss of volatiles from the bio-oil yield.[29] An advantage of CFBs is that they are suitable for very large throughputs, even though the hydrodynamics are more complex. This technology is widely used at very high throughputs in the petroleum and petrochemical industry.

Figure 9 Schematic of the circulating fluidized bed reactor (redrawn, with permission, from Bridgwater.[54] (Copyright 2003, Elsevier, Amsterdam.)

15.3. Vacuum Pyrolysis Reactors. Vacuum pyrolysis (Figure 10) is actually not a true fast pyrolysis, because the heat-transfer rate, both to and through the solid biomass, is much slower than that observed in other reactors.[18,32,91] Thus, pyrolysis products evolve from the solid phase over a longer time frame. However, the vapor residence times are comparable to those in fast pyrolysis. Vacuum pyrolysis involves the thermal decomposition of biomass under reduced pressure.[18,32,91] The complex organic molecules decompose into primary fragments when heated in the reactor. The fragmented products are vaporized and quickly withdrawn from the reactor by vacuum. They are then recovered in the form of pyrolytic oils by condensation. These fragments are often very high-boiling-point compounds; therefore, they could undergo further cleavage to lower-boiling-point fragments in the absence of an applied vacuum.[18,32,91,94,95] Their more-rapid volatilization under vacuum minimizes the extent of secondary decomposition reactions. Thus, the chemical structure of the pyrolysis products more closely resembles the original structures of the complex biomolecules that constitute the original organic material.

Figure 10 Schematic of the vacuum pyrolysis laboratory-scale installation (reprinted, with permission, from Garcìa-Pèrez et al.[94]). (Copyright 2002, Elsevier, Amsterdam.)

Vacuum pyrolysis of biomass is generally conducted at a temperature of ~450 °C and a total pressure of 15 kPa. The main feature of the vacuum pyrolysis process is that a short residence time for volatiles is easily achieved. Therefore, the residence time of the volatile molecules is not coupled to the residence time of the biomass particles, which continue to decompose in the reactor.[29] However, this technology suffers from poor heat- and mass-transfer rates, and it requires larger-scale equipment.

15.4. Ablative Pyrolysis Reactors. Ablative pyrolysis relies on heat transfer occurring when a biomass particle impacts and slides over a solid hot source. Ablative pyrolysis **(**Figure 11) is substantially different in concept, compared to other methods of fast pyrolysis, where the reaction is limited by the rate of heat transfer through a biomass particle. This is why small particles are required. The mode of reaction in ablative pyrolysis is analogous to melting butter in a frying pan: pressing down and moving the butter over the heated pan surface can significantly enhance the rate of melting. This speeds heat transfer; shearing action creates more surface area, which can then contact the heat source, further increasing heat transfer (http://www.pyne.co.uk).

Figure 11 Schematic of the NREL Vortex Ablative bed reactor (redrawn, with permission, from Bridgwater.[54] (Copyright 2003, Elsevier, Amsterdam.)

During ablative pyrolysis, heat is transferred from the hot reactor wall to “melt” wood that is in contact with it under pressure (http://www.pyne.co.uk). The pyrolysis front moves unidirectionally through the biomass particle. As the wood is mechanically moved away, the residual oil film both provides lubrication for successive biomass particles and also rapidly evaporates to give pyrolysis vapors for condensation and collection in the same way as other processes. The rate of reaction is strongly influenced by pressure, the relative velocity of wood on the heat-exchange surface, shear forces that reduce particle size and increase surface area, and the reactor's surface temperature. The unique selling points of ablative pyrolysis are (a) a high pressure of biomass particles on the hot reactor wall is achieved, because of centrifugal force or mechanical force; (b) high relative motion exists between biomass particles and the reactor wall; and (c) reactor wall temperatures are <600 °C (http://www.pyne.co.uk).

The effects of reactor configuration (ablative and wire-mesh pyrolysis reactor) on the yields and structures of pine wood-derived pyrolysis liquids have been studied.[61] Comparison of liquid yields determined for the two reactors has been used to assess the effect of secondary reactions on yields during ablative pyrolysis. Structural charcterization and comparison of liquids produced in the two reactors have been assisted by SEC, UV-fluorescence spectroscopy, and FTIR spectroscopy. Small structural differences were observed, either due to the cracking of lignin-derived macromolecules on the heated reactor surface or low-molecular-weight components that formed during the slow pyrolysis of a small proportion of the feed. Comparison of the ablative liquids with those from other ablative pyrolysis reactors shows similar trends in molecular mass distribution and structures, suggesting that the ablative pyrolysis process inherently cracks some of these liquids during volatilization. Dry organic liquid yields from ablative pyrolysis process reactor were 2.5%−5.3% lower than the wire-mesh reactor in the temperature range of 55−600 °C.

The ablative pyrolysis reactor operates on the principle of "scraping" a continuous stream of biomass particles on a heated surface, under conditions of high relative motion and high-applied pressure.[61,62] In the wire-mesh reactor configuration, formation of a fine dispersion of a small quantity of sample (4−6 mg) and the rapid removal of volatiles from the reaction zone occurs. This ensures that the volatiles released during pyrolysis are captured under conditions that minimize extra particle secondary reactions.

15.5. Auger Reactor. Recently, Mississippi State University constructed an auger-feed pyrolysis reactor that had the following features:

(1) It is compact and does not require carrier gas.

(2) It operates at lower process temperatures (400 °C).

(3) It operates as a continuous process.

Augers are used to move biomass feedstock (wood, organic residue, agricultural residue) through an oxygen-free cylindrical heated tube. A passage through the tube raises the feedstock to the desired pyrolysis temperature (which can be in the range of 400−800 °C), causing it to devolatize and gasify. Char is produced and gases are condensed as bio-oil and noncondensables are collected as biogas. This design consequently reduces energy costs. Also, the vapor residence time can be modified by increasing the length of the heated zone through which the vapors pass prior to entering the condensor train.

A brief description, as well as the operating conditions, advantages, and disadvantages of various reactors used for fast pyrolysis, are presented in Table 35

Table 35. Brief Description, Operating Conditions, Advantages, and Disadvantages of Various Reactors Used for Fast Pyrolysis (Extended forms of 19 and 22, with permission from Elsevier)

bio-oil yield (%)	method of heating	suggested mode of transfer	operational pyrolysis unit	strengths/ advantages	disadvantages/challenges
Fluidized Bed Reactor					
75	heated recycle gas/ hot inert gas	95% conduction, 4% conventional, 1% radiation	400 kg/h at Dynamotive, 250 kg/h at Welman (U.K.), 20 kg/h at RTI	• good temperature control • easy scalability • well-understood technology	• small particle sized are needed • heat transfer to bed has yet to be proven at large scale
Circulating Fluidized Bed Reactor					
75	particle gasification/	80% conduction, 19% conventi	1000 kg/h at Red Arrow (Ensyn),	• good temperature control • large particle sizes may possibly be used	• hydrodynamics more complex than others • char is finer due to more attrition at higher velocities requires attention

	fire tubes	onal, 1% radiation	20 kg/h at VTT (Ensyn)	• suitable for large throughputs • well-understood technology	• heat transfer to bed has yet to be proven at large scale
Rotating Cone Reactor					
65	gasification of char to heat sand	95% conduction, 9% conventional, 1% radiation	120 kg/h at BTG (Netherlands)	• centrifugal force moves heated sand and biomass	• heat transfer to bed has yet to be proven at large scale • small particle sizes needed
Vacuum Reactor					
35−50	wall and sand heating	4% conduction, 95% conventional, 1% radiation	350 0 kg/h at Pyrovac	• lower temperature required • can process larger particles than others • no carrier gas is required	• not a true fast pyrolysis as solids residence time is very high • liquid yields of 35%−50% on dry feed basis
Ablative Reactor					
75	direct contact with hot surface	350 kg/h at Fortum, Finland	• large particle sizes may possibly be used • inert gas is not required • system is more intensive • low temperature (<600 °C)		• reaction rates limited by heat ransfer to the reactor, not to the biomass • process is surface area controlled so scaling is costly • reactor is costly
Auger Reactor					
30−50	ablative	−	200 kg/h at ROI, 1 kg/h at MSU (USA)	• compact, does not required carrier gas • lower process temperature (400 °C)	• moving parts in the hot zone • heat transfer at large scale may be a problem

17. 16. Contributions by Dynamotive and Lurgi

Dynamotive (http://www.dynamotive.com) is an emerging, renewable energy technology company; it has patented Biotherm, which is a fast pyrolysis technology for converting wood and agricultural wastes to a renewable liquid fuel (bio-oil) and char for activated carbon. This is a modification of a process originally developed by Resource Transformations

International, Ltd., which was formed in conjunction with researchers from the University of Waterloo. In this process, a fluidized-bed pyrolytic reactor operates at ∼450−500 °C on waste that is shredded and dried. A cyclone separates the particulate matter, and the remaining gases are condensed to oil. Bio-oil (65%−75%), gas (10%−15%), and inorganic char (10%−25%) are produced. Dynamotive has two plants in Canada, with capacities of 2 and 14 tons/day. A third, with a capacity of 110 tons/day, was commissioned in 2004 at the Erie Flooring and Wood Products plant in West Lorne, Ontario. The bio-oil from this facility will be used to fuel a gas turbine that was developed by Magellan Aerospace to produce up to 2.5 MWe of electricity.

The company has a strong intellectual property position, having acquired patents associated with fast pyrolysis technology in early 2000, and they are developing a scalable 15 tons/day demonstration facility.

Lurgi, which is a subsidiary of the German engineering company Metallgesellschaft AG, has attempted to supply a variety of systems for many significant wastes. Lurgi's gasifier technologies include the following: FB gasifier (nonslagging), FB gasifier/British Gas Lurgi gasifier (slagging), fluidized-bed gasification (CFB), entrained-flow gasification (Destec Gasifier), and the Lurgi Residue (LR) thermal gasification process. Lurgi also has licenses for the Ebara fluidized-bed waste technology for Europe and the patented Pyromelt technology (see Figure 12). [208-211]

Figure 12 Schematic of the Lurgi gasification process.

18. 17. Need for Further Reactor Development

According to Scott et al.,[29] none of the reactor concepts described above fully satisfies all requirements, in their present state of development, as a methodology for the production of an alternative liquid fuel with a reasonably trouble-free operation, proven scale-up technology, and economically competitive performance. Scott et al.[29] devised an improved version of the bubbling fluidized-bed approach for biomass pyrolysis and described its operation. This process allowed easier scaleup and significantly improved energy efficiency. Specific objectives that should be addressed in the design of a bio-oil production process include the following:[29]

(1) Bio-oil vapor quenching requirements should be minimized, using a small recycle ratio (i.e., a small gas/biomass feed ratio).

(2) The biomass pyrolysis reactor should operate at the minimum possible temperature, preferably 400−420 °C.

(3) An independent heat supply allows more design flexibility and easier control.

(4) Preheating of the recycle product gas above 600 °C should be avoided, because this may form microparticulate carbon (soot), because of the decomposition of CO or organic vapors.

(5) The reactor should cause a minimum amount of char particle attrition.

(6) The “blow through” mode of operation used in the Waterloo fast pyrolysis process to elute char should be retained, to avoid the buildup of char when a fluidized bed is used.

(7) Char should be collected separately, to allow flexible use of this fraction.

A comparison of yields from Waterloo fast pyrolysis and the RTI process (an improved version of the bubbling fluidized-bed approach) has been made[29] and is given in Table 36.

Table 36. Comparative Evaluations of Product Yields from the Waterloo Fast Pyrolysis Process and the RTI Processes[a]

		Experimental Yields of Hardwood Sawdust Feed (wt %)		
process	temperature (°C)	char	bio-oil	gas
WFPP	425	30.5	59.6	5.9
WFPP	500	11.8	76.9	11.0
RTI	430	12.5	74.3	10.1
RTI process plus char converter at 800 °C	430	4.5	73.0	19.0

[a] Data taken from ref 29 with permission from Elsevier.

19. 18. Bio-oil Applications

Bio-oil can serve as a substitute for fuel oil [212] or diesel in many static applications, including boilers, furnaces, engines, and turbines for electricity generation.[54,213,214] A surface-active bio-oil (SABO) solution, that was prepared from vacuum pyrolysis bio-oil with a phenol-to-levoglucosan mass ratio of 4.8, was used as a foaming agent in the flotation of sulfured copper mineral. [215] Scheme 10 summarizes some possible uses of bio-oil.

Scheme 10. Application of Bio-Oils (taken from ref 54 with permission from Elsevier)

18.1. Heat Production. The heating value of bio-oil is lower than that for fossil fuel, because of the large number of oxygenated compounds and a significant portion of water. Nevertheless, flame combustion tests showed that fast pyrolysis oils could replace heavy and light fuel oils in industrial boiler applications (http://www.btgworld.com).[54,71] Bio-oil is similar to light fuel oil in its combustion characteristics, although significant differences in ignition, viscosity, energy content, stability, pH, and emission levels are observed. The issues related to the transport, handling, and storage of biomass-derived fast pyrolysis liquid were discussed by Peacocke and Bridgwater. [216] Fractional condensation of biomass pyrolysis vapors can be used to remove a portion of the water, thereby increasing the heating value and reducing the weight of oil per unit of heat generated upon combustion. This possibility has not been fully discussed or described yet in the published literature.

18.2. Electricity Production. The use of a bio-oil requires engine modifications mainly to its high acidity (http://www.btgworld.com). The most important changes involve the fuel pump, the linings, and the injection system. Slight modifications of both the bio-oil and the diesel engine can render bio-oils an acceptable substitute for diesel fuel in stationary engines.[215] Bio-oil blends with standard diesel fuels or bio-diesel fuel is also possible.[217-219] Experience with bio-oil combustion in gas turbines has also been reported.[220]

Emulsions were developed from biomass pyrolysis oil.[221] These emulsions were characterized and tested in diesel engines.[222] Guéhenneux et al.[223] pyrolyzed straw and fescue in a temperature range of 550−650 °C with different residence times. The production of hydrogen and gas oil was studied. A coefficient of pyrolytic volitilization was established, taking into account the quanity of tars produced, quality of plumes, and the proportions of H_2 and CO. Solantausta et al.[224] studied the use of pyrolysis oil as a diesel power plant fuel by analyzing the oil's composition and testing this fuel in a diesel engine. The economics of the system were also analyzed.

18.3. Synthesis Gas Production. Biomass can have a major role in the production of "green" hydrocarbons, because it is the only large-scale renewable source available (http://www.btgworld.com). A comparison between the use of the solid biomass and the use of the liquid bio-oil as feedstock for synthesis gas production encourages serious consideration of the gasification of bio-oil in large-scale syngas generation.[50,225-232] Gasification of bio-oil with pure oxygen and further processing of the crude synthesis gas in Fischer−Tropsch processes may become technically and economically feasible.

The production of synthetic gas/high-Btu gaseous fuel from the pyrolysis of biomass-derived oil (e.g., bio-oil) was studied.[233,234] Pyrolysis of bio-oil at various temperatures in a small tubular reactor was performed at atmospheric pressure. Bio-oil was fed at a flow rate of 4.5−5.5 g/h, along with nitrogen (18−54 mL/min) as a carrier gas. Bio-oil conversion to gas was 83 wt %, whereas gas production was 45 L/100 g of bio-oil at 800 °C and a constant nitrogen flow rate of 30 mL/min. The gas consisted of H_2, CH_4, CO, CO_2, C_2, C_3, and C_4−C_n hydrocarbons. The compositions of product gases were in the following ranges: syngas, 16−36 mol %; CH_4, 19−27 mol %; and C_2H_4, 21−31 mol %. Heating values were in the range of 1300−1700 Btu/SCF. Clearly, a strong potential exists for making syngas, methane, ethylene, and high-heating-value Btu gas from the pyrolysis of biomass-derived oil.

Bio-oil was gasified[233,234] to synthesis gas and gaseous fuels at 800 °C under atmospheric pressure in an Inconel tubular fixed-bed downflow microreactor, using mixtures of CO_2 and N_2, as well as mixtures of H_2 and N_2. Steam gasification was also performed by feeding biomass-derived oil at a flow rate of 5 g/h, along with steam (2.5−10 g/h) and nitrogen (30 mL/min) as a carrier gas. The composition of the various gas components was in the range of 75−80 mol % for syngas (H_2 + CO, including 48−52 mol % H_2) and 12−18 mol % as CH_4, from. Heating values of the product gas were in the range of 460−510 Btu/scf.

18.4. Chemical Production from Bio-oil, and Present and Future Applications. More than 300 compounds have been identified as fragments from the basic components of biomass, viz, the lignin, cellulose and hemicellulose derivatives.[235] Large fractions of acetic acid, acetone, and hydroxyacetaldehyde are reported in the analysis results. Despite this extensive analytical work, only 40%−50% of the oil (excluding the water) has been completely structurally characterized (http://www.btgworld.com). The large, less-severely cracked molecules are not yet specifically identified. All types of functional groups are present in these larger fragments: acids, sugars, alcohols, ketones, aldehydes, phenols and

their derivatives, furans, and other mixed oxygenates. Phenolic compounds may be present in high concentrations (up to 50 wt %) (http://www.btgworld.com). Some lignin-derived fragments have molecular weights in the range of 5000 amu. Structures are variable and dependent on factors such as the feed species used, heat-transfer rates, pyrolysis conditions, and further reactions in the hot gases.

Table 37. Properties of Bio-oils Produced from Different Feedstocks Using Various Reactors

type of feed	reactor/process	temperature (°C)	oil yield (wt %)	residence time	water (wt %)	pH	solids (wt %)	viscosity	reference
hard wood (oak, maple)	Ensyn, Canada				19.9	3.7	0.35	11 cSt at 50 °C	199
Scots	fluidized, 1 kg/h, VTT	530			11.1	2.6	0.18	46 cSt at 50 °C	199
wheat straw	fluidized, 1 kg/h, VTT	530			23.3	2.8	0.30	50 cSt at 50 °C	199
wood (64 %)	ablatic, 20−25 kg/h			< 0.3 s	16.9−32.0	2.5−3.7		20−80 cP at 40 °C	243
oak wood	ablatic, 14.6 kg/h	625	65.7	< 1 s	16.1	2.9		159 cP at 40 °C	25

Acacia		500		15–30 min	5			240 cP at 25 °C	244
maple oak (moisture 5.4%)	ENSYN from RTP facility	525		0.35 s	26			107 cP at 25 °C	244
rice straw (AW)	fluidized bed, 3 kg/h	412		~2–3 s	43	4.2	3–0.1		35
sesame stalk	fixed bed	550	37.20	30 min					127
rapeseed	Heinze	500	46.0	30 min	none			43 cSt at 50 °C	129
olive bagasse	fixed bed	500	34.4	–	none			51 cSt at 50 °C	245
autotrophic *C. prototheoides*	fluidized bed, 4 g/min	500	16.6	2–3 s				0.10 Pa s at 40 °C	146
heterotrophic *C. prot*	fluidized bed, 4	500	57.9	2–3 s				0.02 Pa s at 40 °C	146

othecoides	g/min								
microalgae	fluidized bed, 4 g/min	500	17–27	2–3 s				0.10 Pa s at 40 °C	145
almond shell	fixed bed	400	53.1	30 min	22.3	5.5		1.68 cSt at 50 °C	135
cherry stones		600		30 min	40.0	2.6		1.29 cSt at 50 °C	246
bagasse	vacuum pyrolysis	500 at 8 kPa pressure	43		18.8	2.7	0.38	116.5 cSt at 20 °C, 26.7 cSt at 40 °C, 16.4 cSt at 50 °C, 11.2 cSt at 60 °C, 8.2 cSt at 70 °C, 5.4 cSt at 80 °C, 4.1 cSt at 90 °C	94
soft wood bark	vacuum pyrolysis, 50 kg/h	500 at 14 kPa pressure	20		24		0.34	128 cSt at 20 °C, 38 cSt at 40 °C, 24 cSt at 50 °C, 15 cSt at 60 °C, 10 cSt at 70 °C, 7.5 cSt at 80 °C	27
soft wood bark	vacuum pyrolysis	500			13	3.0		62 cSt at 50 °C, 15 cSt at 80 °C, 11 cSt at 90 °C	96
soft wood	fluidized, 5 kg/h, Hamburg		75		20	2.3		40−200 cP at 40 °C	22

biomass	fluidized, Aten, Itaky	500 at 1 atm	20.5	14.60		15–20	55 cP at 70 °C	18
fir	rotating cone, BTG, Netherlands			4.5			250 cP at 60 °C	18
beech	rotating cone, BTG, Netherlands			14.0	2.7		10 cP at 70 °C	18
wood	transported bed, Ensyn, Canada		83	22	2.5		450 cP at 40 °C	18
pine/spruce								
100% wood	Dynamotive			23.3	2.3	<0.1	73 cSt at 20 °C, 4.3 cSt at 80 °C	107
53% wood, 47% bark	Dynamotive			23.4	2.4	<0.1	78 cSt at 20 °C, 4.4 cSt at 80 °C	107
bagasse	Dynamotive			20.8	2.6	<0.1	57 cSt at 20 °C, 4.0 cSt at 80 °C	107

hardwood	ENSYN/RTP		70–75	0.5 s		10 cSt at 60 °C		247
sunflower oil cake	well-swept fixed-bed	550	48.69		13.13			248
sugar cane bagasse	fixed bed	450			2.8	89.34 cSt at 35 °C		249
jute stick	fixed bed	450			2.9	12.08 cSt at 35 °C		249
straw and stalk of rapeseed plant	tubular reactor	650	17.70	30 min	none			212

Table 37. (Continued)

						Elemental Analysis (wt %)					
type of feed	density	flash point (°C)	pour point (°C)	HHV (MJ/kg)	LHV (MJ/kg)	C	H	N	O	ash (wt %)	reference
hardwood (oak, maple)	1.186 kg/dm^3	56	−36		16.9	55.3	6.6	0.4		0.14	199

Scots	1.266 kg/dm³	76	−18		19.2	56.4	6.3	0.1		0.07	199
wheat straw	1.233 kg/dm³	>106	−9		16.6	58.4	6.0	0.1		0.09	199
wood (64%)	0.94–1.21 g/mL	45–100		22.5–30.2		54.8–72.8	4.8–6.5	0.1–0.6	21–39	0.05–0.95	243
oak wood	1.29 g/mL					46.3	6.8	0.1	46.8	0.05	25
Acacia	1.17 g/cm			25		58.8	6.9	0.6	33.7		244
maple oak (5.4% moisture)	1.19 g/cm			21		55.1	6.7	0.15	38.0		244
rice straw (AW)				17.3						0.1	35
sesame stalk				27		61.69	7.96	0.98	29.37		127
rapeseed	918 kg/m³	83		38.4		74.04	10.29	3.97	11.70		129

olive bagasse	1070 kg /m³	77		31.8	66.9	9.2	2.0	21.9		245
autotrophic *C. protothecoides*	1.06 kg/L			30	62.07	8.76	9.74	19.43		146
heterotrophic *C. protothecoides*	0.92 kg/L			41	76.22	11.61	0.93	11.24		146
microalgae	1.16 kg/L			29	61.52	8.50	9.79	20.19		145
almond shell	1106 kg /m³	110	−15	14.1	48.8	6.2	0.3	44.7		135
cherry stones	1100 kg /m³	72	−21	13.9	46.9	7.9	0.1	45.1		246
bagasse	1211 kg /m³ at 20 °C, 1195 kg /m³at 40 °C	>90		22.4	54.60	6.45	0.73	38.1	0.05	94
softwood bark	1.066 g/mL at 20 °C, 1.051 g/mL at 40 °C	>90	3	32.4	77.56	8.69	0.59	13.3	0.03	27

softwood bark	1188 kg/m³ at 28 °C			27.9	62.6	7.00	1.1	29.0	0.3	96
softwood	1.2 g/cm³			20	55	7				22
biomass				26.3	61.90	6.0	1.05	31.0	1.5	18
fir				22.2	58.12	6.55	0.52	34.81	<0.05	18
beech	1.216 g/cm³ at 15 °C			20.9	55.10	7.20	2.00	35.1		18
wood		55	25	23.1	56.4	6.2	0.2	37.1	0.1	18
pine/spruce										
100% wood	1.20 kg/dm³ at 15 °C			16.6					<0.02	107
53% wood, 47% bark	1.19 kg/dm³ at 15 °C			16.4					<0.02	107
bagasse	1.20 kg/dm³ at 15 °C			15.4					<0.02	107

hardwood				17.5	16.0	54.5	6.4	0.18	38.9	0.16	247
sunflower oil cake				32.2		66.5	9.2	4.5	19.8		248
sugar cane bagasse	1198 kg/m^3	105	−24	20.0		46.27	6.55	0.0	46.9	0.24	249
jute stick	1225 kg/m^3	>70	−14	22.0		47.18	8.36		44.1	0.33	249
straw and stalk of rapeseed plant	909 kg/m^3 at 30 °C			27.2		57.29	6.63	1.03	34.8	0.01	212

A large fraction of the oil is the phenolic fraction, consisting of relatively small amounts of phenol, eugenol, cresols, and xylenols, and much larger quantities of alkylated (poly-) phenols (the so-called water-insoluble pyrolytic lignin). This fraction has exhibited good performance as an adhesive or adhesive extender for waterproof plywood (http://www.btgworld.com).[198] Furfural and furfuryl alcohol are present in amounts up to 30 wt % and 12−30 wt %, respectively.

Liquid alkanes with the number of C atoms ranging from 7 to 15 (C_7−C_{15}) were selectively produced from biomass-derived carbohydrates by acid-catalyzed dehydration, followed by hydrogenation over bifunctional catalysts that contained acid and metal sites in a four-phase reactor.[236] In this process, the aqueous organic reactant becomes more hydrophobic and a hexadecane alkane stream removes hydrophobic species from the catalyst before they proceed further to form coke. These liquid alkanes are of the appropriate molecular weight to be used as transportation fuel components, and they contain 90% of the energy of the carbohydrate and H_2 feeds.

The only current commercially important application of bio-oil chemicals is that of wood flavor or liquid smoke. Several companies produce these liquids by adding water to the bio-oil. A red-colored product is obtained that can be used to brown and flavor sausages, bacon, fish, etc. (http://www.btgworld.com). The most effective browning agents are glucoaldehyde, glyceraldehydes, pruvaldehyde, dihydroxyacetone, acetone, and diacetyl. Because these compounds are also presnt in the bio-oils, these oils can be used as a source of smoke flavors and browning agent. The pyrolytic lignin fraction is comprised of a total phenolic content

from ∼30% to ∼80% (w/w). It is a highly reactive mixture of compounds that has been determined to be suitable for use as an extender within resin formulations without requiring any further extraction or fractionation procedures. Thus, pyrolytic lignin is sometimes called “natural resin”. Phenol/formaldehyde or urea/formaldehyde resins, comprising up to 60% of natural resin, have been prepared and tested in wood-based composites production and determined to exhibit similar properties that are associated with commercially available resins.

The natural resin may substitute for phenol, or for both phenol and formaldehyde within phenol-containing resins. Similarly, the natural resin can replace a substantial portion of the components within urea-containing resins.[100,101,237] Resols with different levels of phenol replacement by phenolic pyrolysis oils, formaldehyde:phenolics molar ratios, and NaOH:phenolics molar ratios were synthesized.[102] The bio-oil was prepared via vacuum pyrolysis at 450 °C and 22.5 kPa. Strandboards were manufactured with resins that had 25−50 wt % of phenol replaced by softwood bark-derived pyrolysis oils. The curing behavior of the formulated resins was also studied using DSC.[103]

Resins that contained up to 50 wt % pyrolysis oil showed slower cure kinetics and a lower extent of condensation reaction versus a neat laboratory-made phenol−formaldehyde resin. Similar slower-curing behavior was observed for the resols that had 25 wt % of the petroleum phenol replaced by pyrolysis oil. Increasing the amount of pyrolysis oil present in the resin decreased the thermal resistance of the resins. Cure kinetics and amount of curing of the resin were improved by adding propylene carbonate (PC) to the resins.[103] Many satisfactory results have been reported. However, resin producers want to market the reproducible, precisely tailored resin compositions that the end users demand. The variability within bio-oils and their fractions has made resin producers cautious in developing commercial resins from pyrolysis liquids.

Recently, a quantitative assessment was conducted of the economic competitiveness of bio-oil standard applications in 14 European countries.[238] A competitive factor (c_F) was developed that represented the total annual cost of a conventional alternative relative to bio-oil application. A wide variation was observed across Europe. A total of six countries had at least one bio-oil application, which was economically competitive now. Overall, heat-only applications were determined to be the most economically competitive, followed by combined heat and power (CHP) applications, with electricity-only applications being only very rarely competitive.[238] With the recent increase in the crude oil price, these quantitative assessments should be continuously updated in the search for commercial opportunities.

20. 19. Conclusions

The fast pyrolysis of biomass in the absence of oxygen has the potential to contribute to the world's need for liquid fuels and, ultimately, for chemicals production. However, the feed complexity and variability makes it difficult to define standard processes. Bio-oil production within the context of biorefineries is likely to be of greater value than self-standing bio-oil plants, much like the manner in which petroleum refinery economics is dependent on the formation of heavy oils, lubricants, fuel oils, gasoline, kerosene, waxes, and such chemicals as the BTX fraction, ethylene, propylene, etc. Therefore, we envision pyrolysis processes in which biomass alone, or biomass cofeeds with waxes, petroleum residues, waste plastics,

oxidized oils, and/or municipal wastes, can be varied and adapted to produce liquid fuels or gases of designed compositions to supply energy for transportation, heating, or electricity generation. We believe synergies with biodiesel production will exist in such refineries where the glycerin byproduct is fed into bio-oil production and is balanced by higher-percentage carbon co-feeds (such as waste plastics or tires).

The use of raw biomass as a source of chemicals production should become more attractive within the biorefinery concept. The current situation resembles the early days of the development of a chemicals industry from coal and coke or the later development of the early petrochemical industry. A huge amount of research and process development will be required. However, this will occur when, and if, either the economic incentive beckons or climate change regulations push us in this direction. Chemical and engineering knowledge is now far more advanced, so technical advances will occur more rapidly when economics dictate a change.

Major technical opportunities exist to develop catalytic biomass pyrolysis processes and subsequent catalytic transformation of the bio-oils and gases produced. This area is certainly understudied and in its infancy. The applications of novel solid feed mixtures for pyrolysis, catalysts, co-gas feeds, and related approaches have not been explored very much. These topics are open for development.

Adapting innovative chemical thinking should lead to major advances. For example, Dumesic[239] estimated that alkanes that were generated from corn would generate 2.2 times more energy than that required to generate these alkanes, if the water removal step can be eliminated. Dumesic[239] then went on to combine hydrogen generation from sorbitol with sorbitol hydrogenation to make hexane as one example. Also, cellulose was transformed by dehydration, aldol condensations, and hydrogenation to make longer-chain alkanes at 250−265 °C in a four-phase reactor system, using a $Pt/SiO_2{-}Al_2O_3$ catalyst. Processes such as this, combined with pyrolytic fuels production, eventually will have a role in augmenting the petrochemical industry. The world's population growth is inexorably pushing us in this direction.

At this time, daunting problems exist with establishing quality norms and standards for pyrolysis products for end uses. So many reactors, processes, and feeds exist that it is difficult to devise a way to accomplish this feat. Table 37 summarizes some bio-oils and their properties obtained from different sources.

This review (and this table) illustrates the feed, product, and process diversity that currently characterizes this topic.

For further bio-oil reading, see the literature cited in refs 251−270.

21. Author Information

Authors

- **Dinesh Mohan** - *Department of Chemistry, Mississippi State University, Mississippi State, Mississippi 39762, USA, Environmental Chemistry Division, Industrial Toxicology Research Centre, Lucknow, India, and Forest Products*

Department, Mississippi State University, Mississippi State, Mississippi 39762, USA

- **Charles U. Pittman** - *Department of Chemistry, Mississippi State University, Mississippi State, Mississippi 39762, USA, Environmental Chemistry Division, Industrial Toxicology Research Centre, Lucknow, India, and Forest Products Department, Mississippi State University, Mississippi State, Mississippi 39762, USA*
- **Philip H. Steele** - *Department of Chemistry, Mississippi State University, Mississippi State, Mississippi 39762, USA, Environmental Chemistry Division, Industrial Toxicology Research Centre, Lucknow, India, and Forest Products Department, Mississippi State University, Mississippi State, Mississippi 39762, USA*

22. References

This article references 270 other publications.

1. **1**

Technical, Environmental and Economic Feasibility of Bio-oil in New-Hampshire's North Country, UNH Bio-oil Team Report (Final Report submitted to NH IRC), August 2002 (available via the Internet at www.unh.edu/p2/biooil/bounhif.pdf).

Google Scholar

2. **2**

Davis, S. C. Transportation Energy Data Book 18, Technical Report ORNL-6941, Oak Ridge National Laboratory, Oak Ridge, TN, September 1998 (available via the Internet at http://cta.ornl.gov/data/Index.shtml).

[Crossref], Google Scholar

3. **3**

Maples, J. D.; Moore, J. S.; Patterson, P. D.; Schaper, V. D. Alternative Fuels for U. S. Transportation. Presented at the TRB Workshop on Air Quality Impacts of Conventional and Alternative Fuel Vehicles, Paper No. A1F03/A1F06, 1998 (available

via the Internet
at http://www.es.anl.gov/Energy_Systems/Publications/publications1998.html).

Google Scholar

4. **4**

Walsh, M. P., Highway Vehicle Activity Trends and Their Implications for Global Warming: The United States in an International Context. In *Transportation and Energy: Strategies for a Sustainable Transportation System*; American Council for an Energy-Efficient Economy: Washington, DC, 1995.

Google Scholar

5. **5**

Emissions of Greenhouse Gases in the United States, Technical Report No. DOE/EIA-0573(2003/es), 2003 (available via the Internet
at http://www.eia.doe.gov/oiaf/1605/ggrpt/).

Google Scholar

6. **6**

Biomass as Feedstock for a Bioenergy and Bioproducts Industry: The Technical Feasibility of Billion-Ton Annual Supply, Technical Report, USDA (U.S. Department of Agricultural Forestry Service), April 2005 (available via the Internet at feedstockreview.ornl.gov/pdf/ billion_ton_vision.pdf).

Google Scholar

7. **7**

Vesterby, M.; Krupa, L. Major Uses of Land in the United States. Statistical Bulletin No. 973. U.S. Department of Agricultural, Economic Research Services: Washington, DC, 1997 (available via the Internet at www.wilderness.net/NWPS/documents/sb973.pdf).

Google Scholar

8. **8**

Alig, R. J.; Plantinga, A. J.; Ahn, S.-E.; Kline, J. D. Land use changes involving forestry in the United States: 1952 to 1997, with projections to 2050. General Technical Report No. PNW-GTR-587, U.S. Department of Agriculture, Forest Service, Pacific Northwest Research Station, Portland, OR, 2003.

Google Scholar

9. **9**

Spurr, S. H.; Vaux, H. J. *Science***1976**, *191*, 752−756.

[Crossref], Google Scholar

10. **10**

Soltes, E. J. Problems and opportunities in the use of wood and related residues for energy in Texas. A report to the Texas House subcommittee on alternate sources of Energy for Agriculture. Texas A&M University: College Station, TX, March 13−14, 1978.

Google Scholar

11. **11**

Soltes, E. J.; Elder, T. J., Pyrolysis. In *Organic Chemicals from Biomass*; Goldstein, I. S., Ed.; CRC Press: Boca Raton, FL, 1981; pp 63−95.

Google Scholar

12. **12**

Knight, J. A.; Bowen, M. D.; Purdy, K. R. Pyrolysis A method for conversion of forestry wastes to useful fuels. Presented at the Conference on Energy and Wood Products Industry, Forest Products Research Society, Atlanta, GA, 1976.

Google Scholar

13. **13**

Peacocke, G. V. C.; Bridgwater, A. V. Ablative fast pyrolysis of biomass for liquids: results and analyses. In *Bio-oil Production and Utilisation*; Bridgwater, A. V., Hogan, E. H., Eds.; CPL Press: Newbury, U.K., 1996; pp 35−48.

Google Scholar

14. **14**

www.dynamotive.com.

Google Scholar

15. **15**

Churin, E.; Delmon, B. What can we do with pyrolysis oils? In *Pyrolysis and Gasification*; Ferrero, G. L., Maniatis, K., Buekens, A., Bridgwater, A. V., Eds.; Elsevier Applied Science: London, 1989; pp 326−333.

Google Scholar

16. **16**

Putun, E. *Energy Sources***2002**, *24* (3), 275−285.

[Crossref], Google Scholar

17. **17**

Demirbas, A. *J. Anal. Appl. Pyrolysis***2004**, *72*, 243−248.

Google Scholar

18. **18**

Bridgwater, A. V.; Peacocke, G. V. C. *Renewable Sustainable Energy Rev.***2000**, *4* (1), 1−73.

[Crossref], Google Scholar

19. **19**

Bridgwater, A. V.; Meier, D.; Radlein, D. *Org. Geochem.***1999**, *30*, 1479−1493.

[Crossref], Google Scholar

20. **20**

Bridgwater, A. V. *Chem. Eng. J.***2003**, *91* (2−3), 87−102.

Google Scholar

21. **21**

Bridgwater A. V. *J. Anal. Appl. Pyrolysis***1999**, *51*, 3−22.

[Crossref], Google Scholar

22. **22**

Meier, D.; Faix, O. *Bioresour. Technol.* **1999**, *68*, 71−77.

[Crossref], Google Scholar

23. **23**

Kelley, S. S.; Jellison, J.; Goodell, B. *FEMS Microbiol. Lett.***2002**, *209*, 107−111.

Google Scholar

24. **24**

Gerdes, C.; Simon, C. M.; Ollesch, T.; Meier, D.; Kaminsky, W. *Eng. Life Sci*. **2002**, *2* (6), 167−174.

[Crossref], Google Scholar

25. **25**

Czernik, S.; Johnson, D. K.; Black, S. *Biomass Bioenergy***1994**, *7* (1−6), 187−192.

[Crossref], Google Scholar

26. **26**

Oasmaa, A.; Meier, D. *J. Anal. Appl. Pyrolysis***2005**, *73* (2), 323−334.

[Crossref], Google Scholar

27. **27**

Boucher, M. E.; Chaala, A.; Roy, C. *Biomass Bioenergy***2000**, *19*, 337−350.

Google Scholar

28. **28**

Boucher, M. E.; Chaala, A.; Pakdel, H.; Roy, C. *Biomass Bioenergy***2000**, *19*, 351−361.

Google Scholar

29. **29**

Scott, D. S.; Majerski, P.; Piskorz, J.; Radlein, D. *J. Anal. Appl. Pyrolysis***1999**, 51, 23−37.

[Crossref], Google Scholar

30. **30**

Bridgwater, A. V. *Therm. Sci.***2004**, *8*, 21−49.

Google Scholar

31. **31**

Demirbas, A. *Energy Convers. Manage.***2000**, *41*, 633−646.

Google Scholar

32. **32**

Bridgwater A. V.; Czernik, S.; Piskorz, J. An overview of fast pyrolysis. In *Progress in Thermochemical Biomass Conversion*, Volume 2; Bridgwater, A. V., Ed.; Blackwell Science: London, 2001, pp 977−997.

[Crossref], Google Scholar

33. **33**

Rowell, R. M. *The Chemistry of Solid Wood*; American Chemical Society: Washington, DC, 1984.

[ACS Full Text], Google Scholar

34. **34**

Elliott, D. C. Chemicals from Biomass. In *Encyclopedia of Energy*, Volume 1, Elsevier: Amsterdam, Boston, 2004.

[Crossref], Google Scholar

35. **35**

Elliott, D. C. Issues in value-added products from biomass. In *Progress in Thermochemical Biomass Conversion*, Volume 2; Bridgwater, A. V., Ed.; Blackwell Science: London, 2001, pp 1186−1196.

[Crossref], Google Scholar

36. **36**

Zugenmaier, P. *Prog. Polym. Sci.***2001**, *26,* 1341−1417.

[Crossref], Google Scholar

37. **37**

Turner, M. B.; Spear, S. K.; Holbrey, J. D.; Rogers, R. D. *Biomacromolecules***2004**, *5* (4), 1379−1384.

[ACS Full Text], Google Scholar

38. **38**

Swatloski, R. P.; Spear, S. K.; Holbrey, J. D.; Rogers, R. D. *J. Am. Chem. Soc*. **2002**, *124* (18), 4974−4975.

[ACS Full Text], Google Scholar

39. **39**

Tang, W. K.; Neill, W. K. *J. Polym. Sci., Part C: Polym. Symp.***1964**, *6*, 65−81.

Google Scholar

40. **40**

Modorsky, S. L.; Hart, V. E.; Stravs, S. *J. Res. Natl. Bur. Stand.***1956**, 54, 343−354.

Google Scholar

41. **41**

Pakhomov, A. M.; Akad-Nauk, I.; Otdel, S. S. S. B. *Khim Nauk*, **1957**, 1457−1449.

Google Scholar

42. **42**

Runkel, R. O. H.; Wilke, K.-D. *Holzals Rohund Werkstoff***1951**, *9*, 260−270.

[Crossref], Google Scholar

43. **43**

McCarthy, J.; Islam, A. Lignin chemistry, technology, and utilization: a brief history. In *Lignin: Historical, Biological and Materials Perspectives*; Glasser, W. G., Northey, R. A., Schultz, T. P., Eds.; ACS Symposium Series 742; American Chemical Society: Washington, DC, 2000; pp 2−100.

Google Scholar

44. **44**

Fengel, D.; Wegner, G. *Wood: Chemistry, Ultrastructure, Reactions*. Walter de Gruyter: Berlin, New York, 1984; Ch. 6.5, pp 167−175.

Google Scholar

45. **45**

Nimz, H. H. *Tappi J.* **1973**, 56, 124.

Google Scholar

46. **46**

Berkowitz, N. *Fuel***1957**, *36*, 355−373.

Google Scholar

47. **47**

Kudo, K.; Yoshida, E. *J. Tap. Wood Res. Soc.***1957**, *3* (4), 125−127.

Google Scholar

48. **48**

Maschio, G.; Koufopanos, C.; Lucchesi, A. *Bioresource Technol.***1992**, *42* (31), 219−231.

Google Scholar

49. **49**

Jakab, E.; Varhegyi, G.; Faix, O. *J. Anal. Appl. Pyrolysis***2000**, *56*, 272−283.

[Crossref], Google Scholar

50. **50**

Bridgwater, A. V. *Appl. Catal., A***1994**, *116*, 5−47.

[Crossref], Google Scholar

51. **51**

Bridgwater, A. V. *Biomass***1990**, *22* (1−4), 279−290.

[Crossref], Google Scholar

52. **52**

Bridgwater, A. V.; Kuester, J. L. *Research in Thermochemical Biomass Conversion*; Elsevier Science Publishers: London, 1991.

Google Scholar

53. **53**

Bridgwater, A. V. *Catal. Today***1996**, *29* (1−4), 285−295.

[Crossref], Google Scholar

54. **54**

Bridgwater, A. V. *Chem. Eng. J.***2003**, *91*, 87−102.

Google Scholar

55. **55**

Demirbas, A. *J. Anal. Appl. Pyrolysis***2005**, *73*, 39−43.

[Crossref], Google Scholar

56. **56**

Emmons, H. W.; Atreya, A. *Proc. Indian Acad. Sci.***1982**, *5*, 259−268.

Google Scholar

57. **57**

Bridgwater, A. V.; Peacocke, G. V. C. *Renewable Sustainable Energy Rev.***2000**, *204* (1−2), 117−126.

Google Scholar

58. **58**

Di Blasi, C. *Prog. Energy Combust. Sci*. **1993**, *19*, 71−104.

[Crossref], Google Scholar

59. **59**

Czernik, S.; Bridgwater, A. V. *Energy Fuels* **2004**, *18*, 590−598.

Google Scholar

60. **60**

Peacocke, G. V. C.; Russel, P. A.; Jenkins, J. D.; Bridgwater, A. V. *Biomass Bioenergy***1994**, *7*, 169−178.

Google Scholar

61. **61**

Peacocke, G. V. C.; Madrali, E. S.; Li, C.-Z.; Guell, A. J.; Kandiyoti, R..; Bridgwater, A. V. *Biomass Bioenergy***1994**, *7* (1−6), 155−167.

Google Scholar

62. **62**

Peacocke, G. V. C.; Russel; Bridgwater, A. V. *Biomass Bioenergy***1994**, *7*, 147−154.

Google Scholar

63. **63**

Piskorz, J.; Scott, D. S.; Radlien, D. Composition of oils obtained by fast pyrolysis of different woods. In *Pyrolysis Oils from Biomass: Producing Analyzing and Upgrading*; American Chemical Society: Washington, DC, 1988; pp 167−178.

[ACS Full Text], Google Scholar

64. **64**

Fratini, E.; Bonini, M.; Oasmaa, A.; Solantausta, Y.; Teixeira, J.; Baglioni, P. *Langmuir***2005**, *22*, 306−312.

Google Scholar

65. **65**

Garcìa-Pérez, M.; Chaala, A.; Pakdel, H.; Kretschmer, D.; Rodrigue, D.; Roy, C. Multiphase Structure of Bio-oils. *Energy Fuels*, **2006**, *20*, 364−375.

Google Scholar

66. **66**

Czernik, S. Storage of biomass pyrolysis oils. In *Proceedings of the Biomass Pyrolysis Oil Properties and Combustion Meeting*, September 26−28, 1994; Paper No. NREL CP-439-7215, pp 67−76.

Google Scholar

67. **67**

Czernik, S.; Bridgewater, A. V. Applications of Biomass Pyrolysis Oils. In *Fast Pyrolysis of Biomass*: A Handbook, Vol. 3; Bridgewater, A. V., Ed.; CPL Press: Newbury, U.K., 2005, pp 105−120.

Google Scholar

68. **68**

Oasmaa, A.; Czernik, S. *Energy Fuels***1999**, *13*, 914−921.

[ACS Full Text], Google Scholar

69. **69**

Demirbas, A. *J. Anal. Appl. Pyrolysis***2004**, *71*, 803−815.

[Crossref], Google Scholar

70. **70**

The conversion of wood and other biomass to bio-oil; ENSYN Group, Inc.: Greely, CA, June 2001.

Google Scholar

71. **71**

Amen-Chen, C.; Pakdel, H.; Roy, C. *Biomass Bioenergy***2001**, *79*, 277−299.

Google Scholar

72. **72**

Elliot, D. C. Analysis and comparison of biomass pyrolysis/gasification condensates Final Report, No. PNL-5943, Pacific Northwest Laboratory, Richland, WA, 1986.

Google Scholar

73. **73**

Fagernas, L. *Chemical and Physical Characterization of Biomass-Based Pyrolysis Oils. Literature Review*; Technical Research Centre of Finland, Espoo, Finland, 1995.

Google Scholar

74. **74**

Standard test methods to water using volumetric Karl Fischer Titration, ASTM Standard E203. In *1996 ASTM Annual Book of Standards*; American Society for Testing and Materials: Philadelphia, PA, 1996.

Google Scholar

75. **75**

Standard test methods for instrumental determination of C, H, and N in petroleum products and lubricants, ASTM Standard D5291. In *1992 ASTM Annual Book of Standards*; American Society for Testing and Materials: Philadelphia, PA, 1992.

Google Scholar

76. **76**

Determination of ash from petroleum products, DIN EN 7, DIN Deutsches Institut fur Normung e.V.: Berlin, 1975.

Google Scholar

77. **77**

Standard test method for kinematic viscosity of transparent and opaque liquids (and the calculation of dynamic viscosity), ASTM Standard D445. In *1988 ASTM Annual Book of Standards*; American Society for Testing and Materials: Philadelphia, PA, 1988.

Google Scholar

78. **78**

Tyson, K. S.; Bozell, J.; Wallace, R.; Petersen, E.; Moens, L. Biomass oil analysis: research needs and recommendations. Technical Report No. NREL/TP-510-34796, National Renewable Energy Laboratory, Golden, CO, 2004.

[Crossref], Google Scholar

79. **79**

Radovanovic, M.; Venderbosch, R. H.; Prins, W.; van Swaaij, W. P. M. *Biomass Bioenergy***2000**, *18*, 209−222.

[Crossref], Google Scholar

80. **80**

Standard test methods for pour point of petroleum oils, ASTM Standard D97. In *1993 ASTM Annual Book of Standards*; American Society for Testing and Materials: Philadelphia, PA, 1993.

Google Scholar

81. **81**

Oasmaa, A.; Peacock, C. *A Guide to Physical Property Characterization of Biomass Derived Fast Pyrolysis Liquids*; Technical Research Centre of Finland, Espoo, Finland, 2001, VTT Publication No. 450.

Google Scholar

82. **82**

Oasmaa, A.; Meier, D. Characterization, Analysis, Norms and Standards. In *Fast Pyrolysis of Biomass, A Handbook*, Volume 3; Bridgwater, A. V., Ed.; CPL Press: Newbury, U.K., 2005; pp 19−60.

Google Scholar

83. **83**

Oasmaa, A.; Kuoppala, E.; Gust, S.; Solantausta, Y. *Energy Fuels***2003**, *17* (1), 1−12.

Google Scholar

84. **84**

Oasmaa, A.; Kuoppala, E.; Solantausta, Y. *Energy Fuels***2003**, *17* (2), 433−443.

Google Scholar

85. **85**

Oasmaa, A.; Kuoppala, E. *Energy Fuels***2003**, *17* (4), 1075−1084.

Google Scholar

86. **86**

Oasmaa, A.; Kuoppala, E.; Selin, J.-F.; Gust, S.; Solantausta, Y. *Energy Fuels***2004**, *18*, 1578−1583.

Google Scholar

87. **87**

Scott, D. C.; Piskorz, J.; Radlein, D. *Ind. Eng. Chem., Process Des. Dev*. **1985**, *24*, 581.

[ACS Full Text], Google Scholar

88. **88**

Graham, R. G.; Freel, B. A.; Bergougnou, M. A. The production of pyrolysis Liquids, Gas and char from wood and cellulose by fast pyrolysis. In *Research in Thermodynamical Biomass Conversion*; Bridgwater, A. V., Kuester, J. L., Eds.; Elsevier Applied Science: London, 1988; pp 629−641.

[Crossref], Google Scholar

89. **89**

Kovac, R. J.; Gorton, C. W.; O'Neil, D. J. Presented at the Thermochemical Conversion Program Annual Meeting, Solar Energy Research Institute, Golden, CO, 1988, Paper No. SERI/CP-231-3355; pp 5−20.

Google Scholar

90. **90**

Diebold, J.; Scahill, J. Production of Primary Pyrolysis Oils in a Vortex Reactor. In *Pyrolysis Oils from Biomass: Producing, Analyzing, and Upgrading*; Soltes, E. J., Milne, T. A., Eds.; ACS Symposium Series No. 376; American Chemical Society: Washington, DC, 1988; pp 31−40.

Google Scholar

91. **91**

Bridgwater, A. V., Ed. *Progress in Thermochemical Biomass Conversion,* Volume 2; Blackwell Science: London, 2001.

[Crossref], Google Scholar

92. **92**

Murwanashyaka, J. N.; Pakdel, H.; Roy, C. *J. Anal. Appl. Pyrolysis***2001**, *60*, 219−231.

[Crossref], Google Scholar

93. **93**

Murwanashyaka, J. N.; Pakdel, H.; Roy, C. *Sep. Purif. Technol*. **2001**, *24*, 155−165.

Google Scholar

94. **94**

Garcia-Perez, M.; Chaala, A.; Roy, C. *J. Anal. Appl. Pyrolysis***2002**, *65*, 111−136.

[Crossref], Google Scholar

95. **95**

Garcia-Perez, M.; Chaala, A.; Roy, C. *Fuel***2002**, *81* (7), 893−907.

[Crossref], Google Scholar

96. **96**

Ba, T.; Chaala, A.; Garcia-Perez, M.; Roy, C. *Energy Fuels***2004**, *18* (1), 188−201.

Google Scholar

97. **97**

Ba, T.; Chaala, A.; Garcia-Perez, M.; Rodrigue, D.; Roy, C. *Energy Fuels***2004**, *18* (3), 704−712.

Google Scholar

98. **98**

Darmstadt, H.; Garcia-Perez, M.; Adnot, A.; Chaala, A.; Kretschmer, D.; Roy, C. *Energy Fuels***2004**, *18* (5), 1291−1301.

Google Scholar

99. **99**

Chaala, A.; Ba, T.; Garcia-Perez, M.; Roy, C. *Energy Fuels***2004**, *18* (5), 1535−1542.

Google Scholar

100. **100**

Pakdel, H.; Roy, C. *Bioresour. Technol.***1996**, *58*, 83−88.

[Crossref], Google Scholar

101. **101**

Pakdel, H. et al. Phenolic Compounds from Vacuum Pyrolysis of Biomass, Bio-oil Production & Utilization. In *Proceedings of the 2nd EU−Canada Workshop on Thermal Bioenergy*, February 1996; pp 124−131.

Google Scholar

102. **102**

Amen-Chen, C.; Riedl, B.; Wang, X.-M.; Roy, C. *Holzforschung***2002**, *56* (2), 167−175.

[Crossref], Google Scholar

103. **103**

Amen-Chen, C.; Riedl, B.; Roy, C. *Holzforschung***2002**, *56* (3), 273−280.

Google Scholar

104. **104**

Amen-Chen, C.; Riedl, B.; Wang, X.-M.; Roy, C. *Holzforschung***2002**, *56* (3), 281−288.

Google Scholar

105. **105**

Amen-Chen, C.; Pakdel, H.; Roy, C. *Biomass Bioenergy***1997**, *13* (1−2), 25−37.

[Crossref], Google Scholar

106. **106**

http://dynamotive.com/biooil/whatisbiooil.html.

Google Scholar

107. **107**

Fast pyrolysis of bagasse to produce biooil fuel for power generation. Presented by Dynamotive Energy Systems Corporation at the 2001 Sugar Conference.

Google Scholar

108. **108**

Demirbas, A. *J. Anal. Appl. Pyrolysis***2004**, *72,* 215−219.

Google Scholar

109. **109**

Beaumont, O. *Wood Fiber Sci.***1999**, *17* (2), 228−239.

Google Scholar

110. **110**

Schroder, E. *J. Anal. Appl. Pyrolysis***2004**, *71*, 669−694.

[Crossref], Google Scholar

111. **111**

Branca, C.; Blasi, C. D.; Elefante, R. *Ind. Eng. Chem. Res.***2005**, *44* (4), 799−810.

Google Scholar

112. **112**

Branca, C.; Blasi, C. D.; Russo, C. *Fuel* **2005**, *84* (1), 37−45.

[Crossref], Google Scholar

113. **113**

Branca, C.; Giudicianni, P.; Di Blasi, C. *Ind. Eng. Chem. Res.***2003**, *42* (14), 3190−3202.

[ACS Full Text], Google Scholar

114. **114**

Şensöz, S.; Can, M. *Energy Sources***2002**, *24* (4), 347−355.

Google Scholar

115. **115**

Şensöz, S.; Can, M. *Energy Sources***2002**, *24* (4), 357−364.

Google Scholar

116. **116**

Guerrero, M.; Ruiz, M. P.; Alzueta, M. U.; Bilbao, R.; Millera, A. *J. Anal. Appl. Pyrolysis***2005**, *74*, 307−314.

[Crossref], Google Scholar

117. **117**

Olsson, M.; Kjallstrand, J.; Petersson, G. *J. Anal. Appl. Pyrolysis***2003**, *67*, 135−141.

[Crossref], Google Scholar

118. **118**

Luo, Z.; Wang, S.; Liao, Y.; Zhou, J.; Gu, Y.; Cen, K. *Biomass Bioenergy***2004**, *26*, 455−462.

[Crossref], Google Scholar

119. **119**

Paris, O.; Zollfrank, C.; Zickler, G. A. *Carbon* **2005**, *43* (1), 53−66.

[Crossref], Google Scholar

120. **120**

Stamatov, V.; Honnery, D.; Soria, J. *Renewable Energy***2005**, in press.

Google Scholar

121. **121**

Diebold, J.; Czernik, S. *Energy Fuels***1997**, *11*, 1081−1091.

[ACS Full Text], Google Scholar

122. **122**

Elliot, D. C. *Biomass Bioenergy***1994**, *7* (1−7), 179−185.

Google Scholar

123. **123**

Nilsson, M.; Ingemarsson, A.; Pedersen, J. R.; Olsson, J. O. *Chemosphere***1999**, *38* (7), 1469−1479.

[Crossref], Google Scholar

124. **124**

Reina, J.; Velo, E.; Puigjaner, L. *Thermochim. Acta***1998**, *320* (1−2), 161−167.

[Crossref], Google Scholar

125. **125**

Pütün, A. E.; Özbay, N.; Önal, E. P.; Pütün, E. *Fuel Process. Technol*. **2005**, *86* (11), 1207−1219.

[Crossref], Google Scholar

126. **126**

Pütün, A. E.; Apaydın, E.; Pütün, E. *Energy* **2004**, *29* (12−15), 2171−2180.

[Crossref], Google Scholar

127. **127**

Ates, F.; Putun, E.; Putun, A. E. *J. Anal. Appl. Pyrolysis***2004**, *71* (2), 779−790.

[Crossref], Google Scholar

128. **128**

Şensöz, S.; Demiral, I.; Gerçel, H. F. *Bioresour. Technol.***2006**, *97*(3), 429−436.

[Crossref], Google Scholar

129. **129**

Şensöz, S.; Angın, D.; Yorgun, S. *Biomass Bioenergy***2000**, *19* (4), 271−279.

[Crossref], Google Scholar

130. **130**

Putun, A. E.; Ozcan, A.; Putun, E. *J. Anal. Appl. Pyrolysis***1999**, *52*, 33−49.

[Crossref], Google Scholar

131. **131**

Kockar, O. M.; Onay, O.; Putun, A.; Putun E. *Energy Sources***2000**, *22* (10), 913−924.

Google Scholar

132. **132**

Drummond, A.-R. F.; Drummond, I. W. *Ind. Eng. Chem. Res*. **1996**, *35* (4), 1263−1268.

Google Scholar

133. **133**

Piskorz, J.; Mejerski, P.; Radlein, D.; Scott, D. S.; Bridgwater, A. V. *J. Anal. Appl. Pyrolysis***1998**, *46*, 15−29.

[Crossref], Google Scholar

134. **134**

Lee, K.-H.; Kang, B.-S.; Park, Y.-K.; Kim, J.-S. *Energy Fuels***2005**, *19* (5), 2179−2184.

Google Scholar

135. **135**

Gonzalez, J. F.; Ramiro, A.; Gonzalez-Garcia, C. M.; Ganan, J.; Encinar, J. M.; Sabio, E.; Rubiales, J. *Ind. Eng. Chem. Res.* **2005**, *44* (9), 3003−3012.

Google Scholar

136. **136**

Das, P.; Sreelatha, T.; Ganesh A. *Biomass Bioenergy***2004**, *27*, 265−275.

Google Scholar

137. **137**

Das, P.; Ganesh, A. *Biomass Bioenergy* **2003**, *25* (1), 113−117.

[Crossref], Google Scholar

138. **138**

Mathias, E. V.; Halkar, U. P. *J. Anal. Appl. Pyrolysis* **2004**, *71*, 515−524.

[Crossref], Google Scholar

139. **139**

Zensor, S.; Angin, D.; Yorgun, S.; Kockar, O. M. *Energy Sources***2000**, *22* (10), 891−899.

Google Scholar

140. **140**

Ozcimen, D.; Karaosmanoglu, F. *Renewable Energy***2004**, *29* (5), 779−785.

[Crossref], Google Scholar

141. **141**

Onay, O.; Beis, S. H.; Kockar, O. M. *J. Anal. Appl. Pyrolysis***2001**, *58*−*59*, 995−1007.

Google Scholar

142. **142**

Haykiri-Acma, H.; Yaman, S.; Kucukbayrak, S. *Renewable Energy***2005**, *31* (6), 803−810.

Google Scholar

143. **143**

Acikgoz, C.; Onay, O.; Kockar, O. M. *J. Anal. Appl. Pyrolysis***2004**, *71*, 417−429.

[Crossref], Google Scholar

144. **144**

Yorgun, S.; Şensöz, S.; Koçkar, Ö. M. *Biomass Bioenergy***2001**, *20* (2), 141−148.

[Crossref], Google Scholar

145. **145**

Miao, X.; Wu, Q.; Yang, C. *J. Anal. Appl. Pyrolysis***2004**, *71,* 855−863.

[Crossref], Google Scholar

146. **146**

Miao, X.; Wu, Q. *J. Biotechnol.***2004**, *110*, 85−93.

[Crossref], Google Scholar

147. **147**

Milne, T. A.; Evans, R. J.; Nagle, N. *Biomass***1990**, *21*, 219−232.

[Crossref], Google Scholar

148. **148**

Ginzburg, B, Z. *Renewable Energy***1993**, *3*, 249−252.

[Crossref], Google Scholar

149. **149**

Dote, Y.; Sawayama, S.; Inoue, S.; Minowa, T.; Yokoyama, S. *Fuel***1994**, *73*, 1855−1857.

[Crossref], Google Scholar

150. **150**

Minowa, T.; Yokoyama, S. Y.; Kishimoto, S. Y.; Okakurat, T. *Fuel* **1995**, *74*, 1735−1738.

[Crossref], Google Scholar

151. **151**

McKendry, P. *Bioresour. Technol*. **2002**, *83*, 37−46.

Google Scholar

152. **152**

McKendry, P. *Bioresour. Technol*. **2002**, *83*, 47−54.

Google Scholar

153. **153**

Demirbas, A. *Energy Sources***2002**, *24*, 337−345.

Google Scholar

154. **154**

Gercel, H. F.; Putun, A. E.; Putun, E. *Energy Sources***2002**, *24* (5), 423−430.

Google Scholar

155. **155**

Boateng, A. A.; Hicks, K. B.; Vogel, K. P. *J. Anal. Appl. Pyrolysis* **2006**, *75*, 55−64.

[Crossref], Google Scholar

156. **156**

Oasmaa, A.; Kuoppala, E.; Selin, J.-F.; Gust, S.; Solantausta, Y. *Energy Fuels***2004**, *18* (5), 1578−1583.

Google Scholar

157. **157**

Fullana, A.; Contreras, J. A.; Striebich, R. C.; Sidhu, S. S. *J. Anal.Appl. Pyrolysis***2005**, *74* (1−2), 315−326.

Google Scholar

158. **158**

Scholze, B.; Meier, D. *J. Anal. Appl. Pyrolysis* **2001**, *60*, 41−54.

[Crossref], Google Scholar

159. **159**

Scholze, B.; Hanser C.; Meier, D. *J. Anal. Appl. Pyrolysis***2001**, *58−59*, 387−400.

Google Scholar

160. **160**

Tuncel, F.; Gercel, H, F. *Energy Sources***2004**, *26* (8), 761−770.

[Crossref], Google Scholar

161. **161**

Richards, G. N.; Zheng, G. *J. Anal. Appl. Pyrolysis* **1991**, *21* (1−2), 133−146.

[Crossref], Google Scholar

162. **162**

Scott, D. S.; Paterson, L.; Piskorz, J.; Radlein, D. *J. Anal. Appl. Pyrolysis***2000**, *57*, 169−176.

Google Scholar

163. **163**

Pan, W.-P.; Richards, G. N. *J. Anal. Appl. Pyrolysis* **1989**, *16* (2), 117−126.

[Crossref], Google Scholar

164. **164**

Pan, W.-P.; Richards, G. N. *J. Anal. Appl. Pyrolysis***1990**, *17* (3), 261−273.

[Crossref], Google Scholar

165. **165**

Dobele, G.; Rossinskaja, G.; Dizhbite, T.; Telysheva, G.; Meier, D.; Faix, O. *J. Anal. Appl. Pyrolysis* **2005**, *74* (1−2), 401−405.

[Crossref], Google Scholar

166. **166**

Piskorz, J.; Radlein, D.; Scott, D. S. In *Proceedings of International Symposium on Advances in Thermochemical Biomass Conversion*; Bridgwater, A. V., Ed.; Blackie Academic: London, 1994; p 1432.

Google Scholar

167. **167**

French, R. J.; Milne, T. A. *Biomass Bioenergy***1994**, *7* (1−6), 315−325.

[Crossref], Google Scholar

168. **168**

Adam, J.; Blazsó, M.; Mészáros, E.; Stöcker, M.; Nilsen, M. H.; Bouzga, A.; Hustad, J. E.; Grønli, M.; Øye, G. *Fuel***2005**, *84* (12−13), 1494−1502.

Google Scholar

169. **169**

Atutxa, A.; Aguado, R.; Gayubo, A. G.; Olazar, M.; Bilbao, J. *Energy Fuels* **2005**, *19* (3), 765−774.

Google Scholar

170. **170**

Alma, M. H.; Kelley, S. S. *Biomass Bioenergy***2002**, *22* (5), 411−419.

Google Scholar

171. **171**

Williams, P. T.; Horne, P. A. *Biomass Bioenergy***1994**, *7* (1−6), 223−236.

[Crossref], Google Scholar

172. **172**

Ateş, F.; Pütün, A. E.; Pütün, E. *J. Anal. Appl. Pyrolysis***2005**, *73* (2), 299−304.

[Crossref], Google Scholar

173. **173**

Ates, F.; Pütün, A. E.; Pütün, E. *Energy Convers. Manage.***2005**, *46* (3), 421−432.

Google Scholar

174. **174**

Garcia, L.; Salvador, M. L.; Arauzo, J.; Bilbao, R. *J. Anal. Appl. Pyrolysis***2001**, *58*−*59*, 491−501.

Google Scholar

175. **175**

Borgund, A. E.; Barth, T. *Org. Geochem.***1999**, *30* (12), 1517−1526.

[Crossref], Google Scholar

176. **176**

Antal, M. J. Jr.; Varhegyi, G.; Jakab, E. *Ind. Eng. Chem. Res*. **1998**, *37*, 1267.

[ACS Full Text], [CAS], Google Scholar

177. **177**

Antal, M. J. *Ind. Eng. Chem. Res*. **1995**, *34*, 703−718.

[ACS Full Text], Google Scholar

178. **178**

Ahuja, P.; Kumar, S.; Singh, P. C. *Chem. Eng. Technol.***1996**, *19*, 272−281.

[Crossref], Google Scholar

179. **179**

Bradbury, A. G. W.; Sakai, Y.; Shafizadeh, F. A. *J. Appl. Polym. Sci.***1979**, *23*, 3271−3282.

[Crossref], Google Scholar

180. **180**

Broido, A.; Nelson, M. A. *Combust. Flame***1975**, *24*, 263−278.

Google Scholar

181. **181**

Curtis, L. J.; Miller, D. J. *Ind. Eng. Chem. Res*. **1988**, *27*, 1775−1783.

[ACS Full Text], Google Scholar

182. **182**

Font, R.; Marcilla, A.; Verdu, E. *Ind. Eng. Chem. Res*. **1990**, *29*, 1846−1957.

Google Scholar

183. **183**

Klose, W.; Wiest, W. *Bioresour. Technol.***1999**, *78*, 53−59.

Google Scholar

184. **184**

Koufopanos, C. A.; Maschio, G.; Lucchesi, A. *Can. J. Chem. Eng*. **1989**, *67*, 75−84.

[Crossref], Google Scholar

185. **185**

Samolado, M. C.; Vasalos, I. A. *Fuel***1991**, *70*, 883−889.

Google Scholar

186. **186**

Thurner, F.; Mann, U. *Ind. Eng. Chem. Res*. **1981**, *20*, 482−489.

Google Scholar

187. **187**

Klose, W.; Damm, S.; Wiest, W. Pyrolysis and activation of different woods thermal analysis (TG/EGA) and formal kinetics. Oral Presentation at 4th International Symposium of Catalytic and Thermochemical Conversions of Natural Organic Polymers at Krasnoyarsk, Russia, 2000.

Google Scholar

188. **188**

Luo, Z.; Wang, S.; Cen, K. *Renewable Energy***2005**, *30*, 377−392.

[Crossref], Google Scholar

189. **189**

Gupta, M.; Yang, J.; Roy, C. *Fuel***2003**, 82, 395−404.

Google Scholar

190. **190**

Tsotsas, E.; Schlunder, E. U. *Comput. Chem. Eng.***1990**, *14*, 1031.

[Crossref], [CAS], Google Scholar

191. **191**

Gupta, M.; Yang, J.; Roy, C. *Fuel***2003**, *82*, 919−927.

Google Scholar

192. **192**

Blasi, S. D. *AIChE J.***2002**, *48* (10), 2386−2397.

Google Scholar

193. **193**

Brown, A. L.; Hames, B. R.; Daily, J. W.; Dayton, D. C. *Energy Fuels***2002**, *17*, 1022−1027.

Google Scholar

194. **194**

Brown, A. L.; Dayton, D. C.; Nimlos, M. R.; Daily, J. W. *Energy Fuels***2001**, *15*, 1276−1285.

Google Scholar

195. **195**

Brown, A. L.; Dayton, D. C.; Daily, J. W. *Energy Fuels***2001**, *15*, 1286−1294.

Google Scholar

196. **196**

Freel, B; Graham, R. G. Bio-oil preservatives, U.S. Patent No. 6,485,841, November 26, 2002.

Google Scholar

197. **197**

Barry, F.; Graham, R. G. Bio-oil Preservatives, PCT/CA99/00984; WO 00/25996.

Google Scholar

198. **198**

Chum, H.; Deibold, J.; Scahill, J.; Johnson, D.; Black, S.; Schroeder, H.; Kreibich, R. E. Biomass pyrolysis oil feedstocks for phenolic adhesives. In *Adhesives from Renewable Resources*; Hemingway, R. W., Conner, A. H., Branham, S. J., Eds.; ACS Symposium Series No. 385; American Chemical Society: Washington, DC, 1989; pp 135−151.

[ACS Full Text], Google Scholar

199. **199**

Sipila, K.; Kuoppala, E.; Fagernas, L.; Oasmaa, A. *Biomass Bioenergy***1998**, *14*, 103−113.

[Crossref], Google Scholar

200. **200**

Shriner, R. L.; Fuson, R. C.; Curtin, D. Y. *The Synthetic Identification of Organic Compounds: A Laboratory Manual*, 4th Edition; Wiley: New York, 1964

Google Scholar

201. **201**

Elder, T. J.; Soltes, E. J. *Wood Fiber***1980**, *12* (4), 217−226.

Google Scholar

202. **202**

Mourant, D.; Yang, D.-Q.; Lu, X.; Roy, C. *Wood Fiber Sci.***2005**, *37* (3), 542−548.

Google Scholar

203. **203**

Robson, A 25 tpd Border Biofuels/Dynamotive plant in the UK. PyNe Newsletter 11, May 2001, Aston University, U.K., pp 1−2.

Google Scholar

204. **204**

Wagenaar, B. M.; Vanderbosh, R. H.; Carrasco, J.; Strenziok, R.; van der Aa, B. Scalling up of the rotating cone technology for biomass fast pyrolysis. In *1st World Conference and Exhibition on Biomass for Energy and Industry*, Seville, Spain, June 2000.

Google Scholar

205. **205**

Czernik, S.; Scahill, J.; Diebold, J. *J. Sol. Energy. Eng.* **1995**, *117*, 2−6.

[Crossref], Google Scholar

206. **206**

Scott, D. S. Can. Patent No. 1,241,541, September 1988.

Google Scholar

207. **207**

Ambler, P. A.; Milne, B. J.; Berruti, F.; Scott, D. S. *Chem. Eng. Sci*. **1990**, *45*, 2179.

[Crossref], [CAS], Google Scholar

208. **208**

Anon. BGL commissioning status. Presented at the Gasification Technology Conference, October 8−11, 2000, San Francisco, CA, 2000.

Google Scholar

209. **209**

Erdmann, C.; Liebner, W.; Seifert, W. Lurgi's MPG and BGL gasifiers at SVZ Schwarze Pumpe status and experiences in IGCC application. Presented at the Gasification Technology Conference, October 8−11, 2000, San Francisco, CA, 2000.

Google Scholar

210. **210**

Olliver R. A.; Wainwright, J. M.; Drnevich, R. F. Application of BGL gasification of solid hydrocarbons for IGCC power generation. Presented at the Gasification Technology Conference, October 8−11, 2000, San Francisco, CA, 2000.

Google Scholar

211. **211**

Koss, U.; Schlichting (Lurgi AS, Germany) Lurgi's MPG gasification plus rectisol gas purification-advanced process combination for reliable syngas production. Presented at the Gasification Technology Conference, October 9−12, 2005, San Francisco, CA, 2005.

Google Scholar

212. **212**

Karaosmanoglu, F.; Tetik, E. *Renewable Energy* **1999**, *16* (1−4), 1090−1093.

[Crossref], Google Scholar

213. **213**

Shihadeh, A.; Hochgreb, S. *Energy Fuels* **2000**, *14*, 260−274.

Google Scholar

214. **214**

Shihadeh, A.; Hochgreb, S. *Energy Fuels***2002**, *16*, 552−561.

Google Scholar

215. **215**

Boocock, D. G. B.; Konar, S. K.; Glaser, G. The formation of petrodiesel by the pyrolysis of fatty acid methyl esters over activated alumina. In *Progress in*

Thermochemical Biomass Conversion; Bridgwater, A. V., Ed.; Blackwell Science: London, 2001; pp 1525−1539.

[Crossref], Google Scholar

216. **216**

Peacocke, G. V. C.; Bridgwater A. V. Transport, handling and storage of biomass derived fast pyrolysis Liquid In *Progress in Thermochemical Biomass Conversion*, Volume 2; Bridgwater, A. V., Ed.; Blackwell Science: London, 2001; pp 1482−1499.

Google Scholar

217. **217**

Baglioni, P.; Chiaramont, D.; Bonini, M.; Soldaini, I.; Tondi, G. Bio-crude-oil/Diesel oil emulsification process and preliminary results of tests on Diesel engine. In *Progress in Thermochemical Biomass Conversion*; Bridgwater, A. V., Ed.; Blackwell Science: London, 2001; pp 1525−1539.

Google Scholar

218. **218**

Lang, X.; Dalai, A. K.; Bakhshi, N. N.; Reaney, M. J.; Hertz, P. B. *Bioresour. Technol.***2001**, *80* (1), 53−62.

[Crossref], Google Scholar

219. **219**

Ikura, M.; Stanciulescu, M.; Hogan, E. *Biomass Bioenergy***2003**, *24*, 221−232.

[Crossref], Google Scholar

220. **220**

Strenziok, R.; Hansen, U.; Kunstner, H. Combustion of bio-oil in a gas turbine. In *Progress in Thermochemical Biomass Conversion*; Bridgwater, A. V., Ed.; Blackwell Science: London, 2001; pp 1452−1458.

[Crossref], Google Scholar

221. **221**

Chiaramonti, D.; Bonini, M.; Fratini, E.; Tondi, G.; Gartner, K.; Bridgwater, A. V.; Grimm, H. P.; Soldaini, I.; Webster, A.; Baglioni, P. *Biomass Bioenergy* **2003**, *25* (1), 85−99.

Google Scholar

222. **222**

Chiaramonti, D.; Bonini, M.; Fratini, E.; Tondi, G.; Gartner, K.; Bridgwater, A. V.; Grimm, H. P.; Soldaini, I.; Webster, A.; Baglioni, P. *Biomass Bioenergy* **2003**, *25* (1), 101−111.

Google Scholar

223. **223**

Guéhenneux, B. G. P.; Brothier, M.; Poletiko, C.; Boissonnet, G. *Fuel***2005**, *84* (6), 733−739.

[Crossref], Google Scholar

224. **224**

Solantausta, Y.; Nylund, N.-O.; Westerholm, M.; Koljonen, T.; Oasmaa, A. *Bioresour. Technol.***1993**, *46* (1−2), 177−188.

[Crossref], Google Scholar

225. **225**

Elliott, D. C.; Sealock, J. L. J.; Low-temperature gasification of biomass under pressure. In *Fundamentals of Thermochemical Biomass Conversion*; Overend, R. P., Milne, T. A., Mudge, L. K., Eds.; Elsevier: London, 1985; pp 937−950.

Google Scholar

226. **226**

Delgado, J.; Aznar, M. P.; Corella, J. *Ind. Eng. Chem. Res*. **1997**, *36*, 1535−1543.

Google Scholar

227. **227**

Antal, M. J., Jr. Synthesis gas production from organic wastes by pyrolysis/steam reforming. In *Energy from Biomass and Wastes*; Klass, D. L., Ed.; Institute of Gas Technology (IGT): Chicago, IL, 1978, pp 495−524.

Google Scholar

228. **228**

Antal, M. J., Jr. A review of the vapor phase pyrolysis of biomass derived volatile matter. In *Fundamentals of Thermochemical Biomass Conversion*; Overend, T. A., Milne, R. P., Mudge, L. K., Eds.; Elsevier: New York, 1985; pp 511−537.

[Crossref], Google Scholar

229. **229**

Gañan, J. A.; Abdulla, Al−K.; Miranda, A. B.; Turegano, J.; Correia, S.; Cuerda, E. M. *Renewable Energy***2005**, *30* (11), 1759−1769.

[Crossref], Google Scholar

230. **230**

Tomishige, K.; Asadullah, M.; Kunimori, K. *Catal. Today***2004**, *89* (4), 389−403.

Google Scholar

231. **231**

Hanaoka, T.; Inoue, S.; Uno, S.; Ogi, T.; Minowa, T. *Biomass Bioenergy***2005**, *28* (1), 69−76.

Google Scholar

232. **232**

Matsumura, Y.; Minowa, T.; Potic, B.; Kersten, S. R. A.; Prins, W.; van Swaaij, W. P. M.; Beld, B.; van de, Elliott, D. C.; Neuenschwander, G. G.; Kruse, A.; Antal, M. J., Jr. *Biomass Bioenergy***2005**, in press.

Google Scholar

233. **233**

Panigrahi, S.; Chaudhari, S. T.; Bakhshi, N. N.; Dalai, A. K. *Energy Fuels* **2002**, *16*, 1392−1397.

Google Scholar

234. **234**

Panigrahi, S.; Chaudhari, S. T.; Bakhshi, N. N.; Dalai, A. K. *Energy Fuels***2003**, *16*, 637−642.

Google Scholar

235. **235**

The Sixth Italian Conference on Chemical and Process Engineering, June 8−11, 2003, Pisa, Italy (available via the Internet at http://www.aidic.it/icheap6).

Google Scholar

236. **236**

Huber, G. W.; Chheda, J. N.; Barrett, C. J.; Dumestic J. A. *Science***2005**, *308*, 1446−1450.

[Crossref], [PubMed], Google Scholar

237. **237**

Kelly, S. S. et al. Use of Biomass Pyrolysis Oils for Preparation of Modified Phenol Formaldehyde Resins. In *Developments in Thermochemical Biomass Conversion*, 1st Edition; Bridgwater, A.V., Boocock, D. G. B., Eds.; Blackie Academic: London, New York, 1997; pp 557−570.

[Crossref], Google Scholar

238. **238**

Brammer, J. G.; Lauer, M.; Bridgewater, A. V. *Energy Policy* **2005**, in press.

Google Scholar

239. **239**

Huber, G. W.; Chheda, J. N.; Barrett, C. J.; Dumesic, J. A. Production of liquid alkanes by aqueous-phase processing of biomass-derived carbohydrates. *Science***2005***, 308*, 1446−1450.

[Crossref], [PubMed], Google Scholar

240. **240**

Van Soest, P. J. *J. Anim. Sci*. **1964**, *23*, 828.

[Crossref], Google Scholar

241. **241**

Solo, M. L. *Mattalorest. Aikakawsh***1965**, *37*, 127.

Google Scholar

242. **242**

Tewfik, S. R. *Energy Edu. Sci. Technol.***2004**, *14*, 1−19.

Google Scholar

243. **243**

Czernick, S. Scahill, J.; Diebold, J. *J. Sol. Energy Eng.***1995**, *117*, 2−6.

Google Scholar

244. **244**

Maggi, R.; Delmon, B. *Fuel***1994**, *73* (5), 671−677.

[Crossref], Google Scholar

245. **245**

Şensöz, S.; Demiral, İ.; Gerçel, H. F. *Bioresour. Technol.***2006**, 97(3), 429−436.

[Crossref], Google Scholar

246. **246**

Gonzalez, J. F.; Encinar, J. M.; Canito, J. L.; Sabio, E.; Chacon, M. *J. Anal. Appl. Pyrolysis***2003**, *67*, 165−190.

[Crossref], Google Scholar

247. **247**

Ray, S. The commercial co-firing of RTP bio-oil at the Manitowoc public utilities power generating station, Manitowoc Public Utilities, Manitowoc, WI, June 1997 (available via the Internet at http:// www.ensyn.com/docs/manitowoc/manitowoc.htm).

Google Scholar

248. **248**

Gerçel, H. F. *Biomass Bioenergy***2002**, *23* (4), 307−314.

[Crossref], Google Scholar

249. **249**

Islam, M. N.; Beg, M. R. A.; Islam, M. R. *Renewable Energy***2005**, *30* (3), 413−420.

Google Scholar

250. **250**

Sinha, S.; Jhalani, A.; Ravi, M. R.; Ray, A. *J. Solar Energy Society of India (SESI)***2000**, *10* (1), 41−62.

Google Scholar

251. **251**

Bridgwater, A. V., Hogan, E. N., Eds. *Bio-oil Production and Utilization*; CPL Press: Newbury, U.K., 1996. (Proceedings of the Second EU−Canada Workshop on the Thermal Processing of Biomass. Overviews the programs and includes papers on

pyrolysis (eight papers), chemicals from pyrolysis oils (three papers), analysis and characterization (four papers), the upgrading of pyrolysis oil (three papers), and applications of bio-oil (five papers); ISBN 187269151X.)

Google Scholar

252. **252**

Bridgwater, A. V., Ed. *Fast Pyrolysis of Biomass: A Handbook*, Volume 1; CPL Press: Newbury, U.K., 2002; 176 pp. (ISBN 1872691072 EUR18913.)

Google Scholar

253. **253**

Bridgwater, A. V., Ed. *Fast Pyrolysis of Biomass: A Handbook*, Volume 2; CPL Press: Newbury, U.K., 2002; 432 pp. (ISBN 1872691471 EUR 20341.)

Google Scholar

254. **254**

Bridgwater, A. V., Ed. *Fast Pyrolysis of Biomass: A Handbook*, Volume 3; CPL Press: Newbury, U.K., 2005; 221 pp. (ISBN 1872691927.)

Google Scholar

255. **255**

Bridgwater, A. V., Ed. *Progress in Thermochemical Biomass Conversion*, Volumes 1 and 2; Blackwell Science: London, 2001. (ISBN 0-632-05533-2.)

[Crossref], Google Scholar

256. **256**

A Review of the Chemical and Physical Mechanisms of the Storage Stability of Fast Pyrolysis Bio-oils; National Renewable Energy Laboratory: Golden, CO, 2000. (ASIN: B0006RHPJQ.)

Google Scholar

257. **257**

Goldstein, I. S. *Organic Chemicals from Biomass*; CRC Press: Boca Raton, FL, 1981.

Google Scholar

258. **258**

Soltes, E. J., Milne, T. A., Eds. *Pyrolysis Oils from Biomass (Production, Analyzing and Upgrading)*; American Chemical Society: Washington, DC, 1988.

[ACS Full Text], Google Scholar

259. **259**

Pyrolysis of Industrial Wastes for Oil and Activated Carbons Recovery; Environmental Protection Technology Series, EPA-600/2-77-091; 1977.

Google Scholar

260. **260**

Pyrolytic Oilscharacterization and Data Development for Continuous Processing; Environmental Protection Technology Series, EPA-600/2-80-122; 1980.

Google Scholar

261. **261**

Elliott, D. C.; Beckman, D.; Bridgwater, A. V.; Diebold, J. P.; Gevert, S. B.; Solantausta, Y. *Energy Fuels***1991**, *5*, 339−410.

Google Scholar

262. **262**

http://www.dynamotive.com/

Google Scholar

263. **263**

http://www.ensyn.com/

Google Scholar

264. **264**

http://www.btgworld.com/

Google Scholar

265. **265**

http://www.pyne.co.uk/

Google Scholar

266. **266**

http://www.wisbiorefine.org/

Google Scholar

267. **267**

www.renewableoil.com

Google Scholar

268. **268**

http://www.aston-berg.co.uk

Google Scholar

269. **269**

www.ieabioenergy.com

Google Scholar

270. **270**
www.juiper.co.uk
Google Scholar

23. Cited By

Citation Statements
beta

•

Supporting

60

•

Mentioning

3145

•

Contrasting

7

This article is cited by 3829 publications.

1. Fan Lin, Mengze Xu, Karthikeyan K. Ramasamy, Zhenglong Li, Jordan Lee Klinger, Joshua A. Schaidle, Huamin Wang. Catalyst Deactivation and Its Mitigation during Catalytic Conversions of Biomass. *ACS Catalysis* **2022**, Article ASAP.
2. Md. Maksudur Rahman, Yun Yu, Hongwei Wu. Valorisation of Waste Tyre via Pyrolysis: Advances and Perspectives. *Energy & Fuels* **2022,** *36* (20) , 12429-12474. https://doi.org/10.1021/acs.energyfuels.2c02053
3. M. Pilar Ruiz, Jimmy A. Faria. Catalysis at the Solid–Liquid–Liquid Interface of Water–Oil Pickering Emulsions: A Tutorial Review. *ACS Engineering Au* **2022,** *2* (4) , 295-319. https://doi.org/10.1021/acsengineeringau.2c00010
4. Haftom Weldekidan, Amar K. Mohanty, Manjusri Misra. Upcycling of Plastic Wastes and Biomass for Sustainable Graphitic Carbon Production: A Critical Review. *ACS Environmental Au* **2022**, Article ASAP.
5. Rafaella Georgiou, Christoph J. Sahle, Dimosthenis Sokaras, Sylvain Bernard, Uwe Bergmann, Jean-Pascal Rueff, Loïc Bertrand. X-ray Raman Scattering: A Hard X-ray Probe of Complex Organic Systems. *Chemical Reviews* **2022,** *122* (15) , 12977-13005. https://doi.org/10.1021/acs.chemrev.1c00953
6. Santanu Bakshi, Marjorie R. Rover, Ryan G. Smith, Robert C. Brown. Conversion of Phenolic Oil from Biomass Pyrolysis into Phenyl Esters. *Energy & Fuels* **2022,** *36* (12) , 6317-6328. https://doi.org/10.1021/acs.energyfuels.2c00769
7. Yupeng Wang, Yucui Hou, He Li, Weize Wu, Shuhang Ren, Jianwei Li. A New Structural Model of Enzymatic Lignin with Multiring Aromatic Clusters. *ACS Omega* **2022,** *7* (22) , 18861-18869. https://doi.org/10.1021/acsomega.2c01812
8. Muhammad Shahzeb Khan, Yikai Min, Mohsen Broumand, Sean Yun, Zekai Hong, Murray J. Thomson. Advancing the Application of Pyrolysis Liquid (Bio-oil) by the Improvement of Its Fuel Properties by Thermo-Catalytic Reforming. *Energy & Fuels* **2022,** *36* (8) , 4381-4395. https://doi.org/10.1021/acs.energyfuels.1c04129
9. Ki-Bum Park, Joo-Sik Kim, Farideh Pahlavan, Elham H. Fini. Biomass Waste to Produce Phenolic Compounds as Antiaging Additives for Asphalt. *ACS Sustainable Chemistry & Engineering* **2022,** *10* (12) , 3892-3908. https://doi.org/10.1021/acssuschemeng.1c07870
10. Ning Li Jianhui Zhao Beibei Yan Xiaoguang Duan Guanyi Chen . Biorenewable Nanocomposite Materials for Wastewater Treatment. **,,,** 281-311. https://doi.org/10.1021/bk-2022-1411.ch011
11. Chaiwat Soanuch, Krittin Korkerd, Vishnu Pareek, Pornpote Piumsomboon, Benjapon Chalermsinsuwan. Fast Pyrolysis Downer Reactor: Effect of Reactor Geometry on the Hydrodynamics. *Industrial & Engineering*

Chemistry Research **2022,** *61* (11) , 4153-4167. https://doi.org/10.1021/acs.iecr.2c00159
12. Abdul Raheem, Qing He, Fareed Hussain Mangi, Chinnathan Areeprasert, Lu Ding, Guangsuo Yu. Roles of Heavy Metals during Pyrolysis and Gasification of Metal-Contaminated Waste Biomass: A Review. *Energy & Fuels* **2022,** *36* (5) , 2351-2368. https://doi.org/10.1021/acs.energyfuels.1c04051
13. Ranjeet Kumar Mishra, Manjusri Misra, Amar K. Mohanty. Value-Added Bio-carbon Production through the Slow Pyrolysis of Waste Bio-oil: Fundamental Studies on Their Structure–Property–Processing Co-relation. *ACS Omega* **2022,** *7* (2) , 1612-1627. https://doi.org/10.1021/acsomega.1c01743
14. Phillip Cross, Kristiina Iisa, Anh To, Mark Nimlos, Daniel Carpenter, Jesse A. Mayer, John C. Cushman, Bishnu Neupane, Glenn C. Miller, Sushil Adhikari, Calvin Mukarakate. Multiscale Catalytic Fast Pyrolysis of Grindelia Reveals Opportunities for Generating Low Oxygen Content Bio-Oils from Drought Tolerant Biomass. *Energy & Fuels* **2022,** *36* (1) , 425-434. https://doi.org/10.1021/acs.energyfuels.1c02403
15. Hoda Shafaghat, Mats Linderberg, Tomasz Janosik, Martin Hedberg, Henrik Wiinikka, Linda Sandström, Ann-Christine Johansson. Enhanced Biofuel Production via Catalytic Hydropyrolysis and Hydro-Coprocessing. *Energy & Fuels* **2022,** *36* (1) , 450-462. https://doi.org/10.1021/acs.energyfuels.1c03263
16. Jon Solar, Blanca M. Caballero, Alexander López-Urionabarrenechea, Esther Acha, Pedro L. Arias. Pyrolysis of Forestry Waste in a Screw Reactor with Four Sequential Heating Zones: Influence of Isothermal and Nonisothermal Profiles. *Industrial & Engineering Chemistry Research* **2021,** *60* (51) , 18627-18639. https://doi.org/10.1021/acs.iecr.1c01932
17. Lin Chen, Wei Yan, Xiujuan Qian, Minjiao Chen, Xiaoyu Zhang, Fengxue Xin, Wenming Zhang, Min Jiang, Katrin Ochsenreither. Increased Lipid Production in Yarrowia lipolytica from Acetate through Metabolic Engineering and Cosubstrate Fermentation. *ACS Synthetic Biology* **2021,** *10* (11) , 3129-3138. https://doi.org/10.1021/acssynbio.1c00405
18. Jasmine Hertzog, Charlotte Mase, Marie Hubert-Roux, Carlos Afonso, Pierre Giusti, Caroline Barrère-Mangote. Characterization of Heavy Products from Lignocellulosic Biomass Pyrolysis by Chromatography and Fourier Transform Mass Spectrometry: A Review. *Energy & Fuels* **2021,** *35* (22) , 17979-18007. https://doi.org/10.1021/acs.energyfuels.1c02098
19. Andreas Eschenbacher, Paul Fennell, Anker Degn Jensen. A Review of Recent Research on Catalytic Biomass Pyrolysis and Low-Pressure Hydropyrolysis. *Energy & Fuels* **2021,** *35* (22) , 18333-18369. https://doi.org/10.1021/acs.energyfuels.1c02793
20. Benjamin Caudle, Maria C. Vieira, Maximilian B. Gorensek, Chau-Chyun Chen. Modeling Phase Equilibrium of Common Sugars Glucose, Fructose, and Sucrose in Mixed Solvents. *Journal of Chemical & Engineering Data* **2021,** *66* (11) , 4193-4205. https://doi.org/10.1021/acs.jced.1c00377
21. Richard Pujro, Juan Rafael García, Melisa Bertero, Marisa Falco, Ulises Sedran. Review on Reaction Pathways in the Catalytic Upgrading of Biomass Pyrolysis Liquids. *Energy & Fuels* **2021,** *35* (21) , 16943-16964. https://doi.org/10.1021/acs.energyfuels.1c01931

22. William de Rezende Locatel, Dorothée Laurenti, Yves Schuurman, Nolven Guilhaume. Can Paints and Varnish Impair the Physicochemical Properties of Wood Pyrolysis Oils?. *Energy & Fuels* **2021,** *35* (21) , 17739-17754. https://doi.org/10.1021/acs.energyfuels.1c02568
23. Najmul Haque Barbhuiya, Ashish Kumar, Ayush Singh, Munish K. Chandel, Christopher J. Arnusch, James M. Tour, Swatantra P. Singh. The Future of Flash Graphene for the Sustainable Management of Solid Waste. *ACS Nano* **2021,** *15* (10) , 15461-15470. https://doi.org/10.1021/acsnano.1c07571
24. Bhavikkumar Mahant, Praveen Linga, Rajnish Kumar. Hydrogen Economy and Role of Hythane as a Bridging Solution: A Perspective Review. *Energy & Fuels* **2021,** *35* (19) , 15424-15454. https://doi.org/10.1021/acs.energyfuels.1c02404
25. Lan Xu, Xin Ma, Priya Murria, Abhijit Talpade, Huaming Sheng, Richard Meilan, Clint Chapple, Rakesh Agrawal, W. Nicholas Delgass, Fabio H. Ribeiro, Hilkka I. Kenttämaa. Fast Determination of the Lignin Monomer Compositions of Genetic Variants of Poplar via Fast Pyrolysis/Atmospheric Pressure Chemical Ionization Mass Spectrometry. *Journal of the American Society for Mass Spectrometry* **2021,** *32* (10) , 2546-2551. https://doi.org/10.1021/jasms.1c00186
26. Cunhao Cui, Xinghua Liu, Chaoqun Zhou, Chunjiang Liu, Zhongyue Zhou, Fei Qi. Online Study on the Catalytic Hydrotreatment of Guaiacol in Liquid Phase by Vacuum Ultraviolet Photoionization Time-of-Flight Mass Spectrometry. *Energy & Fuels* **2021,** *35* (17) , 13863-13870. https://doi.org/10.1021/acs.energyfuels.1c02182
27. Yaowen Zhang, Guoli Fan, Lan Yang, Lirong Zheng, Feng Li. Cooperative Effects between Ni-Mo Alloy Sites and Defective Structures over Hierarchical Ni-Mo Bimetallic Catalysts Enable the Enhanced Hydrodeoxygenation Activity. *ACS Sustainable Chemistry & Engineering* **2021,** *9* (34) , 11604-11615. https://doi.org/10.1021/acssuschemeng.1c04762
28. Archana Bansode, Mehul Barde, Osei Asafu-Adjaye, Vivek Patil, John Hinkle, Brian K. Via, Sushil Adhikari, Andrew J. Adamczyk, Ramsis Farag, Thomas Elder, Nicole Labbé, Maria L. Auad. Synthesis of Biobased Novolac Phenol–Formaldehyde Wood Adhesives from Biorefinery-Derived Lignocellulosic Biomass. *ACS Sustainable Chemistry & Engineering* **2021,** *9* (33) , 10990-11002. https://doi.org/10.1021/acssuschemeng.1c01916
29. Cody Wainscott, Austin C. Edwards, Jason Street, Brian Mitchell, Islam Elsayed, El Barbary Hassan, Todd E. Mlsna. Co-Pyrolysis of Southern Pine and Micronized Rubber Powder with Nickel Oxide and Sodium Carbonate Catalysts. *Industrial & Engineering Chemistry Research* **2021,** *60* (32) , 11915-11926. https://doi.org/10.1021/acs.iecr.1c01520
30. Junmeng Cai, Md. Maksudur Rahman, Shukai Zhang, Manobendro Sarker, Xingguang Zhang, Yuqing Zhang, Xi Yu, Elham H. Fini. Review on Aging of Bio-Oil from Biomass Pyrolysis and Strategy to Slowing Aging. *Energy & Fuels* **2021,** *35* (15) , 11665-11692. https://doi.org/10.1021/acs.energyfuels.1c01214
31. Rashedul Hasan Khondakar, Yun Yu, Hongwei Wu. Cellobiulose as a Key Intermediate during Biomass Hydrothermal Conversion into Biofuels and Biochemicals: Fundamental Decomposition Mechanisms. *Energy &*

Fuels **2021,** *35* (15) , 12200-12207. https://doi.org/10.1021/acs.energyfuels.1c01636
32. Liang Li, Ruben Van de Vijver, Andreas Eschenbacher, Onur Dogu, Kevin M. Van Geem. Primary Thermal Decomposition Pathways of Hydroxycinnamaldehydes. *Energy & Fuels* **2021,** *35* (15) , 12216-12226. https://doi.org/10.1021/acs.energyfuels.1c01662
33. Anton Alvarez-Majmutov, Sandeep Badoga, Jinwen Chen, Jacques Monnier, Yi Zhang. Co-Processing of Deoxygenated Pyrolysis Bio-Oil with Vacuum Gas Oil through Hydrocracking. *Energy & Fuels* **2021,** *35* (12) , 9983-9993. https://doi.org/10.1021/acs.energyfuels.1c00822
34. Qiang Yu, Yonghua Guo, Xiaoxia Wu, Zijun Yang, Hua Wang, Qingfeng Ge, Xinli Zhu. Ketonization of Propionic Acid on Lewis Acidic Zr-Beta Zeolite with Improved Stability and Selectivity. *ACS Sustainable Chemistry & Engineering* **2021,** *9* (23) , 7982-7992. https://doi.org/10.1021/acssuschemeng.1c02290
35. Martin Staš, Miloš Auersvald, Petr Vozka. Two-Dimensional Gas Chromatography Characterization of Pyrolysis Bio-oils: A Review. *Energy & Fuels* **2021,** *35* (10) , 8541-8557. https://doi.org/10.1021/acs.energyfuels.1c00553
36. Zhe Zhang, Min Wang, Hongru Zhou, Feng Wang. Surface Sulfate Ion on CdS Catalyst Enhances Syngas Generation from Biopolyols. *Journal of the American Chemical Society* **2021,** *143* (17) , 6533-6541. https://doi.org/10.1021/jacs.1c00830
37. Qing Zhao, Marko Mäkinen, Antti Haapala, Janne Jänis. Valorization of Bark from Short Rotation Trees by Temperature-Programmed Slow Pyrolysis. *ACS Omega* **2021,** *6* (14) , 9771-9779. https://doi.org/10.1021/acsomega.1c00434
38. Francisco W. S. Lucas, R. Gary Grim, Sean A. Tacey, Courtney A. Downes, Joseph Hasse, Alex M. Roman, Carrie A. Farberow, Joshua A. Schaidle, Adam Holewinski. Electrochemical Routes for the Valorization of Biomass-Derived Feedstocks: From Chemistry to Application. *ACS Energy Letters* **2021,** *6* (4) , 1205-1270. https://doi.org/10.1021/acsenergylett.0c02692
39. Rebecca N. Nishide, Julianne H. Truong, Mahdi M. Abu-Omar. Organosolv Fractionation of Walnut Shell Biomass to Isolate Lignocellulosic Components for Chemical Upgrading of Lignin to Aromatics. *ACS Omega* **2021,** *6* (12) , 8142-8150. https://doi.org/10.1021/acsomega.0c05936
40. Dillon Mazerolle, Benjamin Bronson, Boguslaw Kruczek. Experimental Investigation of Fouling Remediation Strategies for Cross-Flow Microfiltration of Fast Pyrolysis Bio-Oil. *Industrial & Engineering Chemistry Research* **2021,** *60* (7) , 3083-3094. https://doi.org/10.1021/acs.iecr.0c05269
41. Isaac Yeboah, Yahao Li, Kishore Rajendran, Kumar R. Rout, De Chen. Tandem Hydrodeoxygenation Catalyst System for Hydrocarbons Production from Simulated Bio-oil: Effect of C–C Coupling Catalysts. *Industrial & Engineering Chemistry Research* **2021,** *60* (5) , 2136-2143. https://doi.org/10.1021/acs.iecr.1c00113
42. Peter H. Galebach, Micaela Beussman, Jillian Johnson, Thomas Fredriksen, Chengrong Wang, Michael P. Lanci, George W. Huber. Catalytic Conversion of Pyrolysis Oil to Alcohols and Alkanes in Supercritical Methanol over the

CuMgAlOx Catalyst. *ACS Sustainable Chemistry & Engineering* **2021,** *9* (5) , 2067-2079. https://doi.org/10.1021/acssuschemeng.0c07020
43. Lei Shi, Shuping Zhang, Yinhai Su, Dan Xu, Zhongwen wang, Yuanquan Xiong. Investigation of Char Yield and Its Physicochemical Properties with Recycling of Heavy Oil from Biomass Pyrolysis. *Energy & Fuels* **2021,** *35* (3) , 2326-2334. https://doi.org/10.1021/acs.energyfuels.0c03986
44. Amoolya D. Lalsare, Tuhin S. Khan, Brian Leonard, Roman Vukmanovich, Pedram Tavazohi, Lili Li, Jianli Hu. Graphene-Supported Fe/Ni, β-Mo2C Nanoparticles: Experimental and DFT Integrated Approach to Catalyst Development for Synergistic Hydrogen Production through Lignin-Rich Biomass Reforming and Reduced Shale Gas Flaring. *ACS Catalysis* **2021,** *11* (1) , 364-382. https://doi.org/10.1021/acscatal.0c04242
45. Ganapati D. Yadav Ujjal Mondal . Valorization of Bio-Oils to Fuels and Chemicals. **2021,**„ 29-67. https://doi.org/10.1021/bk-2021-1379.ch002
46. Kalpana C. Maheria Aayushi Lodhi Gunjan Sharma . Microalgae Oil Upgrading over Zeolite-Based Catalysts. **2021,**„ 89-124. https://doi.org/10.1021/bk-2021-1379.ch004
47. Huimin Liu, Yicheng Wang, Silan Zhao, Hongyun Hu, Chengyang Cao, Aijun Li, Yun Yu, Hong Yao. Review on the Current Status of the Co-combustion Technology of Organic Solid Waste (OSW) and Coal in China. *Energy & Fuels* **2020,** *34* (12) , 15448-15487. https://doi.org/10.1021/acs.energyfuels.0c02177
48. Pavlo Kostetskyy, Linda J. Broadbelt. Progress in Modeling of Biomass Fast Pyrolysis: A Review. *Energy & Fuels* **2020,** *34* (12) , 15195-15216. https://doi.org/10.1021/acs.energyfuels.0c02295
49. Yinglei Han, Anamaria Paiva Pinheiro Pires, Melba Denson, Armando G. McDonald, Manuel Garcia-Perez. Ternary Phase Diagram of Water/Bio-Oil/Organic Solvent for Bio-Oil Fractionation. *Energy & Fuels* **2020,** *34* (12) , 16250-16264. https://doi.org/10.1021/acs.energyfuels.0c03100
50. Zheng-Hua Li, Huamin Wang, Kimberly A. Magrini, James Edward Lee, Thomas Geeza, Oleg Vitalivich Maltsev, Jacob Pierce Helper. Quantitative Determination of Biomass-Derived Renewable Carbon in Fuels from Coprocessing of Bio-Oils in Refinery Using a Stable Carbon Isotopic Approach. *ACS Sustainable Chemistry & Engineering* **2020,** *8* (47) , 17565-17572. https://doi.org/10.1021/acssuschemeng.0c07323
51. Shanhui Zhao, Yonghao Luo. Multiscale Modeling of Lignocellulosic Biomass Thermochemical Conversion Technology: An Overview on the State-of-the-Art. *Energy & Fuels* **2020,** *34* (10) , 11867-11886. https://doi.org/10.1021/acs.energyfuels.0c02247
52. Bogdan Shumeiko, Miloš Auersvald, Petr Straka, Pavel Šimáček, Dan Vrtiška, David Kubička. Efficient One-Stage Bio-Oil Upgrading over Sulfided Catalysts. *ACS Sustainable Chemistry & Engineering* **2020,** *8* (40) , 15149-15167. https://doi.org/10.1021/acssuschemeng.0c03896
53. Yonghua Guo, Qiang Yu, Huasu Fang, Hua Wang, Jinyu Han, Qingfeng Ge, Xinli Zhu. Ce–UiO-66 Derived CeO2 Octahedron Catalysts for Efficient Ketonization of Propionic Acid. *Industrial & Engineering Chemistry Research* **2020,** *59* (39) , 17269-17278. https://doi.org/10.1021/acs.iecr.0c01238

54. Oraléou Sangué Djandja, Zhi-Cong Wang, Feng Wang, Yu-Ping Xu, Pei-Gao Duan. Pyrolysis of Municipal Sewage Sludge for Biofuel Production: A Review. *Industrial & Engineering Chemistry Research* **2020,** *59* (39) , 16939-16956. https://doi.org/10.1021/acs.iecr.0c01546
55. Xue-Yu Ren, Xiao-Bo Feng, Jing-Pei Cao, Wen Tang, Zhi-Hao Wang, Zhen Yang, Jing-Ping Zhao, Li-Yun Zhang, Yan-Jun Wang, Xiao-Yan Zhao. Catalytic Conversion of Coal and Biomass Volatiles: A Review. *Energy & Fuels* **2020,** *34* (9) , 10307-10363. https://doi.org/10.1021/acs.energyfuels.0c01432
56. Dillon Mazerolle, Benjamin Bronson, Boguslaw Kruczek. Experimental Evaluation and Empirical Modeling of Cross-Flow Microfiltration for Solids and Ash Removal from Fast Pyrolysis Bio-Oil. *Energy & Fuels* **2020,** *34* (9) , 11014-11025. https://doi.org/10.1021/acs.energyfuels.0c01641
57. Chao Li, Lijun Zhang, Mortaza Gholizadeh, Roel Westernhof, Zhenhua Cui, Bingqiang Liu, Yonggui Tang, Xinghui Jin, Zhixiang Xu, Xun Hu. Impact of Acidic/Basic Sites of the Catalyst on Properties of the Coke Formed in Pyrolysis of Guaiacol: A Model Compound of the Phenolics in Bio-oil. *Energy & Fuels* **2020,** *34* (9) , 11026-11040. https://doi.org/10.1021/acs.energyfuels.0c01794
58. Lujiang Xu, Chenchen Shi, Zijian He, Huan Zhang, Mingying Chen, Zhen Fang, Ying Zhang. Recent Advances of Producing Biobased N-Containing Compounds via Thermo-Chemical Conversion with Ammonia Process. *Energy & Fuels* **2020,** *34* (9) , 10441-10458. https://doi.org/10.1021/acs.energyfuels.0c01993
59. Xueyong Ren, Jin Guo, Shuangyin Li, Jianmin Chang. Thermogravimetric Analysis–Fourier Transform Infrared Spectroscopy Study on the Effect of Extraction Pretreatment on the Pyrolysis Properties of Eucalyptus Wood Waste. *ACS Omega* **2020,** *5* (36) , 23364-23371. https://doi.org/10.1021/acsomega.0c03271
60. Tanzina Azad, Jonathan D. Schuler, Maria L. Auad, Thomas Elder, Andrew J. Adamczyk. Model Lignin Oligomer Pyrolysis: Coupled Conformational and Thermodynamic Analysis of β-O-4' Bond Cleavage. *Energy & Fuels* **2020,** *34* (8) , 9709-9724. https://doi.org/10.1021/acs.energyfuels.0c01573
61. Vineet Maliekkal, Paul J. Dauenhauer, Matthew Neurock. Glycosidic C–O Bond Activation in Cellulose Pyrolysis: Alpha Versus Beta and Condensed Phase Hydroxyl-Catalytic Scission. *ACS Catalysis* **2020,** *10* (15) , 8454-8464. https://doi.org/10.1021/acscatal.0c02133
62. Yanling Yang, Mingwu Tan, Aidan Garcia, Zhaoxia Zhang, Jingdong Lin, Shaolong Wan, Jean-Sabin McEwen, Shuai Wang, Yong Wang. Controlling the Oxidation State of Fe-Based Catalysts through Nitrogen Doping toward the Hydrodeoxygenation of m-Cresol. *ACS Catalysis* **2020,** *10* (14) , 7884-7893. https://doi.org/10.1021/acscatal.0c00626
63. Chun Ho Lam, Wei Deng, Lin Lang, Xin Jin, Xun Hu, Yi Wang. Minireview on Bio-Oil Upgrading via Electrocatalytic Hydrogenation: Connecting Biofuel Production with Renewable Power. *Energy & Fuels* **2020,** *34* (7) , 7915-7928. https://doi.org/10.1021/acs.energyfuels.0c01380
64. Liang Cao, He Zhao, Zhenda Tan, Rongqing Guan, Huanfeng Jiang, Min Zhang. Ruthenium-Catalyzed Hydrogen Evolution o-Aminoalkylation of Phenols

with Cyclic Amines. *Organic Letters* **2020,** *22* (12) , 4781-4785. https://doi.org/10.1021/acs.orglett.0c01580
65. Sandeep Badoga, Anton Alvarez-Majmutov, Tingyong Xing, Rafal Gieleciak, Jinwen Chen. Co-processing of Hydrothermal Liquefaction Biocrude with Vacuum Gas Oil through Hydrotreating and Hydrocracking to Produce Low-Carbon Fuels. *Energy & Fuels* **2020,** *34* (6) , 7160-7169. https://doi.org/10.1021/acs.energyfuels.0c00937
66. Fan Zhang, Zhen He, Ren Tu, Zhiwen Jia, Yujian Wu, Yan Sun, Enchen Jiang, Xiwei Xu. Influence of Ultrasonic/Torrefaction Assisted Deep Eutectic Solvents on the Upgrading of Bio-Oil from Corn Stalk. *ACS Sustainable Chemistry & Engineering* **2020,** *8* (23) , 8562-8576. https://doi.org/10.1021/acssuschemeng.0c00837
67. Jipeng Yan, Oluwafemi Oyedeji, Juan H. Leal, Bryon S. Donohoe, Troy A. Semelsberger, Chenlin Li, Amber N. Hoover, Erin Webb, Elizabeth A. Bose, Yining Zeng, C. Luke Williams, Kastli D. Schaller, Ning Sun, Allison E. Ray, Deepti Tanjore. Characterizing Variability in Lignocellulosic Biomass: A Review. *ACS Sustainable Chemistry & Engineering* **2020,** *8* (22) , 8059-8085. https://doi.org/10.1021/acssuschemeng.9b06263
68. Hanping Chen, Haoyu Xiao, Sunwen Xia, Danyan Wu, Yingquan Chen, Xianhua Wang, Haiping Yang, Jianjun Xiao. Catalytic Hydrotreatment of Industrial Wood Tar under Supercritical Ethanol Conditions. *Energy & Fuels* **2020,** *34* (5) , 5983-5989. https://doi.org/10.1021/acs.energyfuels.0c00423
69. Braden Peterson, Chaiwat Engtrakul, Tabitha J. Evans, Kristiina Iisa, Michael J. Watson, Mark W. Jarvis, David J. Robichaud, Calvin Mukarakate, Mark R. Nimlos. Optimization of Biomass Pyrolysis Vapor Upgrading Using a Laminar Entrained-Flow Reactor System. *Energy & Fuels* **2020,** *34* (5) , 6030-6040. https://doi.org/10.1021/acs.energyfuels.0c00649
70. Ping Feng, Weigang Lin, Peter A. Jensen, Wenli Song, Lifang Hao, Songgeng Li, Kim Dam-Johansen. Characterization of Solid Residues from Entrained Flow Gasification of Coal Bio-Oil Slurry. *Energy & Fuels* **2020,** *34* (5) , 5900-5906. https://doi.org/10.1021/acs.energyfuels.9b04437
71. Haoqin Zhou, Robert C. Brown, Zhiyou Wen. Biochar as an Additive in Anaerobic Digestion of Municipal Sludge: Biochar Properties and Their Effects on the Digestion Performance. *ACS Sustainable Chemistry & Engineering* **2020,** *8* (16) , 6391-6401. https://doi.org/10.1021/acssuschemeng.0c00571
72. Yanyang Mei, Shipeng Zhang, Hua Wang, Shuangxi Jing, Ting Hou, Shusheng Pang. Low-Temperature Deoxidization of Lignin and Its Impact on Liquid Products from Pyrolysis. *Energy & Fuels* **2020,** *34* (3) , 3422-3428. https://doi.org/10.1021/acs.energyfuels.0c00202
73. F. A. Agblevor, H. Wang, S. Beis, K. Christian, A. Slade, O. Hietsoi, D. M. Santosa. Reformulated Red Mud: a Robust Catalyst for In Situ Catalytic Pyrolysis of Biomass. *Energy & Fuels* **2020,** *34* (3) , 3272-3283. https://doi.org/10.1021/acs.energyfuels.9b04015
74. A. M. García-Minguillán, L. Briones, D. P. Serrano, J. A. Botas, J. M. Escola. Shifting Pathways in the Phenol/2-Propanol Conversion over the Tandem Raney Ni + ZSM-5 Catalytic System. *Industrial & Engineering Chemistry Research* **2020,** *59* (8) , 3375-3382. https://doi.org/10.1021/acs.iecr.9b07015

75. Conghui Gu, Yujian Zhang, Danping Pan, Shouguang Yao, Kotkin Vladimir, Lei Guan, Kai Wu, Zhulin Yuan. Visual Experimental Analysis of the Residence Time of Flexible Biomass Particles in a Baffled Rotating Cylindrical Tube. *Energy & Fuels* **2020,** *34* (2) , 1851-1858. https://doi.org/10.1021/acs.energyfuels.9b03842
76. Yawei Chen, Kumar Aanjaneya, Arvind Atreya. Catalytic Pyrolysis of Centimeter-Scale Pinewood Particles to Produce Hydrocarbon Fuels: The Effect of Catalyst Temperature and Regeneration. *Energy & Fuels* **2020,** *34* (2) , 1977-1983. https://doi.org/10.1021/acs.energyfuels.9b04314
77. Himanshu Patel, Naijia Hao, Kristiina Iisa, Richard J. French, Kellene A. Orton, Calvin Mukarakate, Arthur J. Ragauskas, Mark R. Nimlos. Detailed Oil Compositional Analysis Enables Evaluation of Impact of Temperature and Biomass-to-Catalyst Ratio on ex Situ Catalytic Fast Pyrolysis of Pine Vapors over ZSM-5. *ACS Sustainable Chemistry & Engineering* **2020,** *8* (4) , 1762-1773. https://doi.org/10.1021/acssuschemeng.9b05383
78. Shukai Zhang, Chong Li, Xiaojuan Guo, Md Maksudur Rahman, Xingguang Zhang, Xi Yu, Junmeng Cai. Kinetic Analysis of Bio-Oil Aging by Using Pattern Search Method. *Industrial & Engineering Chemistry Research* **2020,** *59* (4) , 1487-1494. https://doi.org/10.1021/acs.iecr.9b05629
79. Gengnan Li, Bin Wang, Daniel E. Resasco. Water-Mediated Heterogeneously Catalyzed Reactions. *ACS Catalysis* **2020,** *10* (2) , 1294-1309. https://doi.org/10.1021/acscatal.9b04637
80. Ravinder Kumar, Vladimir Strezov, Tao Kan, Haftom Weldekidan, Jing He, Sayka Jahan. Investigating the Effect of Mono- and Bimetallic/Zeolite Catalysts on Hydrocarbon Production during Bio-oil Upgrading from Ex Situ Pyrolysis of Biomass. *Energy & Fuels* **2020,** *34* (1) , 389-400. https://doi.org/10.1021/acs.energyfuels.9b02724
81. Kanduri Praveen Kumar, Seethamraju Srinivas. Catalytic Co-pyrolysis of Biomass and Plastics (Polypropylene and Polystyrene) Using Spent FCC Catalyst. *Energy & Fuels* **2020,** *34* (1) , 460-473. https://doi.org/10.1021/acs.energyfuels.9b03135
82. Yinglei Han, Anamaria P. P. Pires, Manuel Garcia-Perez. Co-hydrotreatment of the Bio-oil Lignin-Rich Fraction and Vegetable Oil. *Energy & Fuels* **2020,** *34* (1) , 516-529. https://doi.org/10.1021/acs.energyfuels.9b03344
83. Evan Terrell, Lauren D. Dellon, Anthony Dufour, Erika Bartolomei, Linda J. Broadbelt, Manuel Garcia-Perez. A Review on Lignin Liquefaction: Advanced Characterization of Structure and Microkinetic Modeling. *Industrial & Engineering Chemistry Research* **2020,** *59* (2) , 526-555. https://doi.org/10.1021/acs.iecr.9b05744
84. Charles A. Mullen, Gary D. Strahan, Akwasi A. Boateng. Characterization of Biomass Pyrolysis Oils by Diffusion Ordered NMR Spectroscopy. *ACS Sustainable Chemistry & Engineering* **2019,** *7* (24) , 19951-19960. https://doi.org/10.1021/acssuschemeng.9b05520
85. Isabel Hilber, Yves Arrigo, Martin Zuber, Thomas D. Bucheli. Desorption Resistance of Polycyclic Aromatic Hydrocarbons in Biochars Incubated in Cow Ruminal Liquid in Vitro and in Vivo. *Environmental Science & Technology* **2019,** *53* (23) , 13695-13703. https://doi.org/10.1021/acs.est.9b04340

86. Jing Sun, Zhenyu Jiang, Ke Wang, Faqi Li, Zhanlong Song, Wenlong Wang, Xiqiang Zhao, Yanpeng Mao. Experimental Study on Microwave–SiC-Assisted Catalytic Hydrogenation of Phenol. *Energy & Fuels* **2019,** *33* (11) , 11092-11100. https://doi.org/10.1021/acs.energyfuels.9b02595
87. Tingyong Xing, Anton Alvarez-Majmutov, Rafal Gieleciak, Jinwen Chen. Co-hydroprocessing HTL Biocrude from Waste Biomass with Bitumen-Derived Vacuum Gas Oil. *Energy & Fuels* **2019,** *33* (11) , 11135-11144. https://doi.org/10.1021/acs.energyfuels.9b02711
88. Yee Wen Chua, Hongwei Wu, Yun Yu. Interactions between Low- and High-Molecular-Weight Portions of Lignin during Fast Pyrolysis at Low Temperatures. *Energy & Fuels* **2019,** *33* (11) , 11173-11180. https://doi.org/10.1021/acs.energyfuels.9b02813
89. Mehrdad Seifali Abbas-Abadi, Maryam Fathi, Mohammad Ghadiri. Effect of Different Process Parameters on the Pyrolysis of Iranian Oak Using a Fixed Bed Reactor and TGA Instrument. *Energy & Fuels* **2019,** *33* (11) , 11226-11234. https://doi.org/10.1021/acs.energyfuels.9b02845
90. Elias Aliu, Abarasi Hart, Joseph Wood. Reaction Kinetics of Vanillin Hydrodeoxygenation in Acidic and Nonacidic Environments Using Bimetallic PdRh/Al2O3 Catalyst. *Energy & Fuels* **2019,** *33* (11) , 11712-11723. https://doi.org/10.1021/acs.energyfuels.9b02993
91. Héctor Hernando, Begoña Puértolas, Patricia Pizarro, Javier Fermoso, Javier Pérez-Ramírez, David P. Serrano. Cascade Deoxygenation Process Integrating Acid and Base Catalysts for the Efficient Production of Second-Generation Biofuels. *ACS Sustainable Chemistry & Engineering* **2019,** *7* (21) , 18027-18037. https://doi.org/10.1021/acssuschemeng.9b04921
92. Zaikuan Yu, Priya Murria, Mckay W. Easton, John C. Degenstein, Hanyu Zhu, Lan Xu, Rakesh Agrawal, W. Nicholas Delgass, Fabio H. Ribeiro, Hilkka I. Kenttämaa. Exploring the Reaction Mechanisms of Fast Pyrolysis of Xylan Model Compounds via Tandem Mass Spectrometry and Quantum Chemical Calculations. *The Journal of Physical Chemistry A* **2019,** *123* (42) , 9149-9157. https://doi.org/10.1021/acs.jpca.9b04438
93. Maria J. Suota, Edesio L. Simionatto, Dilamara R. Scharf, Henry F. Meier, Vinicyus R. Wiggers. Esterification, Distillation, and Chemical Characterization of Bio-Oil and Its Fractions. *Energy & Fuels* **2019,** *33* (10) , 9886-9894. https://doi.org/10.1021/acs.energyfuels.9b01971
94. Zhiguo Dong, Haiping Yang, Peiao Chen, Zihao Liu, Yingquan Chen, Lei Wang, Xianhua Wang, Hanping Chen. Lignin Characterization and Catalytic Pyrolysis for Phenol-Rich Oil with TiO2-Based Catalysts. *Energy & Fuels* **2019,** *33* (10) , 9934-9941. https://doi.org/10.1021/acs.energyfuels.9b02341
95. Amoolya Lalsare, Yuxin Wang, Qingyuan Li, Ali Sivri, Roman J. Vukmanovich, Cosmin E. Dumitrescu, Jianli Hu. Hydrogen-Rich Syngas Production through Synergistic Methane-Activated Catalytic Biomass Gasification. *ACS Sustainable Chemistry & Engineering* **2019,** *7* (19) , 16060-16071. https://doi.org/10.1021/acssuschemeng.9b02663
96. Jiaming Shao, Chaoqun Xu, Zhihua Wang, Jianping Zhang, Rongtao Wang, Yong He, Kefa Cen. NOx Reduction in a 130 t/h Biomass-Fired Circulating Fluid Bed Boiler Using Coupled Ozonation and Wet Absorption Technology. *Industrial &*

Engineering Chemistry Research **2019,** *58* (39) , 18134-18140. https://doi.org/10.1021/acs.iecr.9b03355
97. Elias Aliu, Abarasi Hart, Joseph Wood. Kinetics of Vanillin Hydrodeoxygenation Reaction in an Organic Solvent Using a Pd/C Catalyst. *Industrial & Engineering Chemistry Research* **2019,** *58* (33) , 15162-15172. https://doi.org/10.1021/acs.iecr.9b02907
98. Henrik Wiinikka, Alexey Sepman, Yngve Ögren, Bo Lindblom, Lars-Olof Nordin. Combustion Evaluation of Renewable Fuels for Iron-Ore Pellet Induration. *Energy & Fuels* **2019,** *33* (8) , 7819-7829. https://doi.org/10.1021/acs.energyfuels.9b01356
99. Kai Sun, Qing Xu, Yuewen Shao, Lijun Zhang, Qing Liu, Shu Zhang, Yi Wang, Xun Hu. Cross-Polymerization between the Typical Sugars and Phenolic Monomers in Bio-Oil: A Model Compounds Study. *Energy & Fuels* **2019,** *33* (8) , 7480-7490. https://doi.org/10.1021/acs.energyfuels.9b01856
100. Shun-Feng Jiang, Guo-Ping Sheng, Hong Jiang. Advances in the Characterization Methods of Biomass Pyrolysis Products. *ACS Sustainable Chemistry & Engineering* **2019,** *7* (15) , 12639-12655

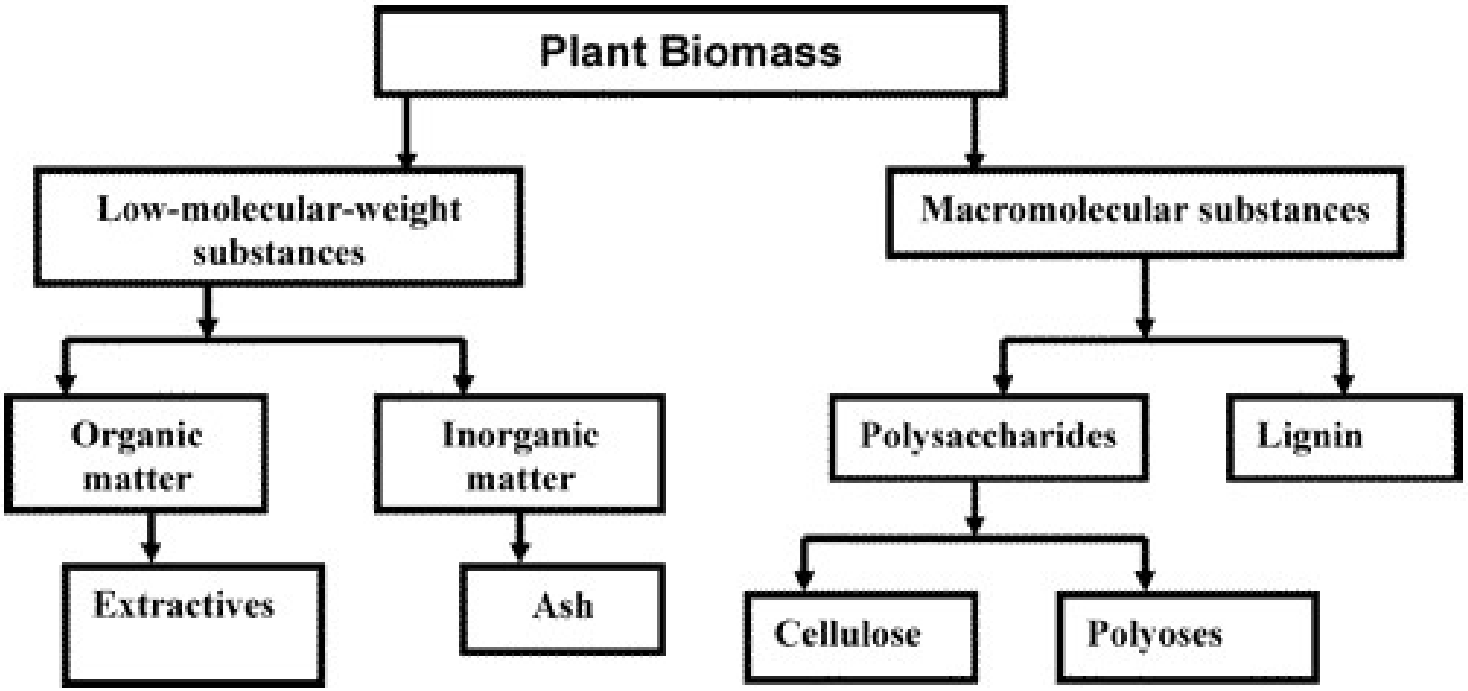

Figure 1 General components in plant biomass.

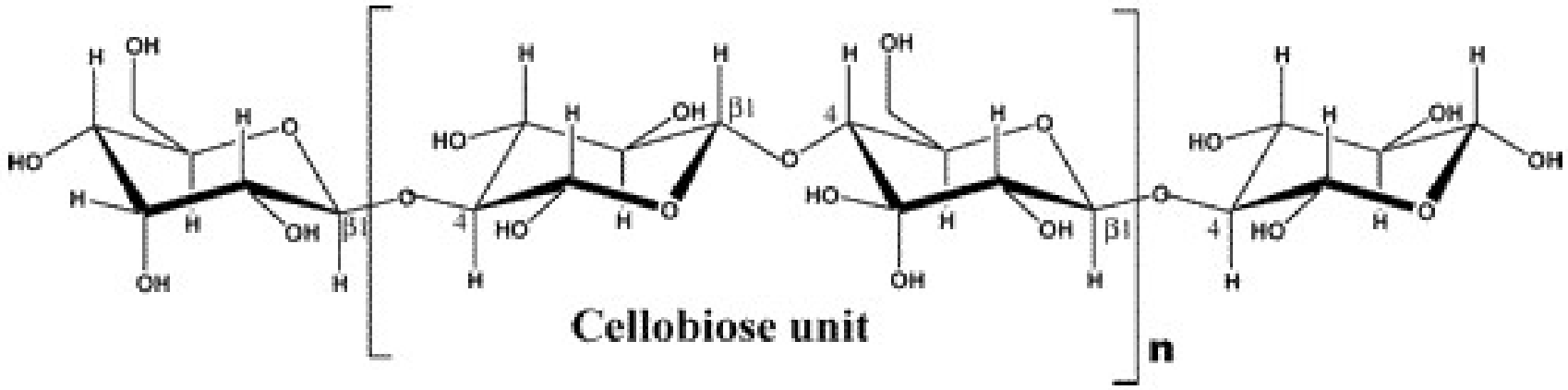

Figure 2 Chemical structure of cellulose.

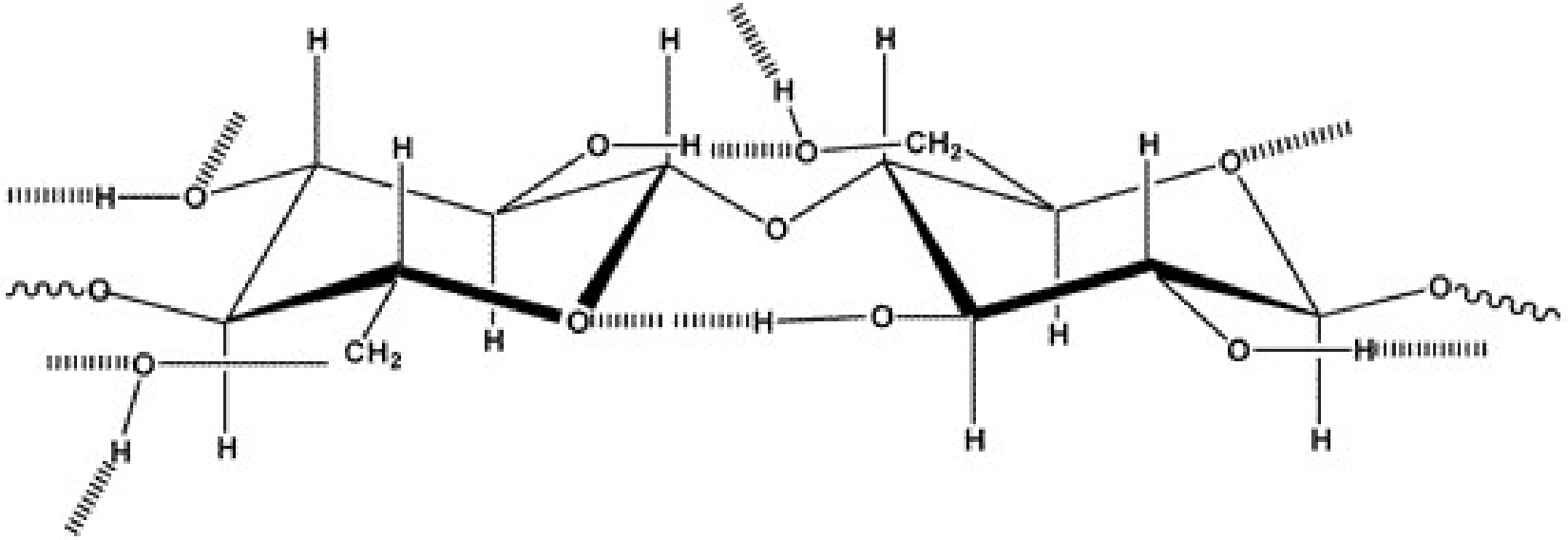

Figure 3 Intrachain and interchain hydrogen-bonded bridging.

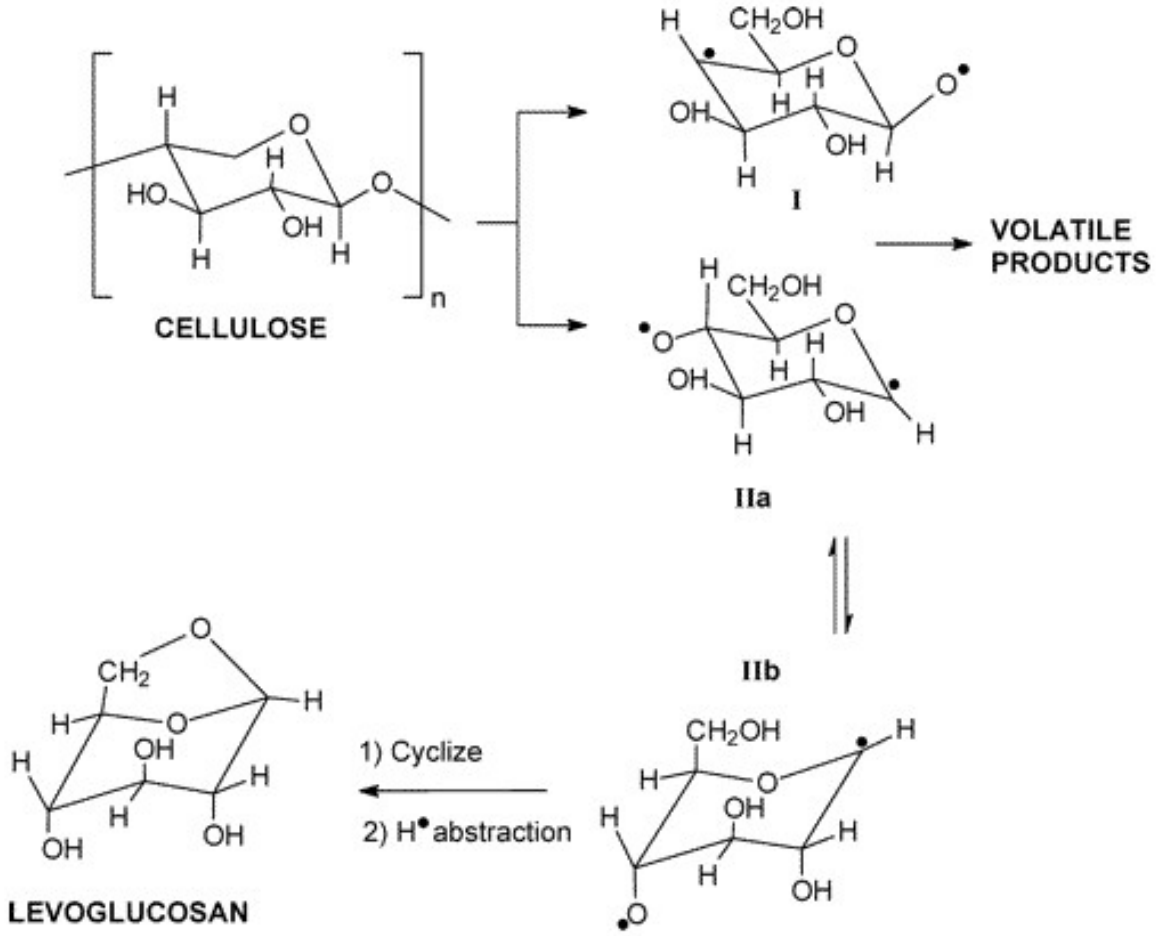
CELLULOSE
I
VOLATILE PRODUCTS
IIa
IIb
1) Cyclize
2) H• abstraction
LEVOGLUCOSAN

Scheme 1

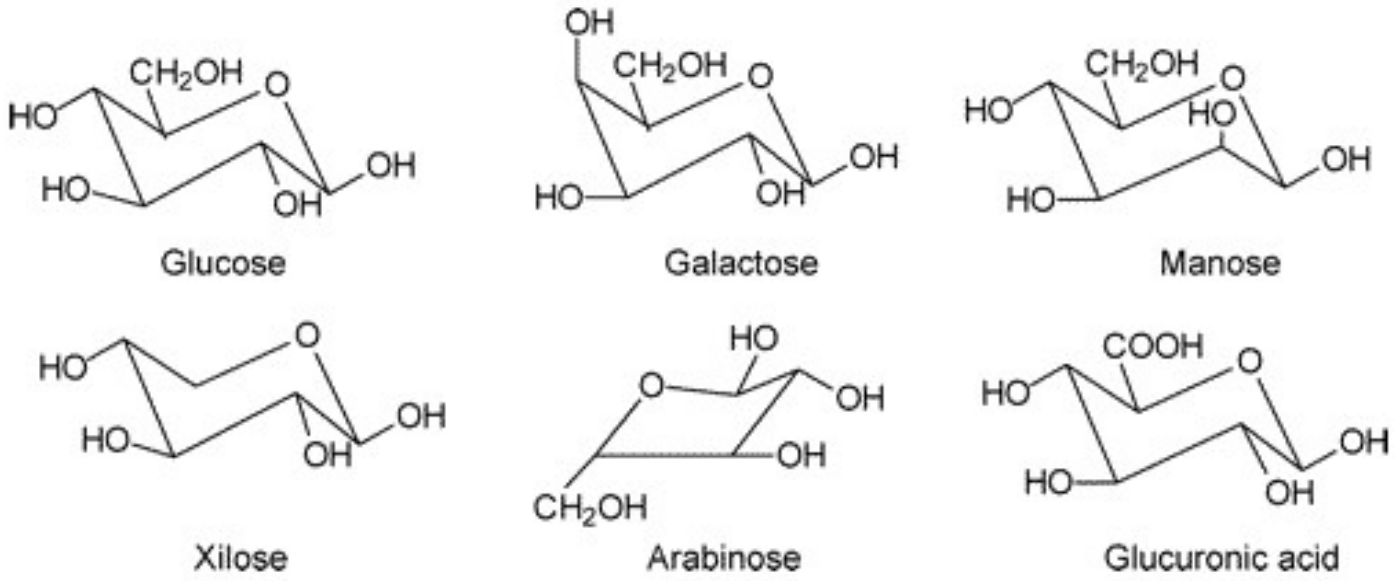

Figure 4 Main components of hemicellulose.

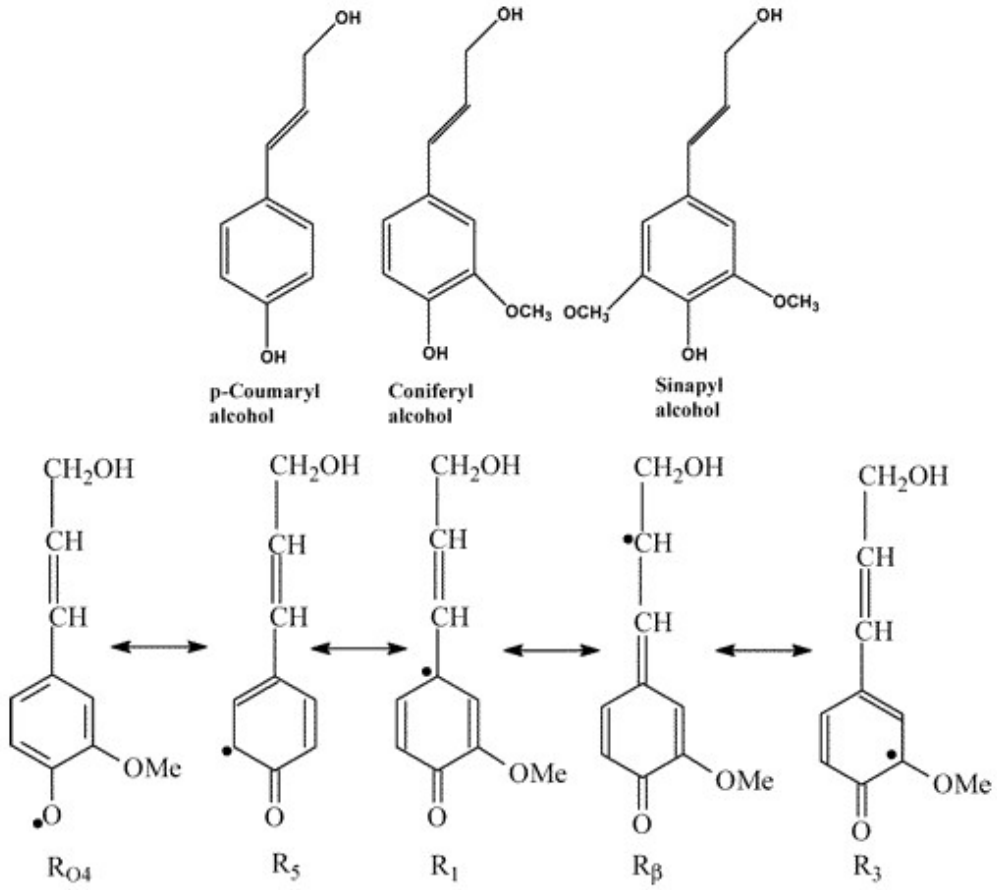

Figure 5 *p*-Coumaryl, coniferyl, and sinapyl structures and resonance hybrid structures of phenoxy radicals produced by the oxidation of coniferyl.

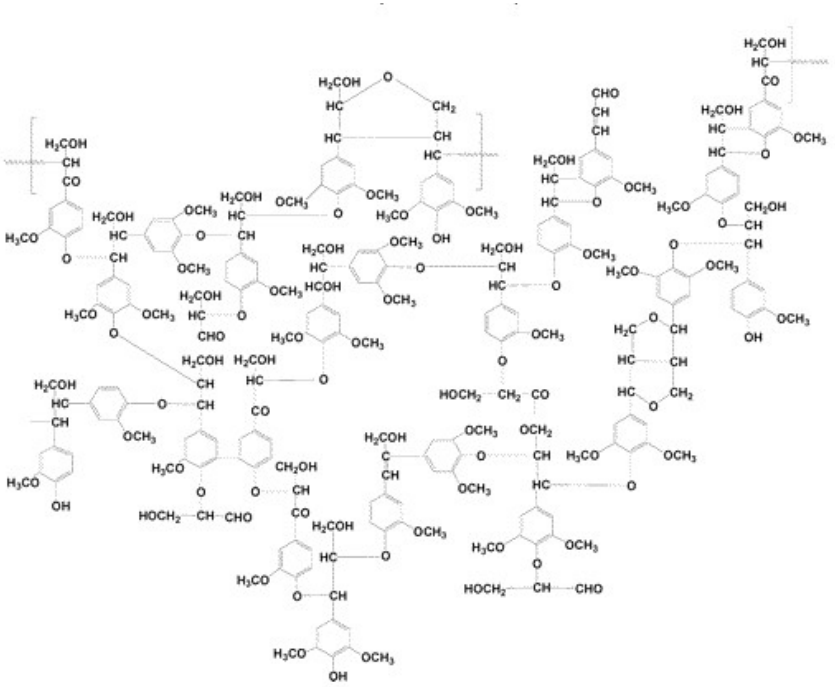

Figure 6 Partial structure of a hardwood lignin molecule from European beech (*Fagus sylvatica)*. The phenylpropanoid units that comprised lignin are not linked in a simple, repeating way. The lignin of beech contains units derived from coniferyl alcohol, sinapyl alcohol, and *p*-coumaryl alcohol in the approximate ratio of 100:70:7 and is typical of hardwood lignin. Softwood lignin contains relatively fewer sinapyl alcohol units. (After Nimz 1974.[45]).

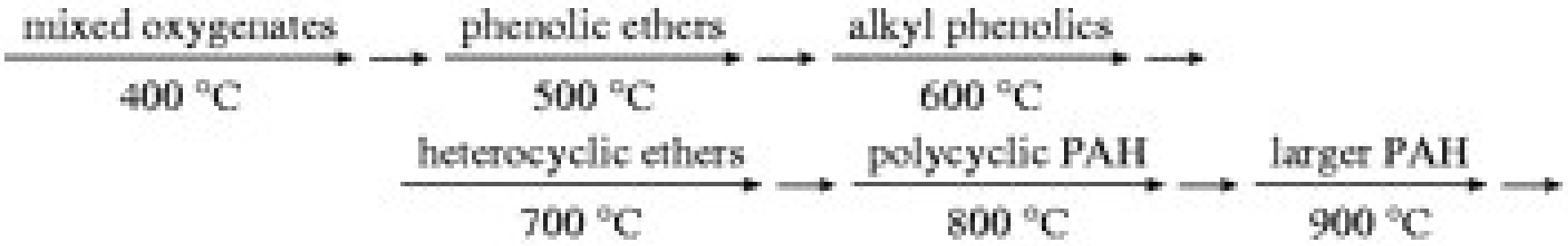

In the middle of 8.1 after “The relationship is described as…”

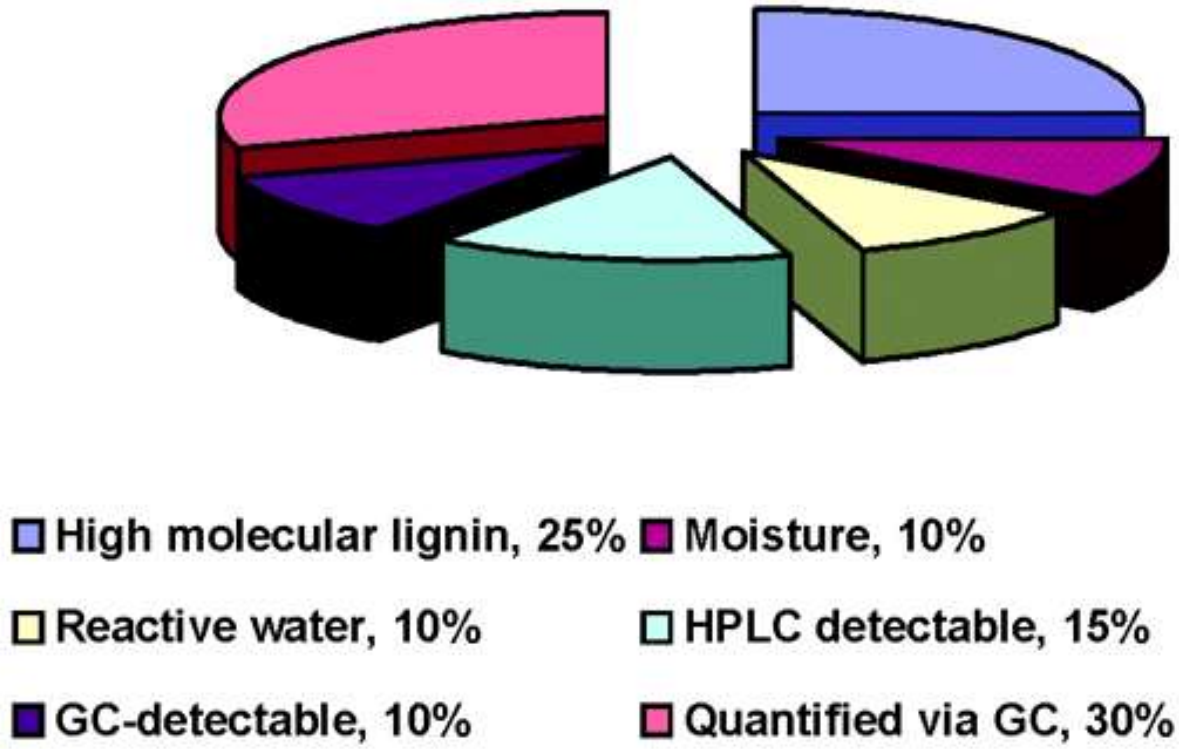

Figure 7 Typical portions of the important fractions in bio-oil.

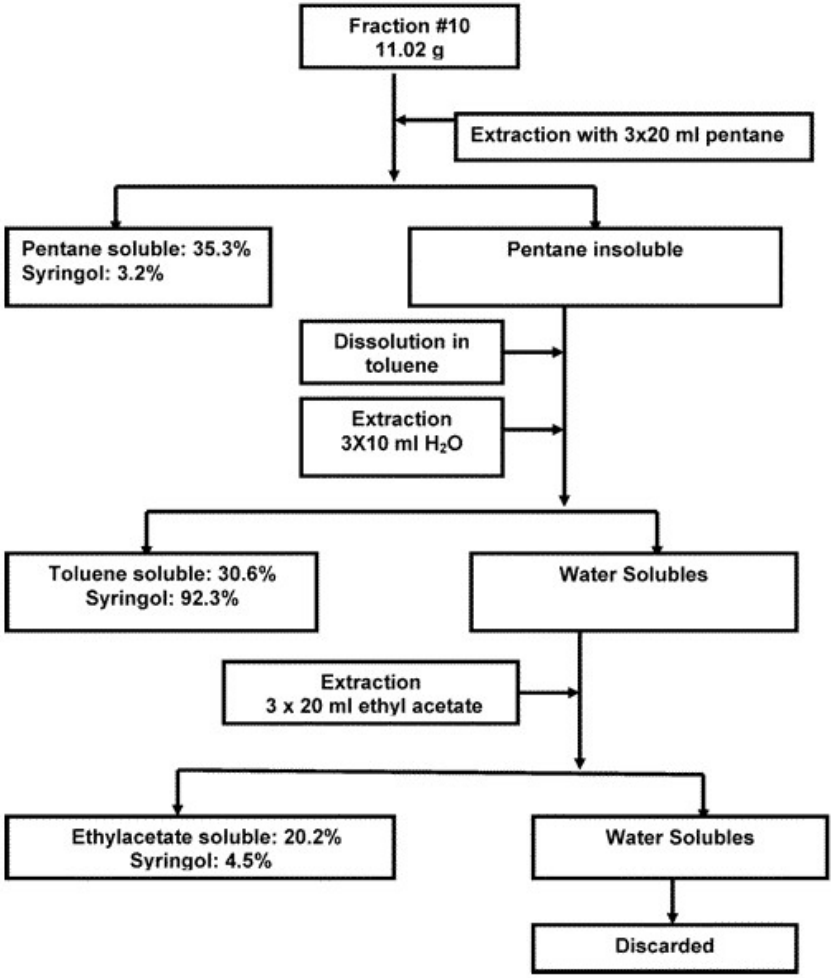

Scheme 2. Syringol Separation and Purification from Birchwood Vacuum Pyrolysis Oil[93]

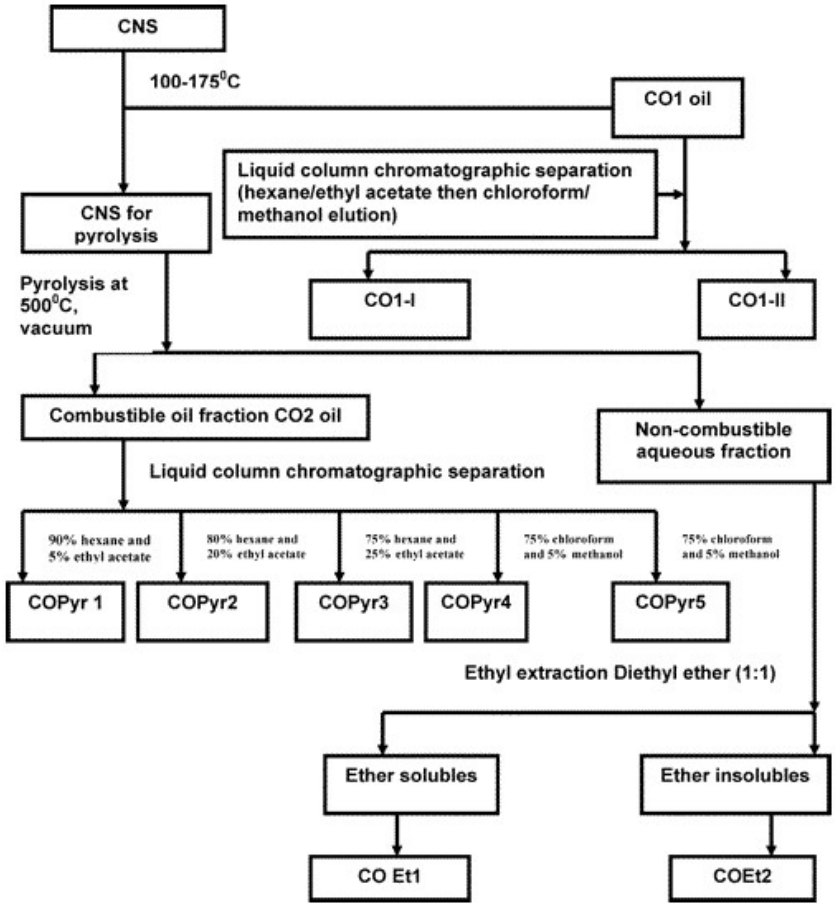

Scheme 3. Schematic Diagram for Separation and Chemical Characterization of Cashew Nut Shell Oil[136,137]

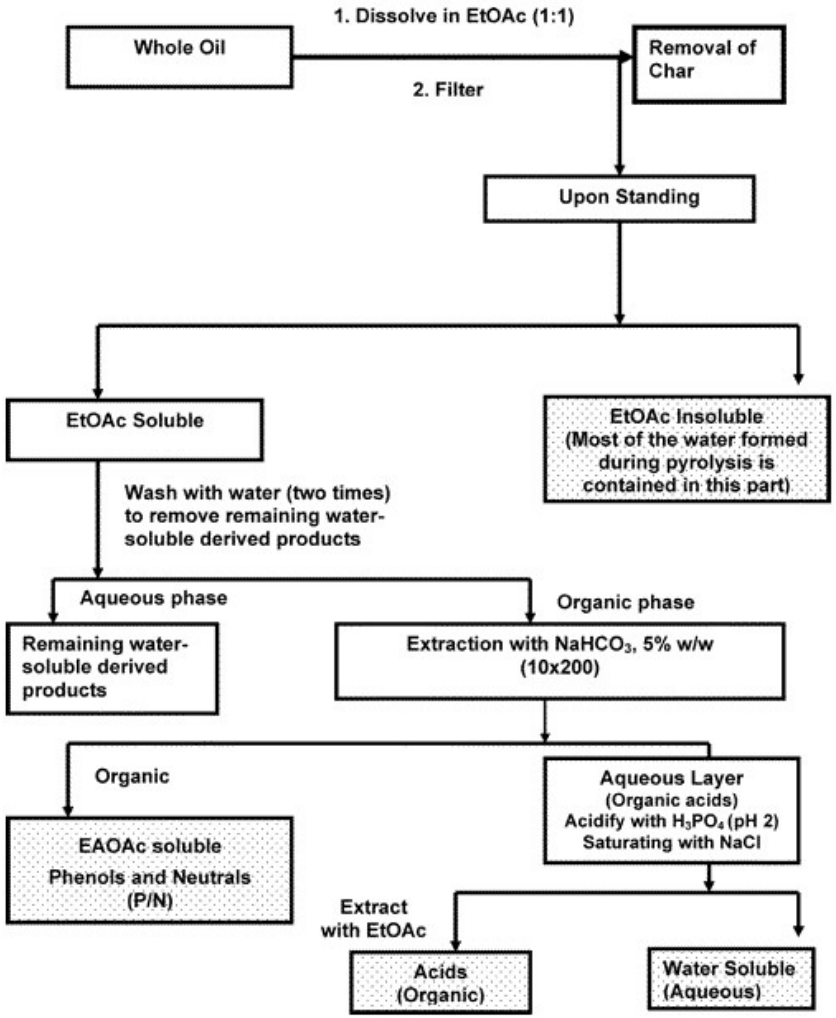

Scheme 4. NREL Bio-oil Fractionation Method[198]

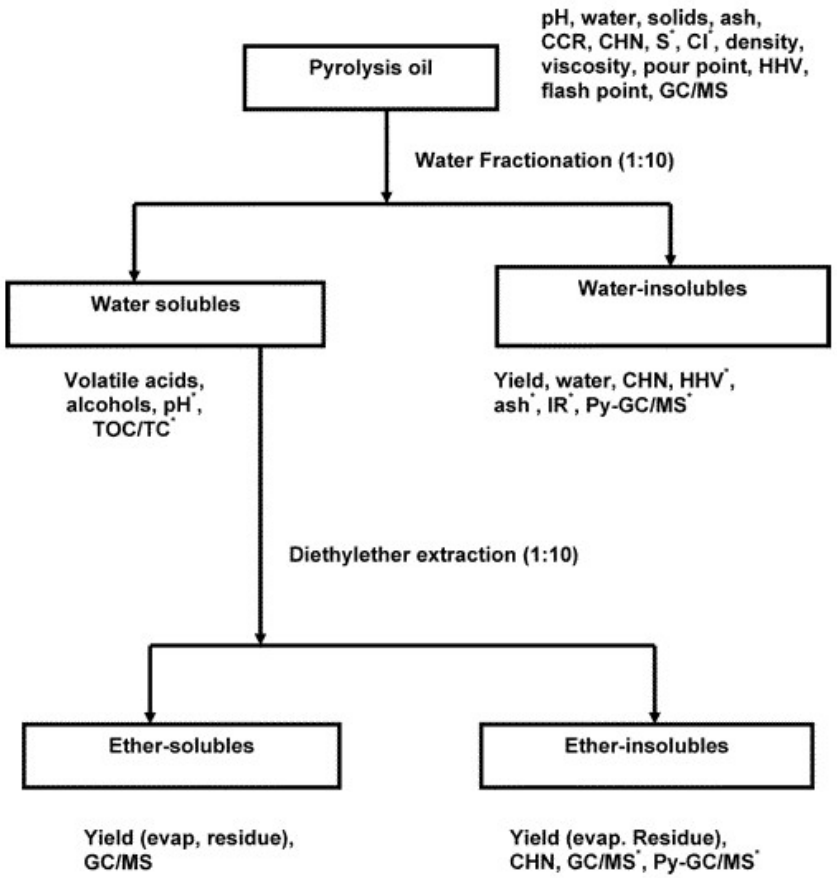

Scheme 5. Solvent Fractionation for the Separation and Characterization of Biomass-Based Flash Pyrolysis Bio-oil[199]

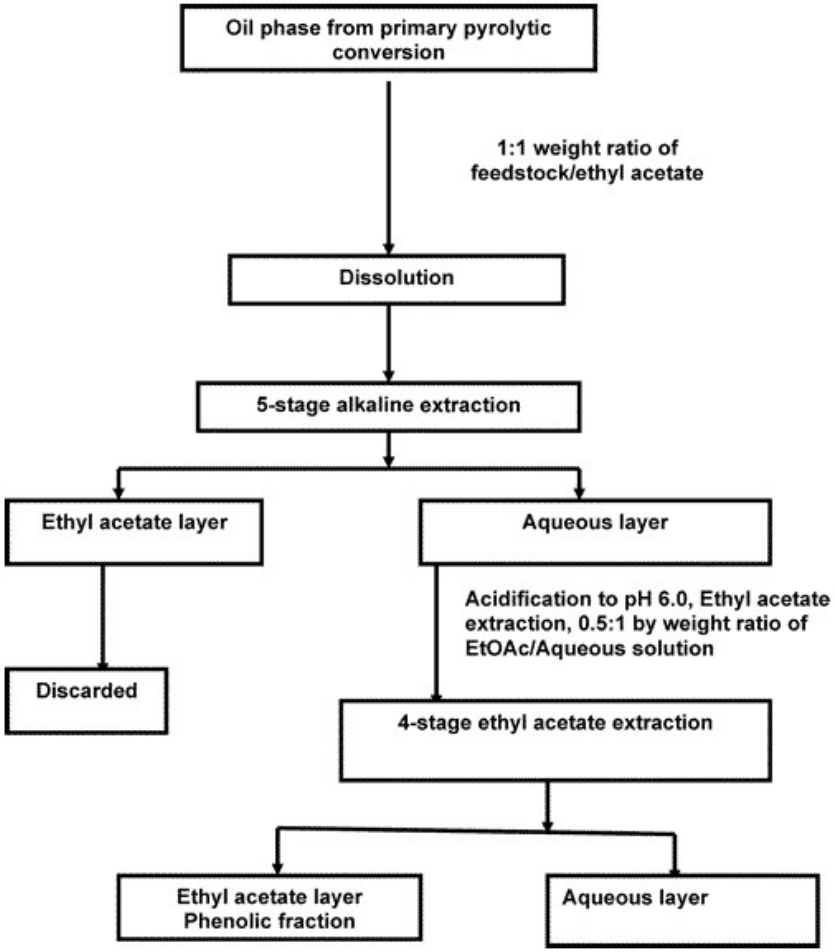

Scheme 6. Extraction Procedure for the Isolation of Phenols from Eucalyptus Tar[105]

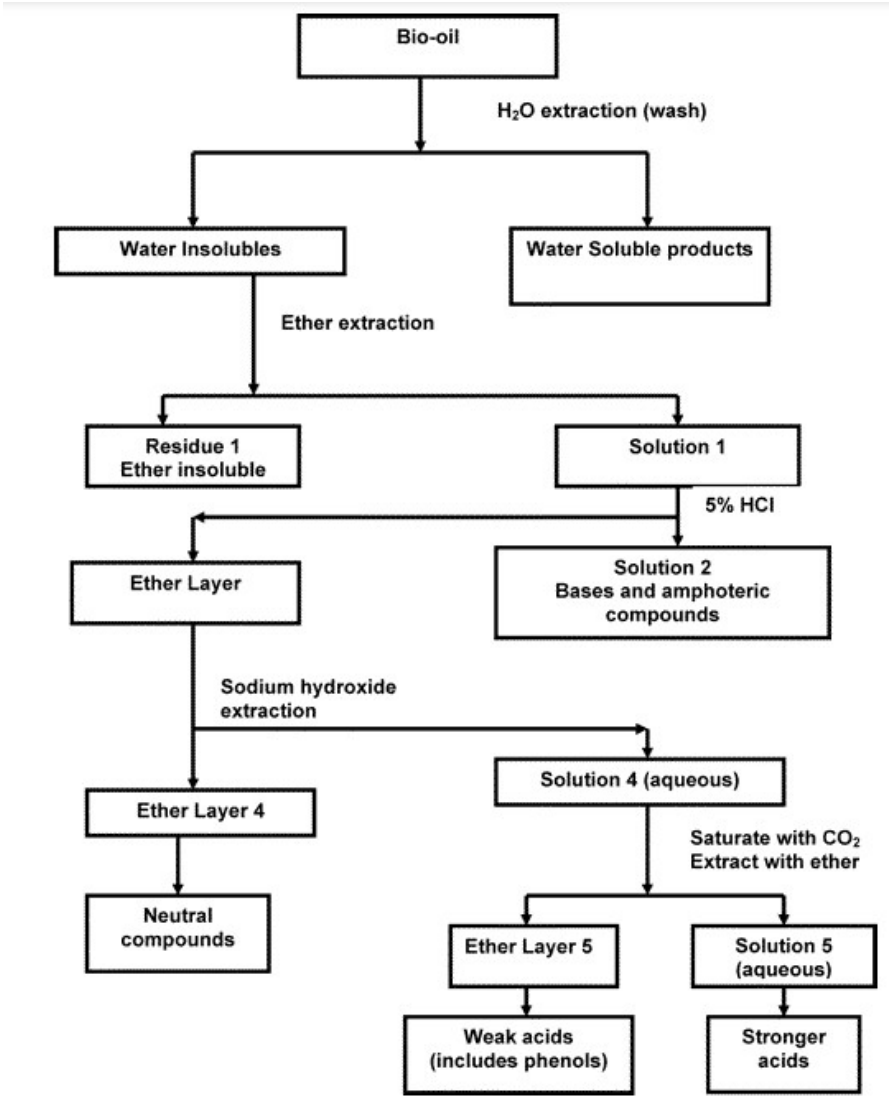

Scheme 7. Bio-oil Extraction Procedure by Shriner et al.[200]

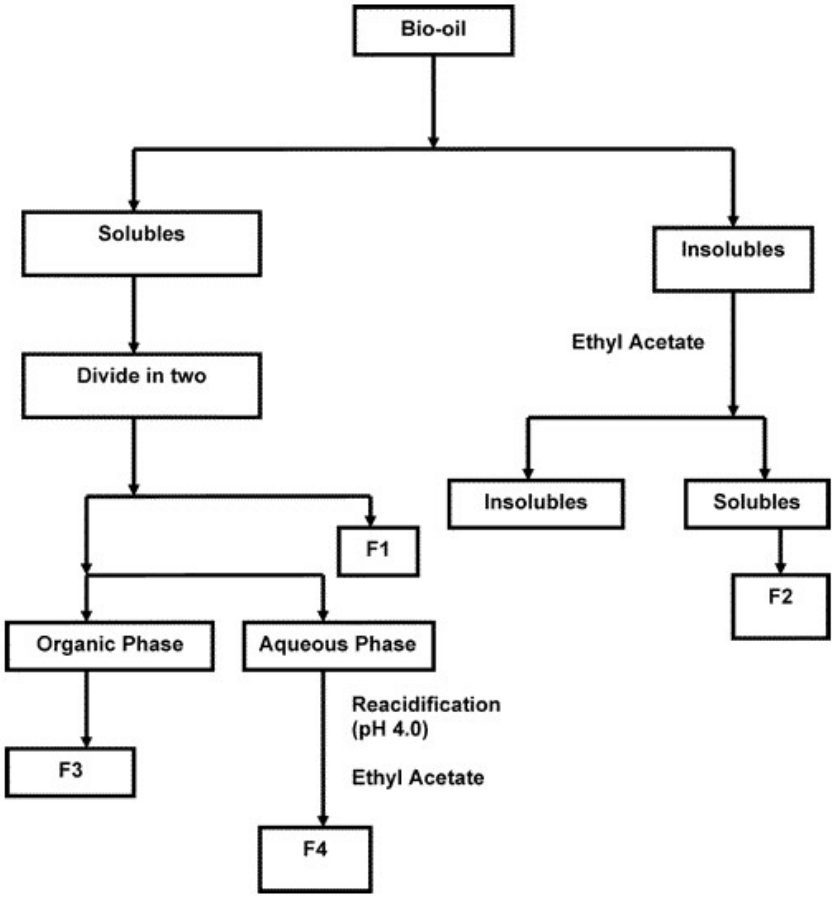

Scheme 8. Aqueous Phase Fractionation of Bio-oil Developed by Christian et al.[202]

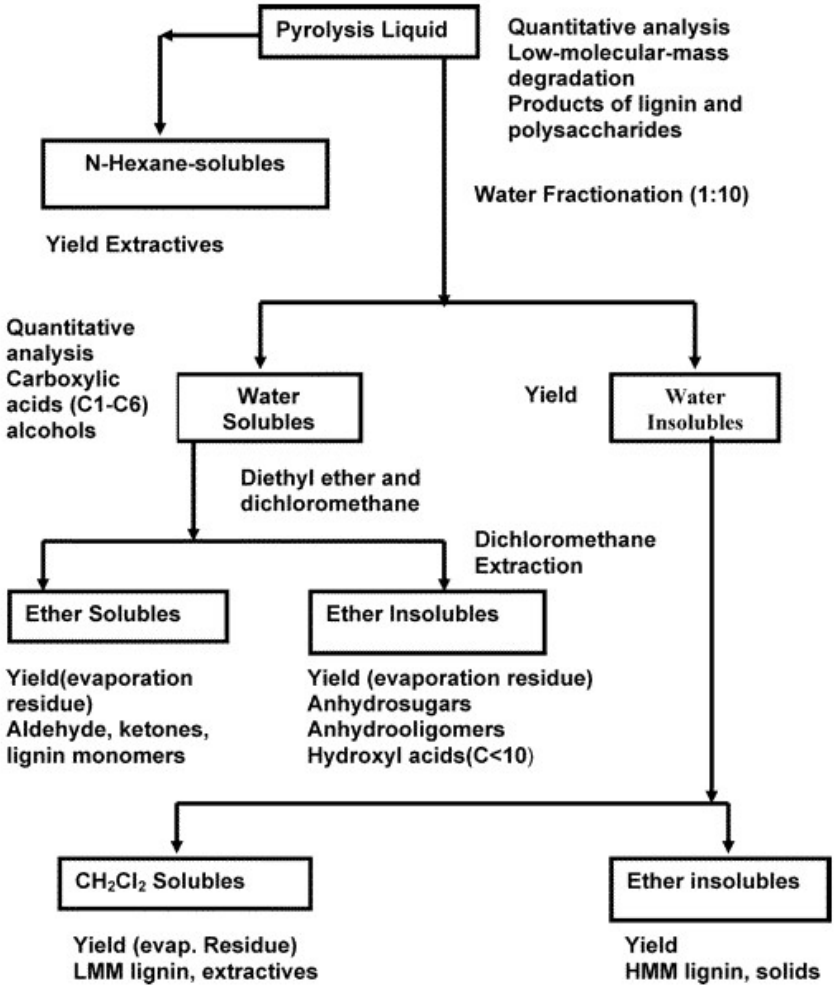

Scheme 9. Fractionation Scheme Developed by Oasmma and Co-workers[83-85]

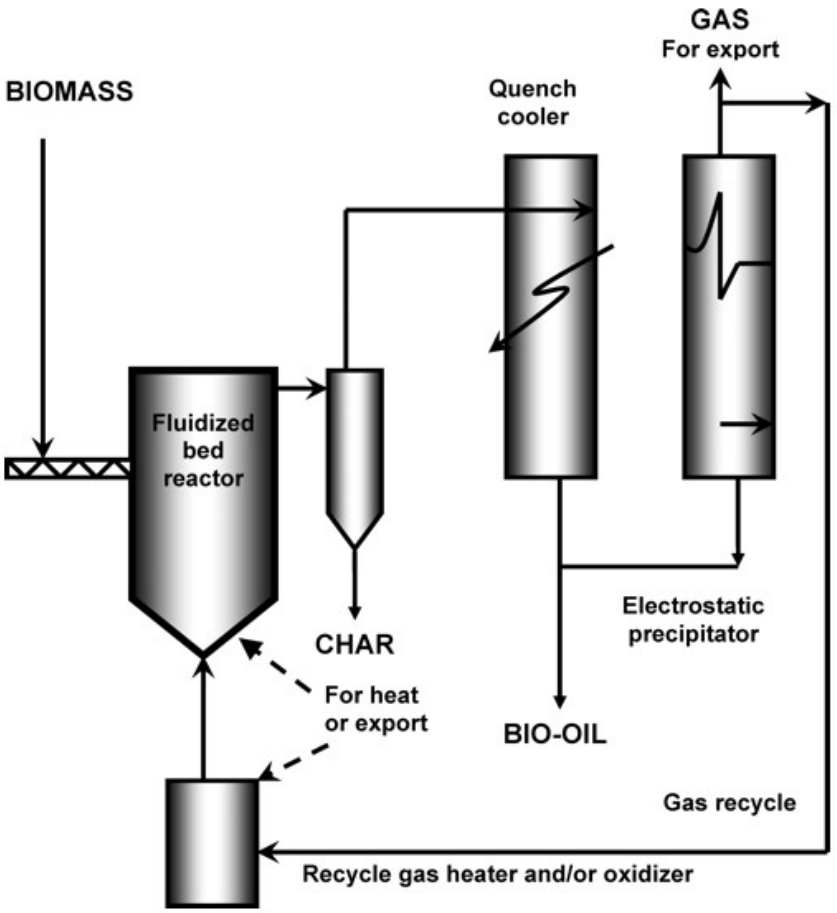

Figure 8 Bubbling fluidized-bed reactor (Redrawn, with permission, from Bridgwater.[54] (Copyright 2003, Elsevier, Amsterdam.)

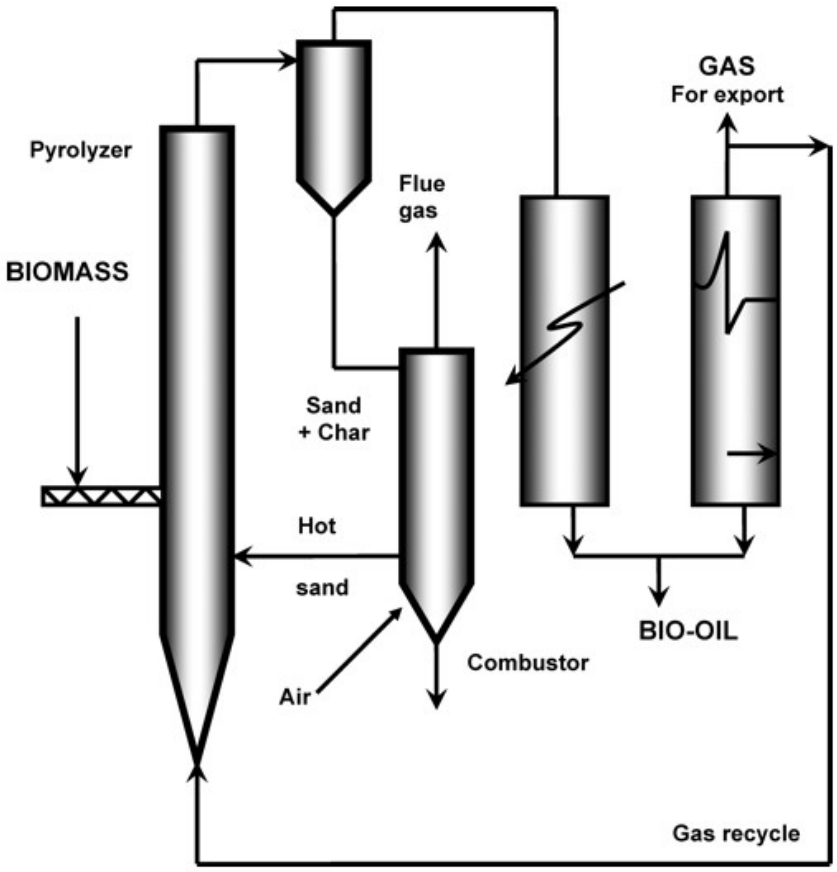

Figure 9 Schematic of the circulating fluidized bed reactor (redrawn, with permission, from Bridgwater.[54] (Copyright 2003, Elsevier, Amsterdam.)

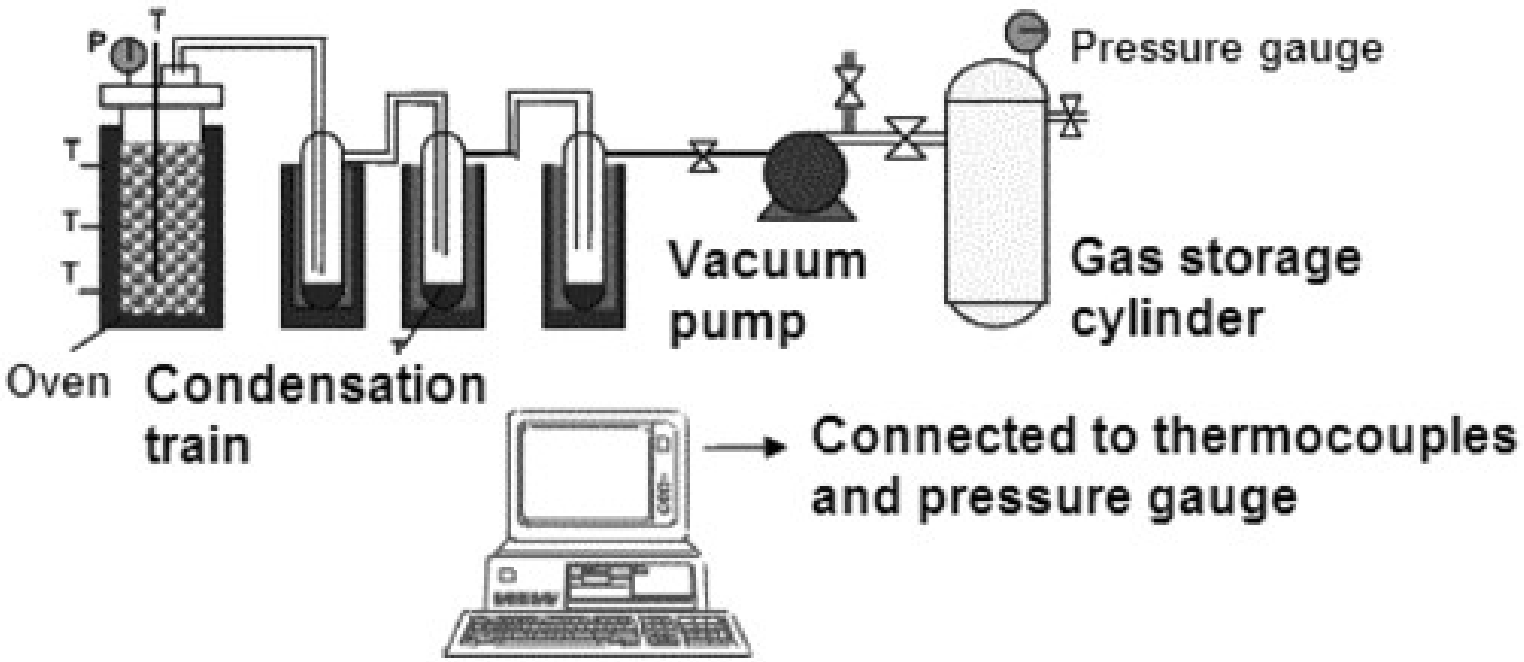

Figure 10 Schematic of the vacuum pyrolysis laboratory-scale installation (reprinted, with permission, from Garcìa-Pèrez et al.[94]). (Copyright 2002, Elsevier, Amsterdam.)

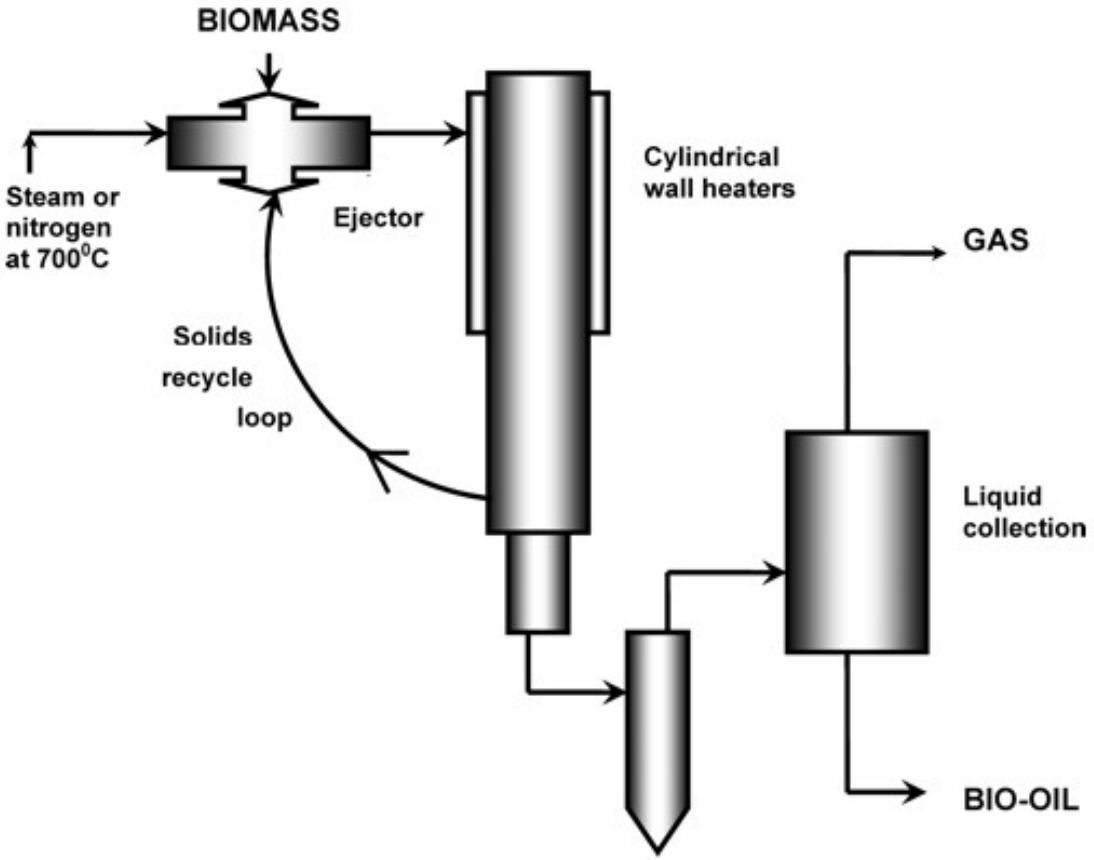

Figure 11 Schematic of the NREL Vortex Ablative bed reactor (redrawn, with permission, from Bridgwater.[54] (Copyright 2003, Elsevier, Amsterdam.)

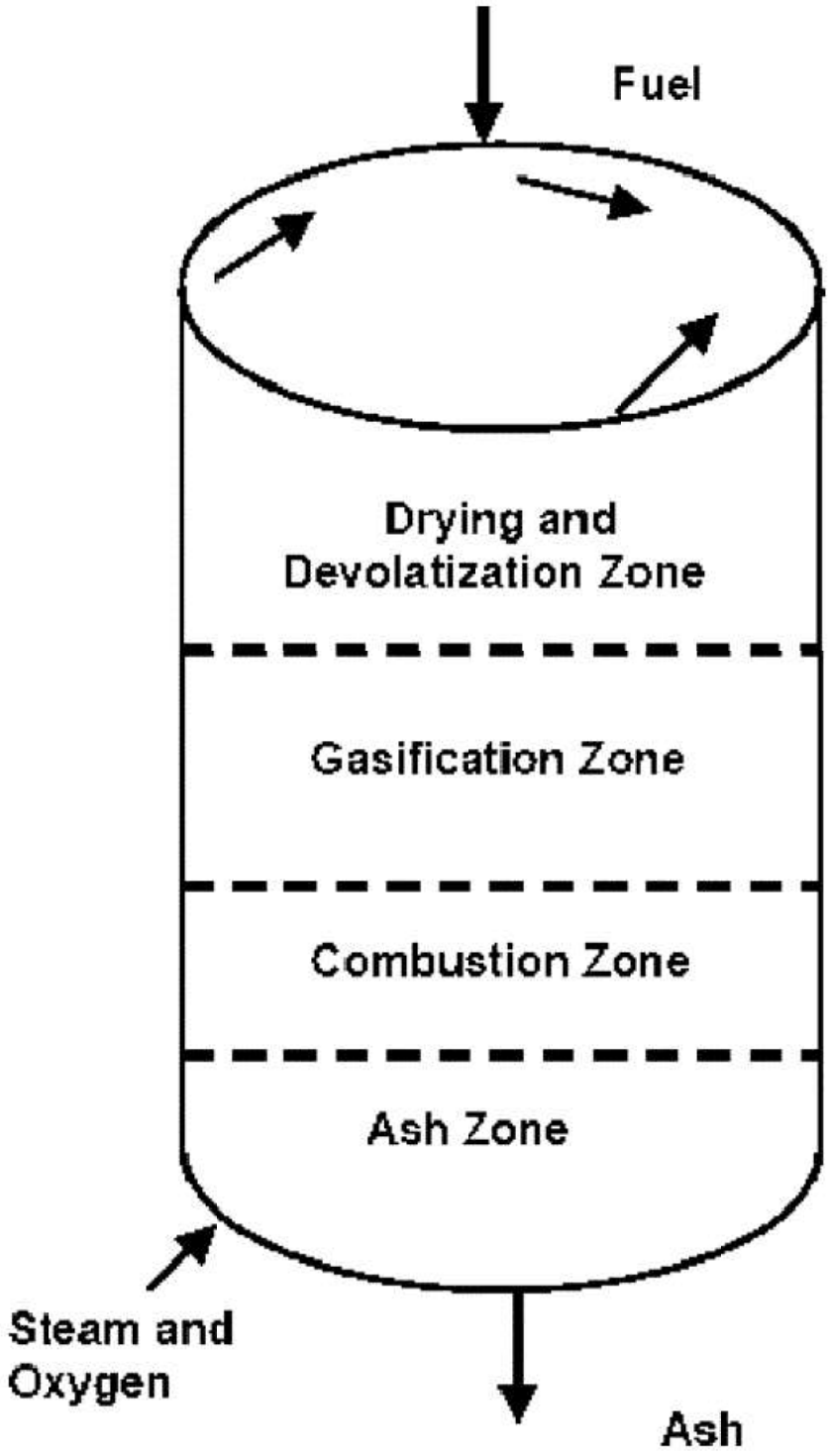

Figure 12 Schematic of the Lurgi gasification process.

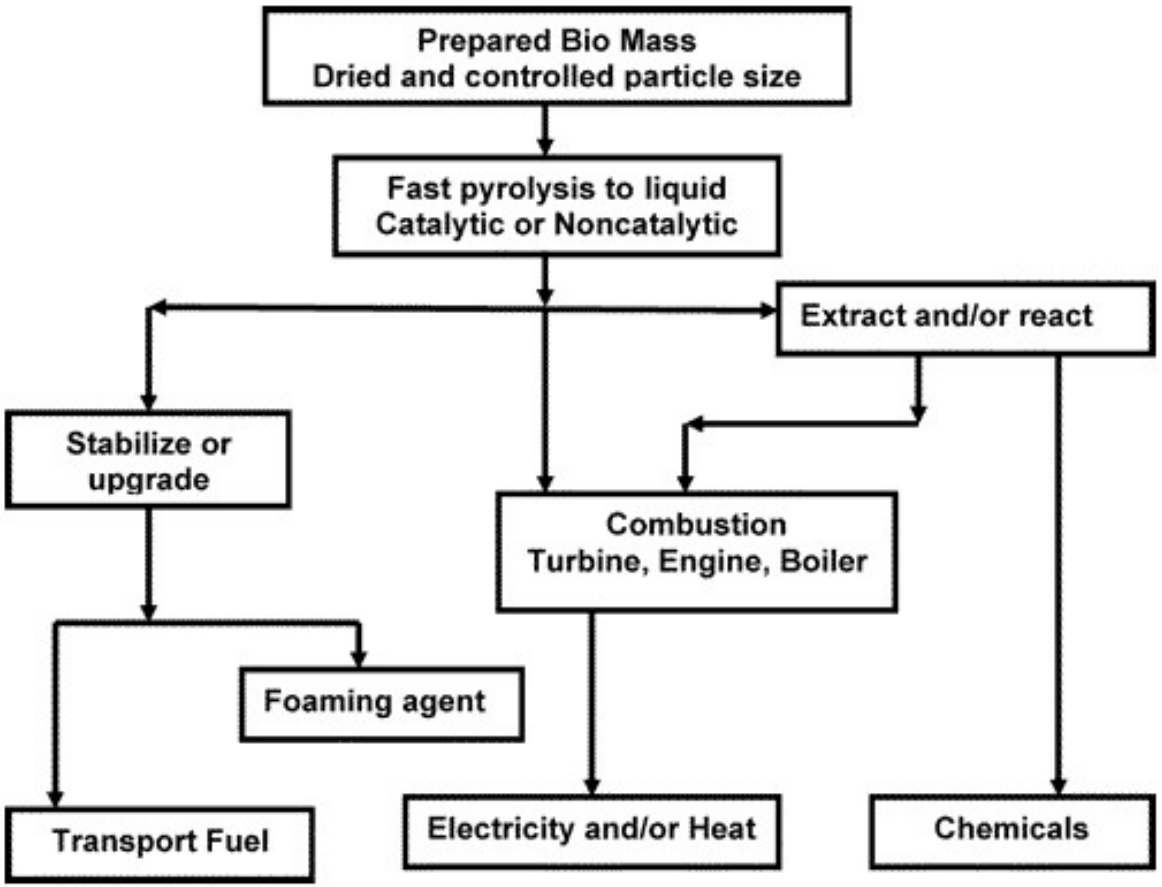

Scheme 10. Application of Bio-Oils (taken from ref 54 with permission from Elsevier)